Institut für Veterinärbiochemie und Molekularbiologie
der Vetsuisse-Fakultät, Universität Zürich

Direktor: Prof. Dr. med. vet. Ulrich Hübscher

Arbeit unter wissenschaftlicher Betreuung von
Dr. sc. nat. Barbara van Loon

Oxidative stress and Mule-driven X-linked intellectual disability

Inaugural-Dissertation

zur Erlangung der Doktorwürde der
Vetsuisse-Fakultät Universität Zürich

vorgelegt von

Cristina Manuela Gattiker

Tierärztin

von Richterswil, Zürich

genehmigt im Auftrag von

Referent: Prof. Dr. med. vet. Ulrich Hübscher

Koreferent: Prof. Dr. med. vet. Hanspeter Nägeli

Zürich 2013

Institut für Veterinärbiochemie und Molekularbiologie
der Vetsuisse-Fakultät, Universität Zürich

Direktor: Prof. Dr. med. vet. Ulrich Hübscher

Arbeit unter wissenschaftlicher Betreuung von
Dr. sc. nat. Barbara van Loon

Oxidative stress and Mule-driven X-linked intellectual disability

Inaugural-Dissertation

zur Erlangung der Doktorwürde der
Vetsuisse-Fakultät Universität Zürich

vorgelegt von

Cristina Manuela Gattiker

Tierärztin

von Richterswil, Zürich

genehmigt im Auftrag von

Referent: Prof. Dr. med. vet. Ulrich Hübscher

Koreferent: Prof. Dr. med. vet. Hanspeter Nägeli

Zürich 2013

Table of Contents

1 Summary

1.1 Abstract

Oxidative damage of proteins, lipids, RNA and DNA is the source of many diseases, which can be prevented by accurate repair machineries. Besides aging and cancer, oxidative DNA damage has been linked to neurodegenerative diseases. One of the most frequent oxidative DNA lesion is 7,8-dihydro-8-oxoguanine (8-oxo-G). During DNA replication, this lesion is often mispaired with adenosine (A) and thereby bears the risk of G:C→T:A transversion mutations. Before DNA replication, 8-oxoguanine glycosylase 1 (OGG1) initiated base excision repair (BER) needs to act on C:8-oxo-G and restore accurate G:C basepair. In case 8-oxo-G becomes a substrate for DNA replication, it is the glycosylase MutY homolog (MutYH) and DNA polymerase (Pol) λ that will repair the newly generated, mutagenic A:8-oxo-G. Among other regulators, the Mcl-1 ubiquitin ligase E3 (Mule) controls these processes by ubiquitinating Pol λ and sending it for proteasomal degradation. So far only little is known about the physiological importance of Mule in regulation of MutYH/Pol λ mediated BER. Here, the effects of mutated Mule on 8-oxo-G repair capacity in patients suffering from X-linked intellectual disability (XLID) were explored. This work addressed (i) the differences in protein amounts of Mule and A:8-oxo-G repair factors, (ii) changes in their presence in different cellular compartments, as well as (iii) the capacity to repair A:8-oxo-G mispairs and (iv) overall bypass accuracy of 8-oxo-G damage. The results show that in relation to a healthy individual, MutYH and Pol λ protein levels are specifically changed in XLID patients with mutated Mule. These changes were characteristically reflected in the subcellular fractions and reveal a functional link between MutYH and Pol λ. A DNA polymerase assay and a novel MutYH glycoslase assay displayed the different repair capacities in XLID patient cells with affected Pol λ and MutYH levels. Namely the reduction in MutYH or Pol λ levels corresponded to decreased removal of mispaired A or increased inaccurate incorporation of dATP opposite 8-oxo-G, respectively. After the Mule knock-down in XLID cells, protein levels of both MutYH and Pol λ could be restored to a certain degree, indicating a direct impact of mutated Mule on these two proteins. Further, also the accurate A:8-oxo-G repair was ameliorated. These findings support a causative effect of mutated Mule in the development of neurodegeneration, demonstrated on XLID and a deficient BER of oxidative DNA lesions.

1.2 Zusammenfassung

Oxidative Schädigung von Proteinen, Lipiden, RNA und DNA sind die Quellen vieler Erkrankungen, die durch intakte Reparaturmechanismen verhindert werden können. Oxidative DNA Schäden werden, neben Alterung und Krebs, mit neurodegenerativen Erkrankungen in Verbindung gebracht. Eine der häufigsten oxidativen DNA Schäden ist 7,8-dihydro-8-oxoguanin (8-oxo-G), welches falsche Basenpaarung mit Adenosin (A) eingeht und dadurch das Risiko von G:C→T:A Transversionsmutationen birgt. Bevor die DNA Replikation stattfindet, stellt die 8-oxoguanin Glykosylase 1 (OGG1) in der Basenexzisionreparatur (BER) korrekte G:C Basenpaare wieder her. Nach der Replikation sind es MutY Homolog (MutYH) und DNA polymerase λ (Pol λ), die das mutagene A:8-oxo-G reparieren. Neben anderen Regulatoren kontrolliert die Mcl1 Ubiquitinligase E3 (Mule) diese Vorgänge durch Ubiquitinierung und Abbau von Pol λ. Um die physiologische Bedeutung der MutYH/Pol λ vermittelten BER zu erläutern, wurden die Auswirkungen mutierten Mules in Patienten mit X-assoziierter mentaler Behinderung (XLID) untersucht. Der Fokus dieser Arbeit liegt auf der Auswirkung auf (i) die Proteinmengen von Mule und A:8-oxo-G Reparaturfaktoren, (ii) ihre Gegenwart in verschiedenen Zellkompartimenten wie auch (iii) die veränderte Reparaturkapazität von A:8-oxo-G und (iv) korrekte Handhabung der 8-oxo-G Läsion. Die Resultate zeigen, dass die Proteinmengen von MutYH und Pol λ im Vergleich mit einem gesunden Individuum in den Zellen von XLID-Patienten mit mutiertem Mule verändert sind. Die subzellulären Fraktionen weisen ebenfalls Abweichungen auf, was auf einen funktionellen Zusammenhang zwischen MutYH und Pol λ deutet. Ein neu entwickelter MutYH Glykosylase und ein DNA Polymerase Assay zeigen die verschiedenen Reparatureigenschaften *in vitro*: Erniedrigte Proteinmengen von MutYH oder Pol λ korrespondieren mit erniedrigter Beseitigung von falsch-gepaartem A oder gesteigerter fehlerhafter Einfügung von A gegenüber 8-oxo-G. Nach dem Knock-down von Mule stiegen die Proteinmengen von MutYH and Pol λ teilweise an, was auf einen direkten Einfluss des mutierten Mule auf die BER von 8-oxo-G hinweist. Des Weiteren verbesserte sich auch die korrekte Reparatur von A:8-oxo-G. Diese Ergebnisse unterstützen einen ursächlichen Zusammenhang zwischen mutiertem Mule und der Entstehung neurodegenerativer Erkrankungen.

2 Introduction

2.1 Oxidative DNA damage

The dependency of living organisms on oxygen has several drawbacks and as such requires control mechanisms to overcome them. One attribute of oxygen especially relevant for the integrity of genetic information is the potential to react with its building blocks. Whereas proteins, lipids or RNA can be replaced when oxidized, DNA cannot [2]. Damage to the DNA can interfere with various processes, such as transcription and replication, and induce mutations. Counteracting DNA damage in the nucleus as well as in the mitochondria is therefore crucial to prevent cellular malfunctions and their consequences, such as developmental impairments, degeneration or cancer [3].

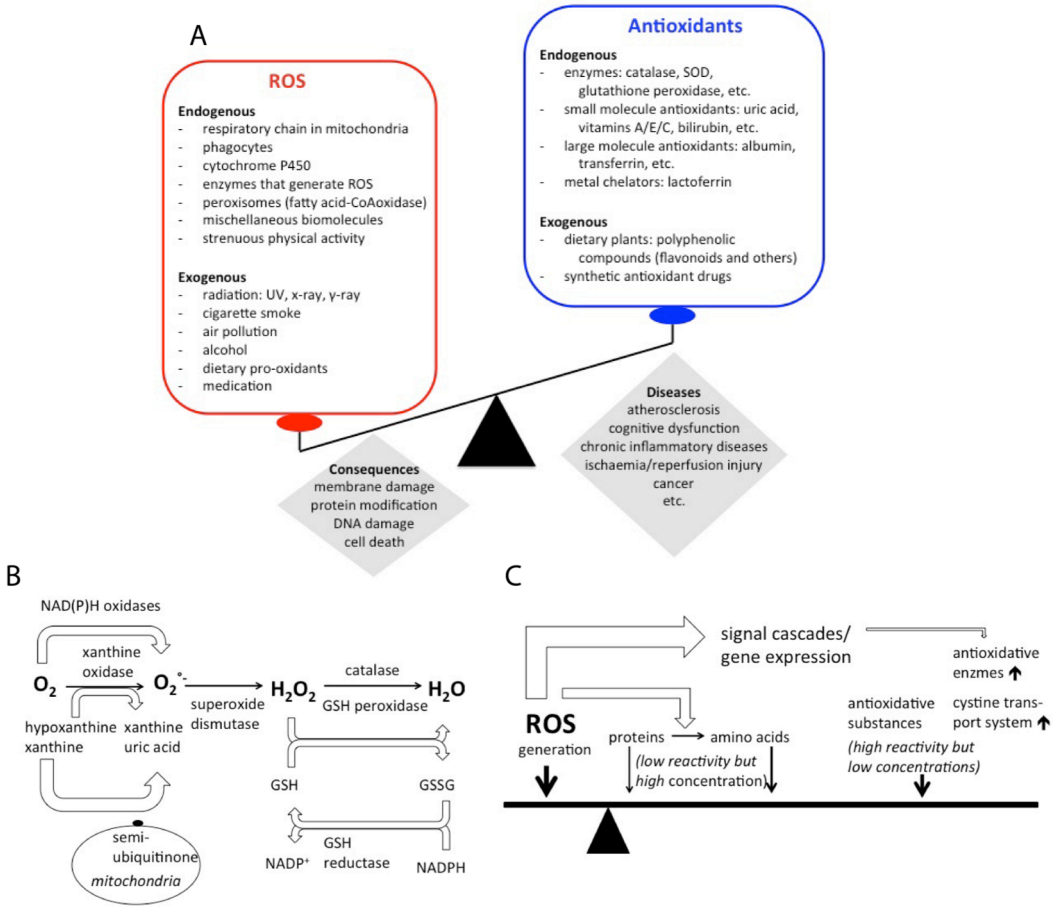

Figure 1. ROS production and neutralization in the cell.
(A) Several endogenous and exogenous substances contribute to the generation and resolution of ROS. (B) Pathways of ROS production and clearance. GSH, glutathione; GSSG, glutathione disulfide. (C) Mechanisms of redox homeostasis. Balance between ROS production and various types of scavengers. The steady-state levels of ROS are determined by the rate of ROS production and their clearance by scavenging mechanisms. Certain antioxidative enzymes including superoxide dismutase (SOD), glutathione peroxidase, catalase, and thioredoxin are potent ROS scavengers but occur in cells only at relatively low concentrations. The same is true for nonenzymic antioxidants. Amino acids and proteins are also ROS scavengers. Amino acids are less effective than the classical antioxidants on a molecular basis, but their cumulative intracellular concentration is higher. (From and modified after Wulf Dröge. (2002) Free Radicals in the Physiological Control of Cell Function. *Physiological Reviews* and O. Firuzi, R. Miri, M. Tavakkoli and L. Saso. (2011) Antioxidant Therapy: Current Status and Future Prospects. *Current Medicinal Chemistry*)

Oxidative DNA damage can be induced by different sources: (i) endogenous products of cellular metabolism and spontaneous oxidative reactions, as well as (ii) exogenous agents ranging from UV-light to irradiation, or toxins and pollutants (Figure 1A). Overall, every mammalian cell accumulates on average 20'000 endogenous DNA lesions per day [4]. In a healthy resting cell, 2% of the absorbed oxygen is transformed into reactive oxygen species (ROS) [5] leading to endogenous oxidative DNA lesions. Those result predominantly from mitochondrial oxidative metabolism, activated inflammatory cells, or enzymes which produce ROS such as superoxide anions, hydrogen peroxide and hydroxyl radicals (Figure 1B) [6,7]. Besides damaging cellular components such as DNA, ROS are involved in the regulation of proliferation, gene expression and signaling [8]. Several enzymatic and non-enzymatic cascades evolved to regulate cellular ROS levels. These include enzymatic antioxidants, such as superoxide dismutase, glutathione peroxidase and catalase, and non-enzymatic antioxidants, for example β-carotene (provitamin A), vitamin E (α-Tocopherol) and C (Ascorbic acid), and glutathione (Figure 1C) [9].

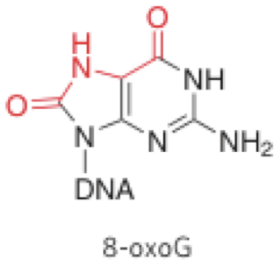

Figure 2. Structure of 7,8-dihydro-8-oxoguanine (8-oxo-G) damage.
(From Sheila S. David, Valerie L. O'Shea, and Sucharita Kundu. (2007) Base excision repair of oxidative DNA damage. *Nature)*

One of the most abundant and best-studied oxidative DNA lesions with mutational capacity is 7,8-dihydro-8-oxoguanine (8-oxo-G). This lesion frequently arises due to the low redox potential of guanine. It carries a hydrogen atom on the nitrogen at position 7 and an oxygen on the carbon at position 8 (Figure 2) [10]. Replicative DNA polymerases (Pols) can bypass 8-oxo-G lesion in an error-prone manner by incorporating incorrect dATP in trans conformation opposite the lesion in syn conformation (Figure 3) [11]. The created mispair escapes proofreading activity of replicative Pols δ and ε, thus persisting in the DNA after completion of replication. If A:8-oxo-G mispairs are not repaired before the next round of replication, G:C→T:A transversion mutations will arise. These mutations are frequently found in many cancer types such as lung, breast, ovarian, gastric, and colorectal cancers [12]. While normal cells encounter approximately 1'000-2'000 8-oxo-G lesions per day, the number of these lesions can reach up to 100'000 in cancer cells [13]. In addition to 8-oxo-G, many other lesions are induced by oxidizing agents, including: abasic sites, bulky base damages, single-strand breaks, protein-DNA adducts and DNA crosslinks (Table 1) [14].

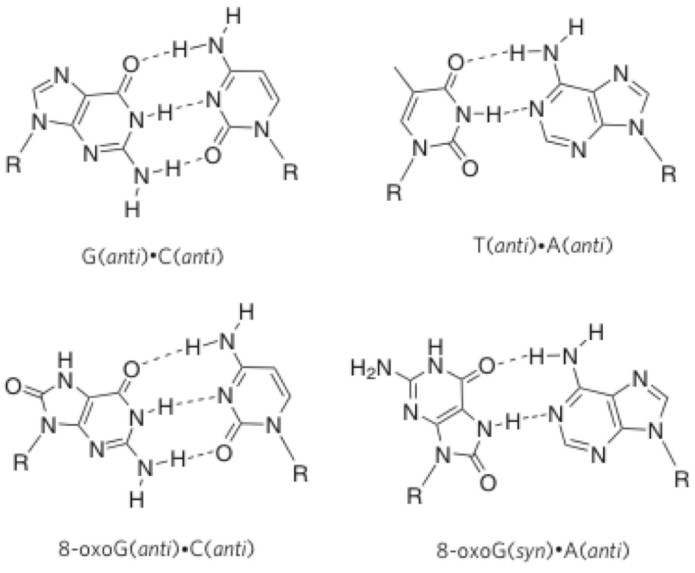

Figure 3. Structures of 8-oxo-G containing base pairs.
The structures of the natural base pairs G:C and T:A are compared with those of C:8-oxo-G and A:8-oxo-G. 8-oxo-G differs from G by an additional oxygen at position C8 and a hydrogen at N7. This subtle change allows 8-oxo-G to base-pair easily with either C or A. (From Sheila S. David, Valerie L. O'Shea, and Sucharita Kundu. (2007) Base excision repair of oxidative DNA damage. *Nature)*

Once DNA is damaged, cells can react in several different ways. Upon registry of the damage cell cycle arrest can occur, enabling initiation of DNA repair or apoptosis. The latter results in elimination of defective cells and prevents tissue malfunction or development of cancer. On the other side, the cell can also enter senescence and restrain from further replication. If damage accumulates, the cell will either gradually loose its function and age, or develop oncogenic potential [15]. To counteract onset of these events several repair pathways have developed [16,17]. Depending on the type of DNA damage, specific DNA repair pathways will be used (Table 1). The importance of efficient and faithful repair of different oxidative DNA lesions is demonstrated by numerous findings showing that not only cancer but also neurodegenerative, pulmonary and cardiovascular diseases as well as ageing correlate with ROS and 8-oxo-G levels [2,18].

Table 1. Classical and atypical forms of oxidative DNA damage and associated DNA repair pathways.
BER/NER: base/nucleotide excision repair, ICR: interstrand crosslink repair, RFR: replication fork restart. (Modified after Brian R. Berquist, David M. Wilson III. (2012) Pathways for repairing and tolerating the spectrum of oxidative DNA lesions . *Cancer Letters)*

Type of lesion	Lesion	Repair Pathway
non-bulky base modifications	7,8-dihydro-8-oxo-guanine (8-oxo-G)	BER
	2,6-diamino-4-hydroxy-5-formamidopyrimidine (Fapy-G)	
	7,8-dihydro-8-oxoadenine	
	4,6-diamino-5- formamidopyrimidine (Fapy-A)	
	cytosine glycol, uracil glycol, 5-hydroxycytosine, 5-hdroxyuracil	
	thymine glycol, 5,6-dihydroxythymine, 5-hydroxymethyluracil, 5-formyluracil	
	apurinic/apyrimidinic site, 2-deoxyribonolactone, 2-deoxypentos-4-ulose, single strand breaks (SSBs)	
bulky base modifications	8,5'-cyclo-2-deoxynucleosides	NER
	etheno-adducts	
	intrastrand crosslinks	
	protein-DNA crosslinks	
interstrand crosslinks	replication blocking lesions	ICR RFR

2.1.1 Base excision repair (BER) - a pathway for removal of small base lesions

2.1.1.1 BER overview

Base excision repair (BER) is one of several different pathways to efficiently repair damaged DNA (Figure 4). BER acts on DNA base lesions generated by alkylation, oxidation, ring saturation or deamination [19,20]. Depending on the number of newly incorporated nucleotides (nt), BER divides in two sub-pathways: short-patch (SP-BER) and long-patch BER (LP-BER) [21]. SP-BER is characterized by incorporation of 1nt (Figure 4A), while in LP-BER a newly synthetized patch of 2 to 12nt is generated (Figure 4B). The BER pathway is generally initiated by DNA glycosylases, enzymes that recognize the damaged base and incise the N-

glycosylic bond between the 2'-deoxyribose and the base. In humans, 11 different DNA glycosylases have been identified so far [22]. If the DNA glycosylase is monofunctional, upon removal of the damaged base it leaves behind an apurinic/apyrimidinic (AP). In the next step the major 5' AP endonuclease, apurinic/apyrimidinic endonuclease 1 (APE1) generates a single nucleotide gap (1nt-gap) with a 3' hydroxyl (3'OH) end and a 5' deoxyribose phosphate (5'dRp) terminus [23]. Pol β, the primary BER Pol which possesses dRp lyase activity, removes the 5'dRp moiety and incorporates 1nt. Bifunctional DNA glycosylases on the other hand, possess also a β lyase activity. They excise the damaged base and cut the sugar phosphate backbone, generating a 3'terminal sugar phosphate (3'ddR5P) and a 5' phosphate residue. The 3'ddR5P moiety is processed by APE1 and a 1nt-gap filled by Pol β.

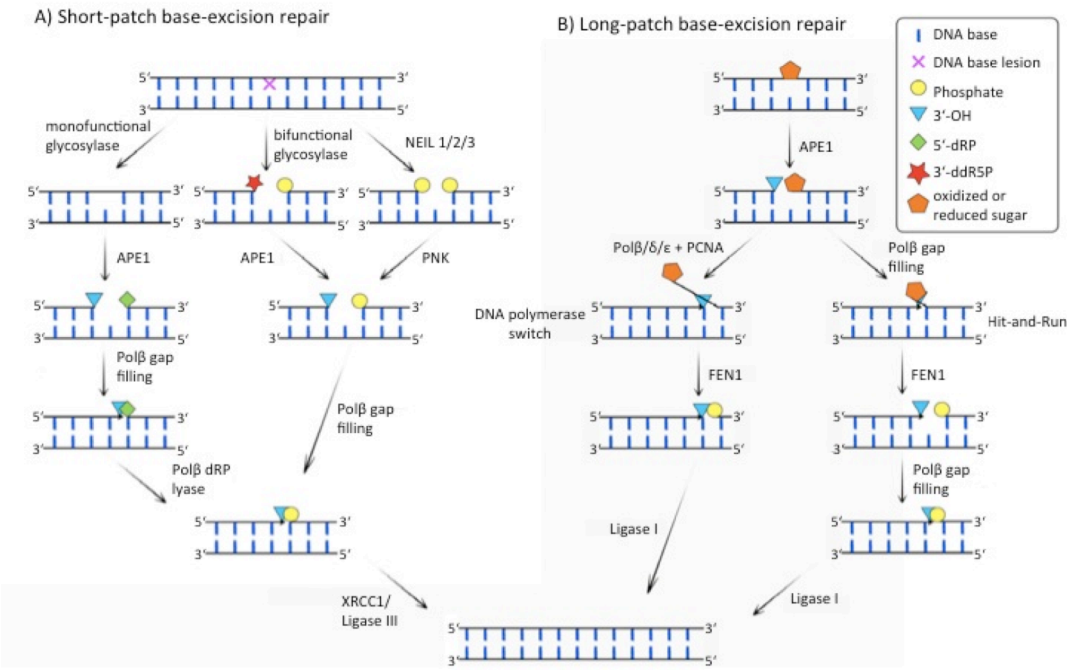

Figure 4. Repair of a damaged DNA base via SP-BER (A) and LP-BER (B).
(A) on the left, a monofunctional glycosylase removes DNA lesion and generates an AP site, processed by APE1, which leaves behind a 1nt-gap with a free 3'OH end and a 5'dRP terminus. In the middle, the BER pathway initiated by a bifunctional glycosylase with β lyase activity is depicted. The glycosylase reaction results in a 3'ddR5P end, which is processed by APE1. On the right, a NEIL family glycosylase upon removal of base lesion with β/δ lyase activity creates a 1nt-gap with 3'P and 5'P ends; the 3'P is removed by PNK. Resulting 1nt-gap is filled by Pol β and the nick sealed by XRCC1/DNA ligase III. (B) The LP-BER pathways are shown: the strand-displacement synthesis on the left and the hit-and-run model on the right. For more details see text. (From Matthias Bosshard, Enni Markkanen, and Barbara van Loon. (2012) Base excision repair in physiology and pathology of the nervous system. *International Journal of Molecular Sciences)*

NEIL1 belongs to the DNA glycosylases of the endonuclease VIII like (Nei)-proteins (NEIL) and has been shown to remove 8-oxo-G from the genome when paired to G, A or C [24]. Its main targets in a physiological environment are 4,6-diamino-5- formamidopyrimidine (FapyA) and 2,6-diamino-4-hydroxy-5-formamidopyrimidine (FapyG) [25], and it even works on bubble structures [26]. In contrast to monofunctional and bifunctional glycosylases, NEIL glycosylases are capable of β/δ elimination leaving behind 3'- and 5'-phosphate residues, after lesion removal and cleavage of the sugar backbone. The 3'-phosphate is then processed by polynucleotide kinase (PNK) to obtain a 3'OH end so that BER can be continued by Pol β

[27-30]. After Pol β mediated DNA synthesis, X-ray repair cross-complementing 1 protein (XRCC1)/DNA ligase III complex seals the resulting nick and completes SP-BER (Figure 4A).
If the 5′ terminus of the 1nt-gap cannot be processed by Pol β dRP lyase activity, LP-BER sub-pathway will take place (Figure 4B). This sub-pathway can occur through strand displacement synthesis or via the hit-and-run mechanism. It has been suggested that strand displacement synthesis is mediated by Pol β, which inserts the first nt, followed by strand a invasion step catalyzed by Pol δ or ε. The generated 5′flap is removed by flap endonuclease 1 (FEN1). The hit-and-run mechanism occurs through alternating insertion of 1nt by Pol β and flap removal by FEN1. Independently of the mechanism, LP-BER is completed through ligation of the sugar backbone by DNA ligase I [31]. Various additional proteins have been associated with LP-BER, such as replication factor C (RF-C), proliferating cell nuclear antigen (PCNA) and replication protein A (RP-A).
Previous work showed that BER still takes place even when Pol β was knocked-down [32,33]. Since Pols β and λ share many structural similarities and belong to the same Pol family, investigations into the relevance of Pol λ in this repair pathway have been made. It was indeed shown that Pol λ participates in BER [34].

2.1.1.2 BER of 8-oxo-G

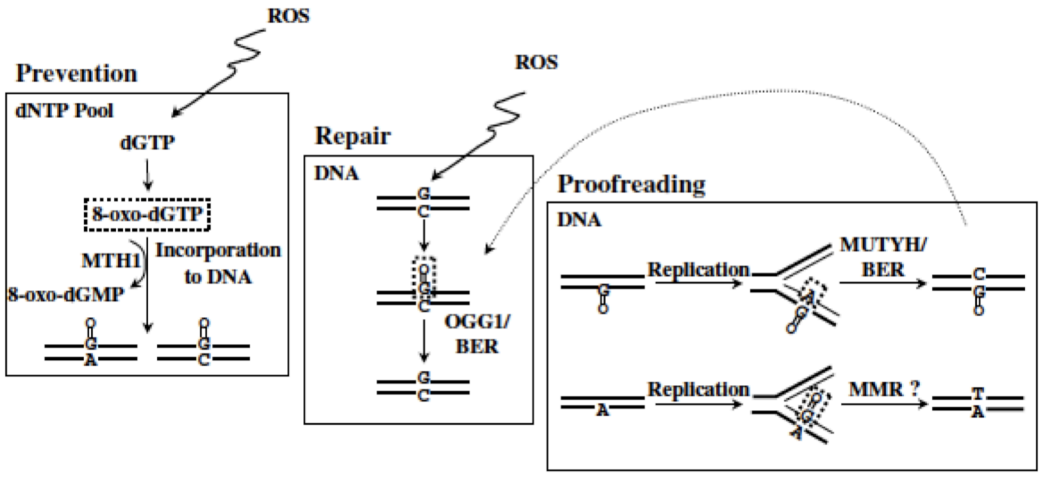

Figure 5. The major protective mechanisms against the oxidative DNA lesion 8-oxo-G. Prevention, involving MTH1-catalyzed hydrolysis of 8-oxo-dGTP, to prevent its incorporation into DNA by Pols during DNA synthesis. Repair, involving OGG1-initiated BER, to repair the C:8-oxo-G base pair to the original C:G base pair. Proofreading operates on the A:8-oxo-G mispair. When A is in the newly synthesized DNA strand, it is eliminated by MutYH DNA glycosylase, thereby enabling the formation of a C:8-oxo-G base pair that can be repaired by OGG1-initiated BER. When A is in the template strand, the newly incorporated 8-oxo-G might be removed through mismatch repair (MMR). (From Tamar Paz-Elizur, Ziv Sevilya, Yael Leitner-Dagan, Dalia Elinger, Laila C. Roisman, Zvi Livneh. (2008). *Cancer Letters*)

Three different enzymes are associated with the 8-oxo-G metabolism (Figure 5). The 8-oxo-G damage, created by oxidation of guanine (G) paired with cytosine (C), is recognized and removed by the bifunctional 8-oxo-guanine glycosylase 1 (OGG1) [35]. The native G:C base pair is restored by subsequent SP-BER. If 8-oxo-G becomes a substrate for replicative Pols before OGG1 repair takes place, dATP will be misincorporated opposite 8-oxo-G. The A:8-oxo-G mispair is recognized by the monofunctional MutY homolog (MutYH) DNA glycosylase [36], which cuts out the adenosine (A) to prevent generation of G:C→T:A transversion mutations

in the next round of DNA replication [37]. After MutYH and APE1 generated a 1nt-gap, Pol λ with the associated dRP lyase activity removes the 5'dRp moiety and, in the presence of co-factors PCNA and RP-A, places a correct dCTP opposite 8-oxo-G with extension of an additional 1nt [38,39]. FEN1 and DNA ligase I finalize the repair pathway [39]. It was indeed shown that while the repair of C:8-oxo-G by OGG1 is generally followed by SP-BER, the MutYH initiated repair of A:8-oxo-G mispairs is mediated by LP-BER pathway [21,31]. Further, exposure of cells to oxidative stress, results in increases levels of MutYH and Pol λ and their gathering at the site of DNA damage [39].

Besides in the DNA, oxidation can also lead to damages in the nucleotide pool and generate 8-oxo-dGTP. If 8-oxo-dGTP becomes a substrate of Pol, it will be incorporated in the DNA opposite an A, since 8-oxo-G in syn conformation mimics T. The human MutT homolog (MTH1) is an 8-oxo-dGTPase that hydrolyzes 8-oxo-dGTP so that this damaged nucleotide cannot be incorporated into the DNA. If preserved, the misincorporation of 8-oxo-dGTP would misguide MutYH to remove the assumed mispaired A from the parental strand and thereby produce T:A→G:C transversion mutations [40].

The OGG1 and MutYH repair machineries scan the DNA explicitly for 8-oxo-G lesions and do so against a high background of undamaged bases. Oxidative stress leads to higher levels of repair proteins to combat the damage. Alterations in levels of BER components could also be targeted to increase sensitivity of cancer cells for therapy [41]. Indeed changes in the three proteins involved to combat 8-oxo-G damage were associated with diseases such as cancer, neurodegeneration or premature aging. One such example is a recent study showing increased levels of 8-oxo-G in thyroid adenoma and carcinoma, together with a decrease in gene expression of BER proteins in carcinoma and an increase in adenoma [42].

2.1.2 DNA glycosylases

2.1.2.1 DNA glycosylases through families

DNA glycosylases remove faulty bases by cleaving the N-glycosylic bond between the base and the sugar, thereby creating an AP-site [43]. They are specific for different base lesions and show either monofunctional or bifunctional activity, as mentioned above. DNA glycosylases can be further grouped into four superfamilies with distinguishing structural characteristics (Table 2): uracil DNA glycosylases (UDGs), helix-hairpin-helix (HhH) glycosylases, 3-methyl-purine glycosylase (MPG, also known as AAG) and NEIL glycosylases [22]. All of them exert their repair function by a flip out mechanism through which the specific base is isolated from the DNA helix and placed into a selective active site pocket [44]. The different glycosylases then use either an internal Lys or Pro as the active site nucleophile for the removal of the corresponding base [25]. Even though structurally different, many glycosylases have overlapping substrate specificity and therefore complement an efficiently connected BER system [45,46].

The glycosylases that engage in oxidative DNA damage are endonuclease III-like protein 1 (NTH1), NEIL1, OGG1, MutYH and single-stranded selective monofunctional uracil DNA glycosylase 1 (SMUG1) [40]. With respect to 8-oxo-G lesions, OGG1, MutYH and NEIL1 are the most relevant. Nonetheless, all the named glycosylases act together and maximize repair efficiency in the cell [47]. Deficiencies in DNA glycosylases lead to the accumulation of base alterations and finally manifest in the development of diseases [48]. Gene expression, posttranslational modifications, subcellular localization and recruitment of DNA glycosylases to damaged DNA all influence cellular damage recognition and removal capacity [49].

Table 2. Mammalian DNA glycosylases, their substrates, modes of action, and mutant phenotypes.
(From Angelika L. Jakobs, Primo Schär. (2012) DNA glycosylases: in DNA repair and beyond. *Chromosoma*)

Type of base lesion		Name	Physiological substrates	Mono (M)/ bi(B) functional	Mouse knockout (ko)/ knockdown (kd) phenotype
Uracil in ssDNA dsDNA	UNG	Uracil-N glycosylase	U, 5-FU, ss and dsDNA	M	ko: viable, B-cell lymphomas, disturbed antibody diversification
	SMUG1	Single-strand-specific monofunctional uracil DNA glycosylase 1	U, 5–hmU, 5-FU, ss and dsDNA	M	kd: moderate increase in mutation frequency (C→T)
Pyrimidine derivates in mismatches	MBD4	Methyl-binding domain glycosylase 4	T, U, 5-FU, εC, opposite G, dsDNA	M	ko: viable, elevated mutation frequency (C→T)
	TDG	Thymine DNA glycosylase	T, U, 5-FU, εC, 5-hmU, 5-fC, 5-caC; opposite G, dsDNA	M	ko: embryonic lethal, aberrant DNA methylation and imbalanced chromatin marks in CpG-rich promoters
Oxidative base damage	OGG1	8-OxoG DNA glycosylase 1	8–oxoG, FaPy, opposite C, dsDNA	B	ko: viable, accumulation of 8-oxoG, elevated mutation frequency (G→T)
	MYH	MutY homolog DNA glycosylase	A opposite 8–oxoG, C or G, 2–hA opposite G, dsDNA	M	ko: viable, see OGG1
Alkylated purines	MPG	Methylpurine glycosylase	3–meA, 7-meG, 3-meG, hypoxanthine, εA, ss and dsDNA	M	ko: viable, elevated levels of ethenoA and hypoxanthine
Oxidized, ring-fragmented or –saturated pyrimidines	NTHL1	Endonuclease III-like 1	Tg, FaPyG, 5-hC, 5-hU, dsDNA	B	ko: viable
	NEIL1	Endonuclease VIII-like glycosylase 1	Tg, FaPyG, FaPyA, 8-oxoG, 5–hU, 5–hC, ss and dsDNA	B	ko: metabolic syndrome, increased damage levels in mitochondrial DNA kd: hypersensitive to γ radiation
	NEIL2	Endonuclease VIII-like glycosylase 2	As NTHL1 and NEIL1	B	Unknown
	NEIL3	Endonuclease VIII-like glycosylase 3	FaPyG, FaPyA, prefers ssDNA	B	ko: normal

U, uracil; , *A*, adenine; , *T*, thymine; , *C*, cytosine, *G*, guanine; , *ss* single stranded; , *ds*, double stranded; , *5–hm*, 5–hydroxymethyl; , *5-FU*, 5 fluorouracil; , *ε*, etheno; , *5-fC*, 5-formylcytosine; , *5-caC*, 5-carboxylcytosine; , *8–oxoG*, 8–oxo-7,8-dihydroguanine; , *Tg*, thymine glycol; , *FaPy* 2,6-diamino-4-hydroxy-5-*N*-methylformamidopyrimidine; , *me*, methyl; , *h*, hydroxyl

2.1.2.2 MutY glycosylase homolog

MutYH is the human homolog to the *E. coli* MutY glycosylase. In humans, it is encoded on chromosome 1 [50]. Numerous different isoforms have been identified so far: some of which are directed to the mitochondria via an N-terminal domain and others that localize in the nucleus through their C-terminal nuclear localization sequence [51,52]. Isoform 2 consists of 535 amino acids (Figure 6). MutYH carries the characteristic HhH motif important for the recognition of A:8-oxo-G mispairs as well as subsequent removal of the undamaged A. Besides A:8-oxo-G, human MutYH recognizes other mispairs such as A:G or 2-OH-A:G and reliably removes the A or 2-OH-A respectively [53] (Table 2). MutYH from other species shows additional substrate specificities. Besides the HhH motif, the iron-sulphur cluster (4Fe-4S) in the catalytic core supports binding and repairing of the DNA [54]. An unique carboxy-terminal domain and a pseudo-HhH moderate substrate specificity by recognizing 8-oxo-G [50,55,56]. Highly-structured domains are also important for binding to APE1, RP-A and PCNA. As MutYH exerts its activity on newly replicated DNA, association with those proteins at the DNA increases the glycosylase's affinity and activity for A:8-oxo-G mispairs [57,58]. Besides the interaction with other proteins, posttranlational modifications influence MutYH activity. Phosphorylation of MutYH for example increases its cleavage activity [59]. Further, MutYH levels increase during S-phase and mitosis, which at least partially correlates with its established role in A:8-oxo-G repair [60].

Impairment of MutYH function has been associated with several diseases. Even though the alterations in activity are often quite modest, sensitivity to oxidative stress is increased in a way that genetic mutations accumulate and finally result in pathological changes [61]. Certain MutYH variants exhibit hampered binding and cleavage activity, while other have decreased stability compared to wild-type (WT) protein, resulting in reduced protein levels [62]. The most widespread and well-studied disease associated with MutYH deficiency is MutYH-associated adeomatous polyposis (MAP), a pre-stage of colorectal cancer [63]. Germ-line mutations cause variant proteins to evolve, which may account for a variety of hereditary cancers [64]. In MAP, it is often the adenomatous polyposis coli (APC) tumor suppressor gene, which is mutated secondarily because of insufficient MutYH activity [65,66]. This is in contrast to familial adenomatous polyposis (FAP), where the APC gene is primarily mutated [67]. Genetic and environmental factors as well as tissue-specific expression, alternative DNA repair pathways, inflammatory response and the immune system influence the development of cancer [68,69]. This is also true for MAP, where phenotype, cancer risk and survival vary according to the genetic background and extent of inflicted oxidative DNA damage [70,71]. Besides the colon, researchers suspect cancers of other organs to be associated with MutYH polymorphisms. This applies to gastric [72] and endometrial [73] cancers while others such as childhood acute lymphoblastic leukemia [74] or squamous oral carcinoma [75] showed no correlation. Former studies propose that MutYH also induces apoptosis when oxidative damage exceeds a certain threshold [76]. Knock-down of both MutYH and OGG1 leads to the accumulation of 8-oxo-G [77] and predisposition to lung and ovarian tumors as well as lymphomas [78].

Overall, it is elevated oxidative stress in certain tissues that pushes cells with deficient MutYH towards cancer or, supposedly, neurodegeneration. Fast replicating tissues, as the intestines, are characterized with high oxygen consumption due to their active metabolism. Similarly, neuronal metabolism is very active with enhanced oxygen usage [79]. Tissues requiring large amounts of oxygen are in particular sensitive to MutYH status. Therefore, it is possible to reason that MutYH also participates in repair of nuclear and mitochondrial DNA in the brain, where specific isoforms of the protein exist [80]. While MutYH largely appears together with PCNA during brain development and neurogenesis, some isoforms dominate later during development [77,81]. This suggests that MutYH mediates nuclear DNA damage repair in replicating neurons and is later on shifted to mitochondria in adult permanent brain cells [81]. Mitochondria are abundant in neurons (in the cell body as well as in synapses [82]) because of their high metabolism that asks for an efficient system to repair oxidatively damaged DNA [83].

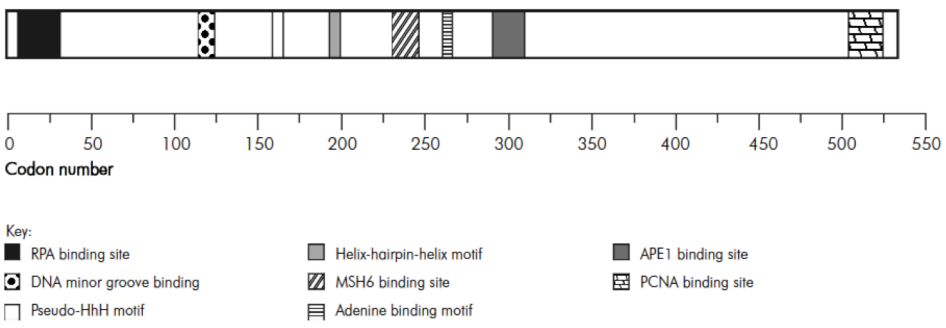

Figure 6. Functional domains of MutYH.
(From Carla Kairupan, Rodney J. Scott. (2007) Base excision repair and the role of MutYH. *Hereditary Cancer in Clinical Practice*)

Deficiencies in the MutYH mediated DNA repair pathway could have severe consequences on brain homeostasis. Hypoxia drastically increases oxidative damage and accordingly, it was shown that MutYH levels rise after stroke [84]. In case of mitochondrial dysfunctions in Parkinson's disease, elevations in the levels of MTH1, OGG1 and MutYH were detected [85,86]. As increased oxidative stress is thought to be one of the main issues in Parkinson's disease [87], the repair proteins cannot deal with the total amount of DNA damage, leading to neuronal death [88]. The importance of functional MutYH initiated DNA repair in the nervous system is also demonstrated through altered MutYH levels observed in retinal degeneration of rodents or Equine Cerebellar Abiotrophy in Arabian horses. The former is attributed to an age-dependent decrease of MutYH expression among other repair proteins [89], while the latter correlates with a single-nucleotide polymorphism in the MutYH gene [90]. Together these findings clearly demonstrate the crucial role of MutYH in the maintenance of normal brain function.

2.1.3 DNA polymerases

2.1.3.1 Eukaryotic DNA polymerase families

A set of Pols synthesizes DNA during cellular processes such as replication, repair, recombination, translesion synthesis and immunoglobulin recombination. The eukaryotic Pols are grouped into four families. The members of family A (γ, ν, θ) and B (α, δ, ε, ζ) are mainly involved in replication and translesion synthesis (TLS); replicative Pols are underlined. Some of them have a 3'→5' exonuclease proofreading activity. Family Y Pols (η, ι, κ, Rev1) can bypass various lesions that would otherwise lead to replication fork stalling. The Pols of family X (β, λ, μ, TdT) are engaged in different DNA repair steps [91].
The overall architecture of Pols is conserved in all species and kingdoms from prokaryotes to eukaryotes. The catalytic core resembles a right hand with palm, finger and thumb domains. The palm carries the catalytic activity with the phosphoryl transfer function. It attaches a dNMP to the 3'OH group of the DNA primer and discharges a pyrophosphate. The fingers associate with incoming nucleotides and singe-stranded DNA while the thumb binds to the double-stranded (ds) DNA. Fingers and thumb are not conserved to the same extent as the palm and, besides other differences, account for the specific functions of Pols.
Defects in Pols relate to a wide spectrum of diseases, for example cancer and hypersensitivity to oxidative DNA damaging agents [92]. This not only holds true for mutations impairing Pol activity, but also for augmented levels or hyperactivity of these proteins. For instance, Y- and X-family Pols are regarded as error-prone when compared to replicative Pols. If their activity is increased, they work to a higher extent on the DNA and thus can induce mutations. This feature of cancer cells is called mutator phenotype. More serious outcome arises when DNA replication stress occurs, resulting among others in DNA ds breaks (DSBs) and chromosome instability [93,94]. Alterations in Pols can therefore not only contribute to cancer by induction of mutations, but also affect propagation of clones in cancer development. At the same time, response to chemotherapy or radiation as treatment options can be decreased if cancer cells have up-regulated TLS Pols [94]. After treatment, instead of damaging the DNA to a point where the cell enters apoptosis, Pols efficiently bypass harmful lesions and survival is possible [93,95]. The study of Pols and their properties is an interesting and continuously evolving field that enables gain of insights into the molecular processes during pathogenesis as well as possible treatment protocols.

2.1.3.2 Structure of DNA polymerase λ

The X-family Pols are involved in BER where they fill small DNA gaps. Pol λ is the most widespread X-family Pol among different species and thus is potentially the ancestor of all X-family members [96]. Pols λ and β share approximately 32% homology [97]. In humans, Pol λ is encoded on chromosome 10 [98] and has a predicted size of 63kDa. Highest Pol λ expression levels are detected in highly proliferative germline tissues, especially in testis. It is therefore suggested that Pol λ potentially plays a role in meiosis. In addition, it is also transcribed in the brain, which indicates a role not only in germline but also in somatic cells [99,100].
Pol λ (Figure 7) contains two non-enzymatic domains at its N-terminus: the breast cancer susceptibility gene 1 C-terminal (BRCT) domain and a proline-rich domain. These two domains account for the preference to fill the short DNA gaps, in which efficiency and fidelity of Pol λ are the highest. While the BRCT-domain mediates protein-protein and protein-DNA interactions [101], the proline-rich domain increases the fidelity of Pol λ up to a 100-fold [102]. In general, Pol λ works better on damaged than on undamaged DNA and does so, in the case of 8-oxo-G damage, with a higher fidelity than Pol β [103]. It is also up to 20-fold more efficient on AP sites, with a greater affinity for dNTPs, than Pol β [104].

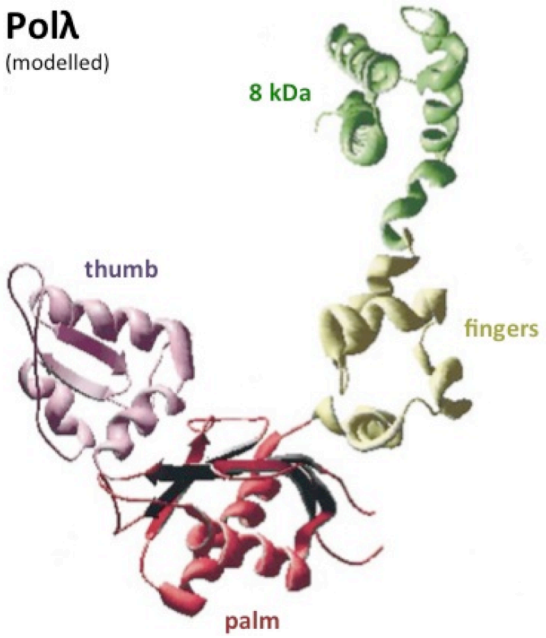

Figure 7. Structure of human DNA polymerase λ core.
8kDa domain (green), endowed with a dRPase activity and providing additional DNA binding capacity; fingers, providing contacts to handle the DNA primer strand through its Helix-hairpin-Helix motif; palm, constituting an appropriate surface to accommodate the substrate molecules (nucleotides and DNA) and to present the pair of metal ions adequately for catalysis; thumb, providing template selectivity and reaction cycling via conformational changes. (From Miguel Garcia-Diaz, Orlando Dominguez, Luis A. Lopez-Fernandez, Lain Teresa de Lera, Maria L. Saniger, Jose F. Ruiz, Maro Parraga, Maria J. Garcia-Ortiz, Tomas Kirchhoff, Jesus del Mazo, Antonio Bernad, and Luis Blanco. (2000) DNA Polymerase lambda (Pol λ), a Novel Eukaryotic DNA Polymerase with a Potential Role in Meiosis. *Journal of Molecular Biology*)

2.1.3.3 Functions of DNA polymerase λ

Previously, it was shown that Pol λ engages in different DNA repair pathways, from BER, to AP site TLS, oxidative DNA damage bypass and non-homologous end joining (NHEJ) of DSBs [105-108]. For BER, the 8kDa lyase domain is crucial in the step of the AP site processing to remove the 5'dRP moiety [97]. The HhH motif is another key structure. It allows binding to both ends of the gapped DNA, and serves as a stabilizer to assure correct assembly of the free DNA ends [109]. The processivity of Pol λ is enhanced when the 5'end of the gap carries a phosphate group [110]. However, as other family X members, it does not possess exonuclease activity, cannot proofread and is thus not considered to be highly accurate. Functionally, Pol λ forms a complex with MutYH glycosylase at the position of A:8-oxo-G mispair and participates in BER [39,111]. When MutYH removes the misincorporated A, a correct C has to be incorporated. Two auxiliary proteins, PCNA and RP-A, promote repair synthesis mediated by Pol λ and at the same time inhibit recruitment of Pol β, a main BER Pol, to the 1nt-gap opposite 8-oxo-G (Figure 8). Under these conditions, Pol λ incorporates dCTP 1200-fold better than dATP, rendering it the main Pol involved with A:8-oxo-G repair [38,112].

Even though Pol λ inserts correct nucleotides opposite 8-oxo-G lesions with a high fidelity, it has an inclination for frameshift deletions. This happens because the Pol performs strand slippage and thereby causes -1 base deletions. Previous studies suggest that the frameshift either happens due to misalignment of the active site or when the primer relocates after misincorporation of a nucleotide [113-115]. Maybe this attribute of Pol λ is connected to its role in NHEJ and V(D)J recombination in the production of immunoglobulins [116]. When summarizing the properties of Pol λ, it is possible to conclude that this Pol is an enzyme efficient in short gap-filling synthesis with very little strand displacement, however it is prone to frameshift generation.

Besides direct protein-protein interactions, posttranslational modifications of Pol λ tune its activity in the cell. Phosphorylation of Pol λ by Cdk2/cyclin A on Thr553 stabilizes the protein and gathers it in the nucleus so that it can act in late S and G2 phases of the cell cycle [117]. As a result, Pol λ accumulates in the period when DNA is replicated and acts on A:8-oxo-G mipairs generated by replicative Pols. When phosphorylated, Pol λ has a higher affinity for MutYH and is more efficiently recruited to the chromatin [118]. Interestingly, the polymerase activity is not affected by phosphorylation [119]. On the other side, Pol λ tightly associates with PCNA during S phase when it is hypophosphorylated [119]. This interaction enhances the assembly and activation of the necessary proteins at the DNA damage sites [38,117,119,120]. Levels of Pol λ not only increase after replication but also when cells are challenged by ROS [121]. Indeed it was shown that when phosphorylated, Pol λ is protected from ubiquitination and subsequent degradation [119]. The main E3 ubiquitin ligase responsible for ubiquitinating Pol λ is Mule (for more details see subchapter 2.2.3.). Taken together these findings highlight the involvement of Pol λ in the repair of A:8-oxo-G mispairs.

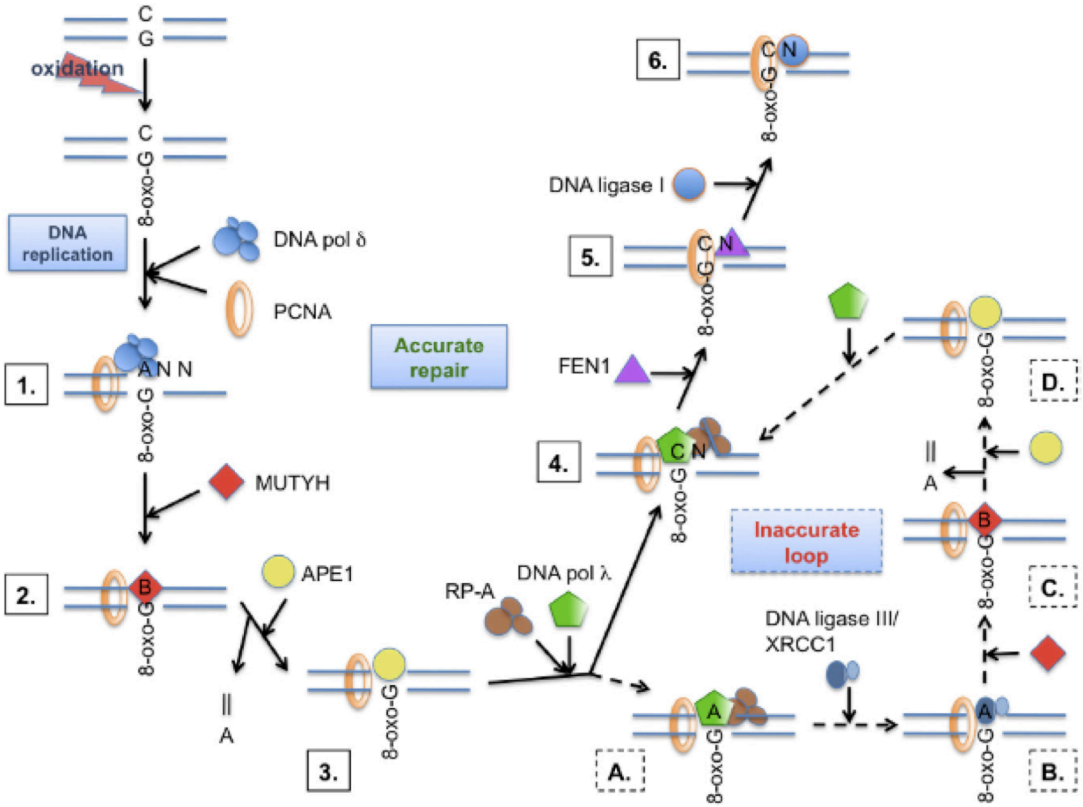

Figure 8. Model for the MutYH initiated LP-BER of 8-oxo-G, after misincorporation by the replication machinery.

1) DNA replication over an 8-oxo-G by Pol δ. 2) recognition of an A:8-oxo-G mispair by MutYH, removal of the A and formation of an AP site (designated also as *B*). 3) recruitment of APE1 mediated by MutYH/PCNA and generation of 5'P, 3'OH gapped intermediate. 4) protection of the 1nt-gap by RP-A and PCNA mediated recruitment of Pol λ, with accurate gap filling (dCTP incorporation). 5) PCNA mediated recruitment of FEN1 and removal of 1nt-flap. 6) ligation of the nick by recruited DNA ligase I and further faithful OGG1 initiated Pol β mediated SP-BER of C:8-oxo-G product. Alternatively an inaccurate loop is initiated: (*A*) Pol λ catalyzes inaccurate gap filling; (*B*) recruitment of DNA ligase III/XRCC1-mediated by PCNA and ligation of the nick; (*C*) recognition of A:8-oxo-G mispair by MutYH, removal of A and generation of AP site (designated as *B*); and (*D*) recruitment of APE1 mediated by MutYH/PCNA, generation of 5'P, 3'OH gapped intermediate. This creates an opportunity for Pol λ to catalyze accurate LP-BER. (From Barbara van Loon, Ulrich Hübscher. (2009) An 8-oxo-guanine repair pathway coordinated by MUTYH glycosylase and DNA polymerase λ. *PNAS*)

2.2 Regulation of BER through ubiquitination

2.2.1 Ubiquitination

Ubiquitination is a type of posttranslational modification that plays an important role in proteasomal degradation as well as non-proteolytic regulation. Four classes of enzymes belong to the ubiquitination machinery: activating E1, conjugating E2, ligating E3 and accessory E4 enzymes. They all participate in the attachment of ubiquitin to target proteins (Figure 9) [122]. Ubiquitin (Ub) itself is a protein that consists of 76 amino acids. Ubiquitination is a sequential process that starts by activation of free Ub and its linkage by C-terminus to E1 through a thio-ester bond in an ATP dependent manner. Ub is subsequently handed over to an E2 protein, which then associates with an E3 ubiquitin ligase. In the final step, Ub is

transferred onto the target protein. The covalent bond is created between the C-terminal Gly of Ub and the ε-amino group of a Lys in the target protein [123]. The E3 family of ubiquitin ligases has many different members that belong either to the homologous to the E6AP carboxyl terminus (HECT), ring between ring fingers (RBR), really interesting new gene (RING) or U-box subfamilies [124]. The diversity of ubiquitin ligases contributes to the substrate specificity [125,126].

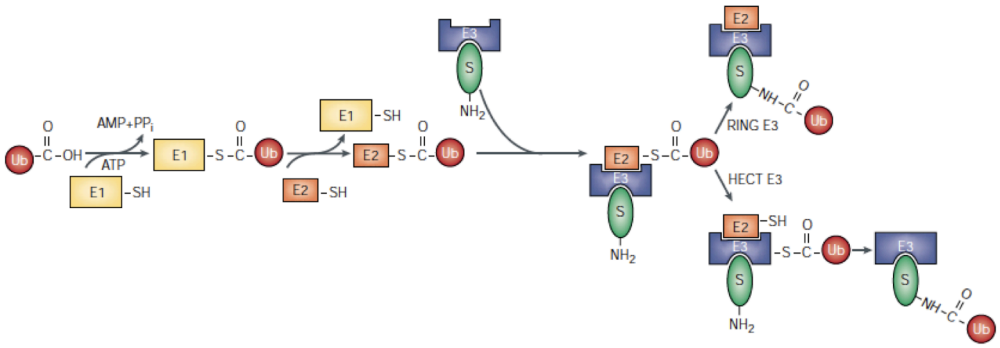

Figure 9. The ubiquitination pathway.
See text for more details. (From Alan M. Weissman. (2001) Themes and variations on ubiquitylation. *Nature Reviews)*

Various proteins contain ubiquitin binding domains (UBDs) and specifically recognize certain types of Ub chains. The structure of ubiquitin chains, defined by the linkage and distribution of Ub units, dictates the selection of binding partners [127]. In case of monoubiquitination, Ub is solitarily attached to a target protein and thereby mediates change in its activity or subcellular localization. Furthermore, there are eight different polyubiquitin chains characterized by the type of isopeptide links (Lys48, Lys63, Lys6, Lys11, Lys27, Lys33, Met1). Most of them are formed between one of the seven conserved Lys and the C-terminus of Ubs. Further, linear polyubiquitin chains exist, consisting of Ubs linked through their N-termini (Met1).

The type of linkage between the Ubs as well as between the Ub chain and the target determines the fate of the protein. The polymers can be homotypic or heterotypic, with either single or mixed linkage types. Also the length of the chains influence the signal character [128] and a minimum of four ubiquitins appear to be necessary for proteasomal targeting [129]. Most known are Lys48- and Lys63-linked polyubiquitin chains, the former directing proteins to proteasomal degradation whereas the latter mainly recruits binding partners in cell-signaling [130]. The other polyubiquitin chains are named atypical but their abundance and significance is being continuously unraveled [131-133]. Ubiquitination is therefore not merely a type of post-translational modification that marks proteins for degradation, but can influence subcellular localization, enzymatic activity and interaction capacity of proteins. It participates in pathways of apoptosis, cell proliferation, differentiation, neuronal activity, cellular trafficking and signaling, DNA repair and many more [134-138].

As ubiquitination plays a role in many cellular processes, it is also regulated by a variety of other proteins. Deubiquitinating enzymes (DUBs) reverse ubiquitination by hydrolysis [139]. Up to date, many different DUBs have been discovered, some of which are characterized by high specificity. Similarly to E3 ligases, DUBs are tightly regulated by other proteins and the picture of the ubiquitin proteasome system (UPS) grows constantly [140]. Furthermore, defects in the ubiquitination pathway are known to cause cancer, neurodegenerative and metabolic disorders [141].

2.2.2 Mule - E3 ubiquitin ligase

Mcl1 ubiquitin ligase E3 (Mule; also known as HUWE1, ARF-BP1, Lasu1, Ureb, HectH9, and E3 histone) is a 482 kDa protein encoded on the X-chromosome. It is expressed in most tissues and locates to the cytoplasm with the exception of testis and brain, where it is largely found in the nucleus [142]. Mule belongs to the HECT family of E3 Ub ligases, characterized by the common C-terminal HECT domain. The HECT domain was first characterized in human papilloma virus (HPV) E6-associated protein (E6-AP) [143,144]. If E6-AP is mutated, a neurological disorder called Angelman syndrome arises [145,146].
The N-terminal region of the HECT domain (N-lobe) is required for interaction with E2 enzymes. The conserved Cys of the C-terminus (C-lobe) binds Ub in thioester complexes, transfers it to a substrate protein and participates in elongation of polyubiuitin chains [147,148]. To complete this action, the flexible hinge loop between N- and C-lobe has to undergo conformational changes and bring the catalytic Cys of HECT close to the active site of E2. The N-terminus outside the HECT domain accounts for substrate specificity.
Many tumor suppressors are substrates of E3 Ub ligases and alterations in their protein levels through E3 enzymes are linked to cancer [149,150]. In line with this observation, Mule was found to be overexpressed in lung, breast and colorectal carcinomas [151,152]. E3 antagonists could consequently serve as targets for therapeutical intervention in specific cancers [153,154]. Conversely, another group found the anti-apoptotic protein myeloid cell leukemia sequence 1 (Mcl-1) to be ubiquitinated by Mule and degraded thereafter [155]. This seems to be a contradiction as Mule cannot be an anti-apoptotic mediator in case of p53-ubiquitination and at the same time promote apoptosis when ubiquitinating Mcl-1. However, the processes are never absolute and maintaining a balance under unstressed conditions is vital, as revealed by the regulatory network around Mule (Figure 10). Its activity is directly influenced by the alternate reading frame (ARF) protein. ARF is induced in the nucleus after DNA damage, binds Mule and thereby stabilizes p53 to arrest cell cycle. Little ARF is present in the cytoplasm so that degradation of Mcl-1 by Mule leads to apoptosis [156]. This demonstrates that Mule is involved in complex pathways to regulate DNA damage and changes in the protein may have intertwined effects.

2.2.3 Mule in BER

Mule interacts with many proteins and participates in the regulation of cell proliferation, apoptosis, DNA damage response and BER [151,155,157]. It has recently been shown that Mule monoubiquitinates Pol β, which is further polyubiquitinated by the E3 ubiquitin ligase carboxyl terminus of Hsc70-interacting protein (CHIP) and sent for proteasomal degradation (Figure 10) [158]. However, when base lesions are introduced in DNA, Pol β needs to accumulate and be active in BER. This is where the ARF protein plays an important role. ARF is a tumor suppressor that, upon occurrence of DNA damage, stabilizes p53 and consequently leads to induction of cell cycle arrest or apoptosis [159]. Mule on the other side leads to the proteasomal degradation of p53 [160], which is why ARF closes the regulation circle by inhibiting Mule upon DNA damage [150,154,161]. By doing so, ARF guarantees that p53 and Pol β are stabilized to intervene in cell cycle and enable DNA damage repair, respectively. Similarly to Pol β, another BER protein, Pol λ, is ubiquitinated by Mule and degraded thereafter [121]. The consequence of Pol λ ubiquitination and degradation is a reduction in correct TLS of 8-oxo-G damage [111,119].

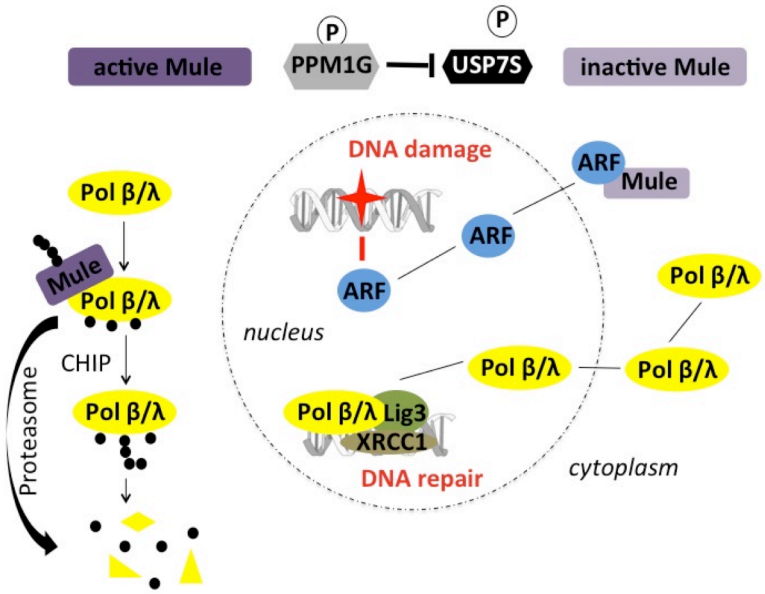

Figure 10. Regulation of BER by Mule and ARF.
If not required for DNA repair, Pol β is ubiquitinated by Mule and further targeted via CHIP mediated polyubiquitylation for subsequent degradation by the proteasome (left side of scheme). However, after detection of DNA damage, ARF accumulates and inhibits the activity of Mule, thus stabilizing Pol β and λ to enable DNA repair (right side of scheme). In parallel, protein phosphatase magnesium dependent 1G (PPM1G) dephosphorylates USP7S, which is then downregulated. The repair of DNA damage will result in a decreased release of ARF with a concomitant increased activity of Mule that will downregulate Pol β and λ levels. A new adjustment cycle will therefore begin on the detection of increased levels of DNA damage. (Modified after Svetlana V. Khoronenkova, Grigory L. Dianov. (2011) Ubiquitin ligase ARF-BP1/Mule modulates base excision repair. *FEBS letters*)

Besides targeting other proteins, Mule has the ability to self-ubiquitinate and thus initiate its own degradation [150]. The extent of Mule ubiquitination is under direct control of deubiquitinating enzyme ubiquitin-specific protease 7S (USP7S, also known as HAUSP). It has recently been shown that USP7S deubiquitinates Mule and thereby allows the E3 ubiquitin ligase to keep the levels of p53 low in unstressed cells [162]. Without this system, p53 would accumulate in intact cells and cause delayed proliferation as well as apoptosis [163]. Besides tumor suppressors and DNA repair proteins, USP7 regulates the activity of other substrates important for the immune system, virus replication and epigenetic control [164] (Figure 11).

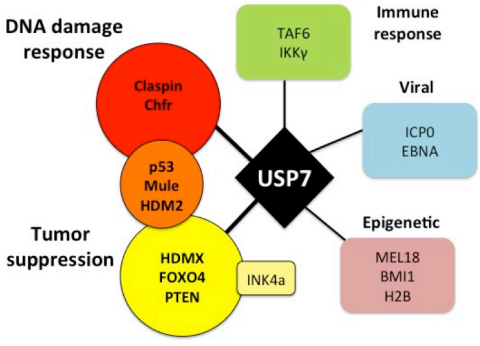

Figure 11. USP7 interacts with multiple substrates.
USP7 substrates are grouped into various functional groups. (Modified after Benjamin Nicholson, K.G. Suresh Kumar. (2011) The Multifaceted Roles of USP7: New Therapeutic Opportunities. *Cell Biochemistry and Biophysics*)

In summary, upon induction of DNA damage, p53 as well as DNA repair proteins need to be activated. The elements of this axis are controlled by common regulatory proteins, which modify the stability or activity of the former by changing their phosphorylation or ubiquitination status (Figure 12) [165]. While accumulation of p53 affects cells through overactivation of cell cycle arrest and apoptosis, abundant Mule was found to be overexpressed in a number of tumors [151,160]. It impedes BER in cancer cells and upregulates tranascription by ubiquitinating Myc and thereby enhancing its activity. Mule thus promotes the proliferation and accumulation of mutations. The inactivation of USP7S upon DNA damage destabilizes Mule and enables the cell to trigger the repair pathways (Figure 12). Overall, regulatory chains are very complex and pose many opportunities for therapeutic interventions as well as causes of disease [140,166].

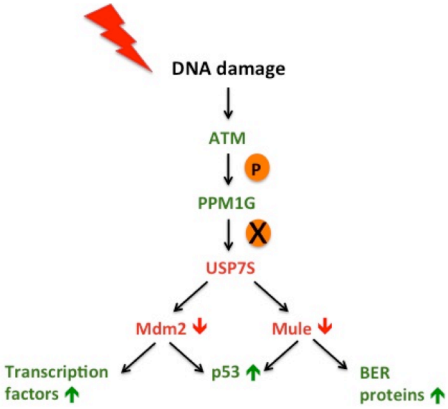

Figure 12. Proposed mechanism for the USP7-dependent regulation of Mule and Mdm2 protein levels after DNA damage.
In response to DNA damage, ATM is activated and stimulates activity of PPM1G. PPM1G dephosphorylates and destabilizes USP7S, which leads to both Mdm2 and Mule self-ubiquitination and degradation, with the consequent stabilization of p53 and other substrates of Mdm2 and Mule. In unstressed cells, the deubiquitination enzyme USP7S is stabilized by phosphorylation, and thus stabilizes both Mdm2 and Mule, which results in proteasomal degradation of p53 and other substrates. (Modified after Svetlana V. Khoronenkova and Grigory L. Dianov. (2012) USP7S-dependent inactivation of Mule regulates DNA damage signalling and repair. *Nucleic Acids Research*)

2.3 Neurodegeneration

The nervous system is a highly specialized organ with numerous terminally differentiated cells. Due to a low proliferation rate, the regeneration capacity of the nervous system is much smaller in comparison to other tissues. For this reason, most of the neurons have to survive as long as their organism. Even small changes in neuronal metabolism, architecture or activity disturb physiological functions and quickly manifest symptomatically.
Neurons build a complex system, however they do not constitute a homogenous cell population. They are involved in myriads of processes and as such differ considerably in morphology and function. As a result, neurons are characterized by individual gene expression patterns and consequently react differently upon exposure to stress or damaging agents. Diseases with particular symptoms emerge depending on the type of repair deficiency, damaging agent and character of the involved neuron. This principle is referred to as selective neuronal vulnerability (SNV) and facilitates the understanding of pathogenesis as

well as symptomatology [167]. Based on studies over the previous years, it has become apparent that neurons, once differentiated, have to suppress cell cycle to survive [168]. If they fail to do so, the result is not cell division and proliferation but apoptosis [169]. Several neurodegenerative disorders have been found to correlate with an elevation in the expression of cell cycle proteins [170]. If neuronal DNA is damaged and reentry into cell cycle takes place, the course of disease instead of repair will be promoted [171]. The integrity of the source of all biological processes, the DNA, therefore has to be closely monitored and damage repaired efficiently. If initiation or activity of any repair pathway is defective, genetic lesions may accumulate and finally lead to cell death [172,173] and neurodegeneration [174]. In proliferating cells, repair pathways are more accessible than in postmitotic cells. While for example accurate homologous recombination (HR) repairs DNA strand breaks during proliferation, the more error-prone NHEJ prevails in mature cells [175]. Thus, some diseases arise as the nervous system is still developing, while others when it has already matured. This potentially explains why many patients with neurodegenerative disorders often do not suffer from cancer, sterility or immune dysfunctions; a set of back-up repair pathways is available in cells with an active cell cycle.

2.3.1 Oxidative DNA damage in the nervous system

The brain is an organ with a very high metabolism and as such consumes 20% of the circulating oxygen in the body [176]. The neuronal cells synthesize many proteins but also need a lot of ATP to maintain intracellular ion homeostasis important for their excitability. The blood-brain barrier effectively shields the brain from exogenous damaging agents so that endogenous side-products represent the most significant source of damage to neurons [177]. Roughly 2% of the absorbed oxygen ends as ROS, the majority of which are generated in mitochondria [5,178]. Unfortunately, ROS in the brain are not neutralized as effectively as in other organs, since concentrations of classical antioxidants in the nervous system are much lower. This might cause a higher rate of oxidative DNA damage in neuronal tissue [179]. Indeed, mitochondrial dysfunction is a strong cause of metabolic diseases in general and neurodegeneration in particular [180,181]. Since the concentration of iron is high in certain brain regions, it further contributes to ROS production through the Fenton reaction [182]. On the other side, ROS are secondary messengers that deliver information and modulate gene expression as well as protein activity [183]. They play an important role in the maintenance of synaptic plasticity, the capacity of synapses to modulate their signaling intensity [184]. The impact of oxidative stress also differs according to the type and the amount of ROS, making it necessary to tightly regulate their production and decomposition. If ROS accumulate, they can lead to pathological changes and induce apoptosis in different ways [185-189]. Interestingly, many genes on the X-chromosome also contribute to synaptic plasticity, which together with oxidaive stress holds interesting implications for neurological diseases [190].
To synthesize anti-oxidant proteins and repair oxidized components, energy in the form of ATP is necessary. If ATP levels in neurons are low, for example due to mitochondrial dysfunctions or modifications at the promoters of genes encoding proteins for energy production, the cells will not be able to compensate for the harmful effects of ROS. Consequently, cells will suffer from oxidative stress with damage to DNA, RNA or lipids. Previous studies have shown that the DNA repair enzymes are up-regulated in vulnerable neurons [191]. If the DNA damage response (DDR) is deficient, a variety of neurodegenerative diseases arise, such as amyotrophic lateral sclerosis, Alzheimer's disease or Parkinson's disease.

Besides ROS and ATP imbalances, Ca^{2+} dysregulation also contributes to degenerative diseases. Ca^{2+} influences numerous cellular processes, such as gene transcription, cell survival, neurotransmitter release and excitability, as well as neurite outgrowth and synaptic plasticity. If the transport of Ca^{2+} or its binding are disturbed, mitochondria can be over-stimulated, resulting in increased generation of ROS. If the mitochondrial membrane is severely damaged, caspase-dependent apoptosis is initiated and the cell dies [192]. Glutamate, an excitatory neurotransmittor, additionally increases intracellular levels of Ca^{2+}. Its influx through glutamate receptor-ion channels is enhanced in aged individuals, as glutamate levels increase. Synapses are thereby destroyed through glutamate excitotoxicity. Taken together, all these different players contribute to oxidative neurodegeneration and finally engage in a vicious circle (Figure 13).

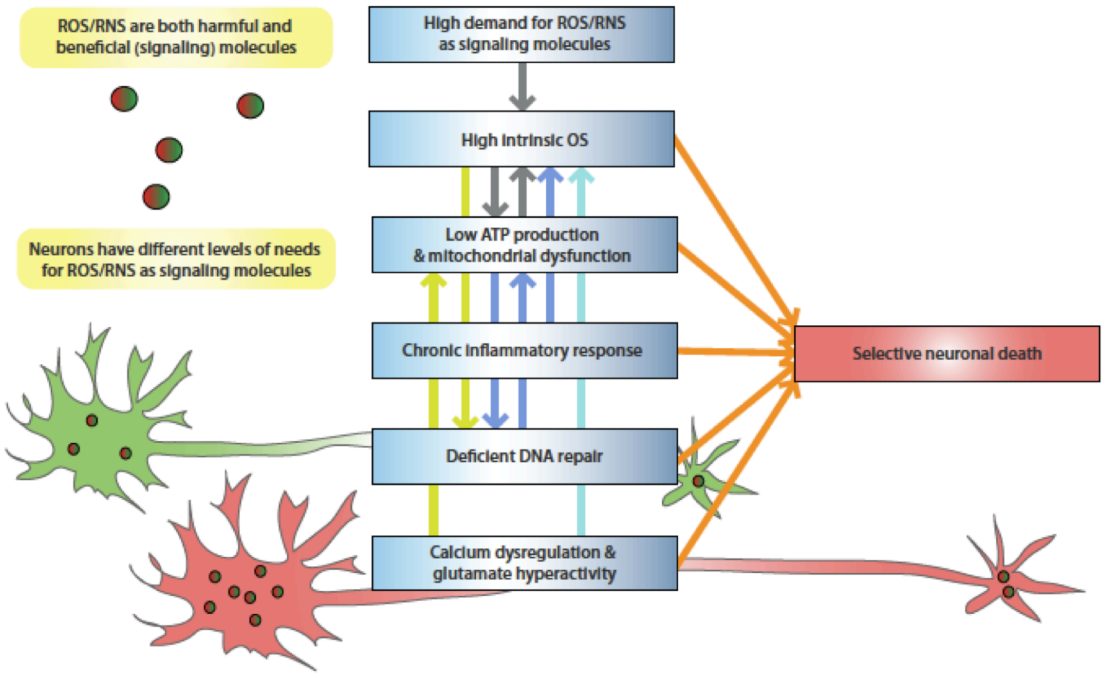

Figure 13. Molecular and cellular factors that contribute to the selective vulnerability of neurons to oxidative stress.
The colored arrows that link the mechanistic factors in the figure denote direct relationships between them. (From Xinkun Wang and Elias K. Michaelis. (2010) Selective neuronal vulnerability to oxidative stress in the brain. *Frontiers in Aging Neuroscience).* OS: oxidative stress.

Vulnerable neurons do not always accumulate all types of DNA damages but they are more prone to axon, dendrite and synaptic pathologies than resistant neurons. Clinical approaches have been developed, trying to reduce oxidative stress by supplementing antioxidants such as vitamin E or metal chelators, thus aiming to support the organism in detoxifying ROS and thereby prohibit its sequelae such as proteasomal malfunction and misfolding, mitochondrial dysfunction, apoptosis and inflammation [193]. Finally the goal would be to target specific diseased regions of the nervous system and thereby provide optimal treatment for individual patients.

2.3.2 Neurodegeneration and BER

Neurons possess high transcriptional activity as they permanently stimulate cells that surround them and are stimulated themselves. This increases the mutagenic potential, as well as the effects of DNA damage, since synthesis of corrupted proteins considerably disturbs cell function and transcription can even be blocked entirely [194]. Flaws of neuronal functions can be measured by several different methods: behavioral experiments, microscopy and immumohistochemistry as well as long-term potentiation (LTP). The LTP designates the quality of synapses to be excited after a series of high-frequency stimulation. In organisms with reduced DNA damage repair, those properties often decay in an age-dependent manner and end in neurodegenerative diseases [195,196].

BER proteins are highly expressed in the brain to prevent oxidative stress. They are present in the nucleus as well as in the mitochondria as both organelles contain DNA and are under constant pressure of ROS. Consistent with this, the brain expresses the BER enzymes relevant for 8-oxo-G metabolism and alterations in several of these proteins are associated with neurodegenerative diseases [197]. Recently, it has been shown that a type of NER, transcription-coupled repair (TCR), is also involved in the repair of oxidative DNA damage in neurons[198]. This is of particular importance since neurons use their genome mainly for transcription of RNA and defects therein will have the greatest impact on the normal function [199]

Table 3. Examples of neurodegenerative diseases associated with deficiencies in DNA repair proteins.
Different defects in DNA repair can lead to a variety of neurodegenerative diseases. (Modified after Matthias Bosshard, Enni Markkanen, and Barbara van Loon. (2012) *International Journal of Molecular Sciences*)

Repair pathway	Disease	Affected proteins
BER and SSBR	X-linked intellectual disability	Mule
	Alzheimer's disease	OGG1, XRCC1, UNG, APE1, Pol β
	Parkinson's disease	OGG1, MutYH, APE1
	Huntington's disease	OGG1, FEN1, Pol δ, Pol ε
	Amyotrophic lateral sclerosis	OGG1
	Ataxia-oculomotor apraxia-1	APTX
	Spinocerebellar ataxia with axonal neuropathy-1	TPD1
MMR	Huntington's disease	HD
NER	Cockaine Syndrome	CSA, CSB, XPG
DSBR	Ataxia telangiectasia	NBS1
	Ataxia telangiectasia-like disorder	
	Nijmegen breakage syndrome	
Mitochondrial	Alzheimer's disease	various
	Parkinson's disease	various
	Amyotrophic lateral sclerosis	ALS2

In aging organisms, the BER proteins often decrease and DNA lesions build up [200]. Previous findings have also shown changes in certain components of the BER pathway in different neurodegenerative diseases (
) [201]. Alzheimer's disease, amyotrophic lateral sclerosis, Huntington's disease and Parkinson's disease are the most known and represented neuronal disorders that, among many other pathological processes, are connected to deficient BER. Besides their role in neurodegeneration, the BER enzymes are also important during reperfusion after ischemic brain damage. In this time period, cells accumulate ROS and need higher repair efficiency accomplished by up-regulated repair proteins [202].
A very recent study gained new insight into association between neurodegeneration and MutYH [203]. As mentioned previously, MutYH can cause apoptosis when cells are under strong oxidative stress. It does so by exerting its glycosylase function and leaving behind AP sites. Due to high amount of damage, they are not further repaired but instead converted into harmful single-strand breaks (SSBs). Poly(ADP-ribose) polymerase 1 (PARP1) binds to the SSBs and thereby increases poly(ADP-ribose) polymer (PAR) formation [204]. This reaction depletes nicotinamide adenine dinucleotide (NAD+) and ATP pools, leading to nuclear translocation of apoptosis-inducing factor (AIF) [205]. Parallel mitochondrial dysfunction activates calpains and initiates the release of cytochrom c, the second pathway of apoptosis. The caspase cascade is activated and triggers the degradation of the cellular organelles [206]. In context with PARP toxicity, intracellular Ca^{2+} levels rise, which is another indication of apoptosis and promotes SNV [207-209].
While MutYH in this pathway prevents cancer by provoking apoptosis in peripheral tissues, it can cause neurodegeneration in the central nervous system as the cells cannot be replaced. A careful balance of this enzyme is required to ensure adequate repair of A:8-oxo-G mispairs but at the same time to prevent SSB after massive oxidative damage and MutYH hyperactivation. However, all the networks and regulation mechanisms are not yet fully understood and need further investigation.

2.3.3 X-linked intellectual disability (XLID)

Intellectual disability (ID) describes a lack of cognitive abilities, low level of intelligence and missing adaptive behavior appropriate for the corresponding age group [210]. It affects 2 to 3% of the Western population with a male overrepresentation of 30% [211]. Patients display limited intellectual functions with lacking conceptual, social and practical skills [212]. Besides genetic causes, prenatal factors such as malnutrition or teratogenic substances can lead to ID. Also perinatal complications and postnatal events such as infections or injuries can damage the brain [213]. Mild cases of ID have an intelligence quotient (IQ) between 50 and 70, while severe forms score below an IQ of 50 [214].
XLID, formerly known as X-linked mental retardation (XLMR), is a form of ID originating from mutations on the X-chromosome. Because males only have one X-chromosome, they are predominantly affected, with an approximate prevalence of 0.1% in the total population [215]. Other factors that affect the disposition for XLID are differences in the expression of X-genes in the brains of males and females or variable protein amounts due to genes that evade X-inactivation [216].
About 40% of the 885 proteins encoded on the X-chromosome are expressed in the brain, and over 150 of those are predicted to be involved in different forms of XLID. In general, many intelligence genes lie on the X and it is therefore disproportionally represented in causes for ID [217-219]. So far, mutations in 82 X-genes have been identified [220]. They encode signaling pathways, transcription factors, arrange cytoskeletal organization, cell adhesion and

migration as well as maintenance of the cell membrane potential (Figure 14) [221]. This makes XLID a very heterogeneous disease. Although clinicians distinguish between non-syndromic (mental disabilities alone) and syndromic (additional disabilities) forms, there is no correlation to the genetic background. Mutations of different genes can evoke similar symptoms. At the same time, different conditions can trace back to the same gene. Diagnosis and identification of candidate genes is hence a very laborious process.

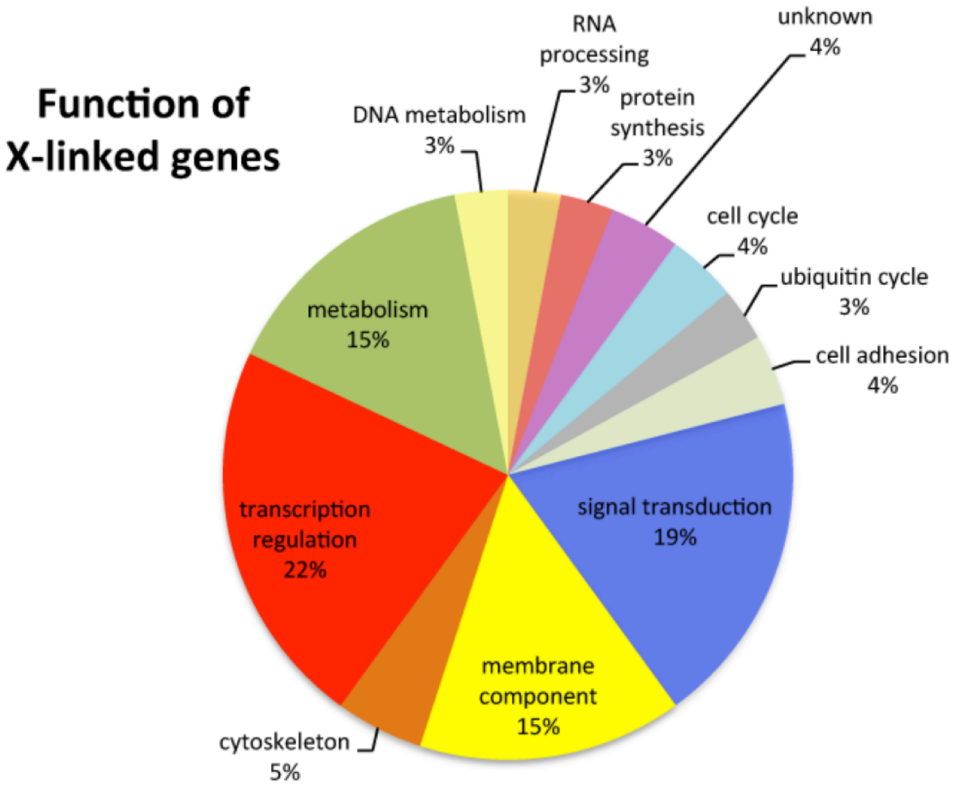

Figure 14. Molecular functions of proteins encoded by 82 known XLID genes, according to the available Gene Ontology annotations (www.geneontology.org).
(Modified after Pietro Chiurazzi, Charles E Schwartz, Jozef Gecz, and Giovanni Neri. (2008) XLMR genes: an update. *European Journal of Human Genetics)*

Examples of distinct XLID forms are the Fragile X mental-retardation syndrome with a cloning of the fragile X-linked mental retardation type 1 (FMR1) gene or the Rett syndrome with a mutation of the methyl-CpG-binding protein 2 (MECP2) [222]. Overall, non-syndromic XLID is the most frequent form [217]. As mentioned above, many of the proteins altered in XLID are involved in neurogenesis and neuronal functions. A change in their amount or structure leads to the malfunctions responsible for the final symptoms: imperfect dendrite development [223], neurite outgrowth [224], deformed actin cytoskeleton, or synaptic transmission and detection problems [225,226].
Neurons generally do not regenerate and they disappear without replacement after apoptosis. To fully grasp the mechanisms of neurodegeneration and subsequent ID, one has to go down to the single cellular processes and study all the players involved. Furthermore, identification of genes causing XLID also leads to a more profound understanding of the complexities in brain development and cognitive function. With new insights, even treatment options may arise [227], a very promising and exciting outlook for neuropathologic diseases.

2.3.3.1 XLID and Mule

Ubiquitination with its various chain linkage types and effector mechanisms is involved in a range of neuronal functions such as synaptogenesis and signal transduction [228]. The development of the brain is a very complex and highly specialized process where each step is crucial for a correct outcome. Also Mule plays important roles in neurogenesis and is expressed in the brain among other tissues [160]. Knock-down of Mule in mice leads to neonatal lethality with severely disturbed brain architecture and differentiation. In malignant brain tumors, Mule can be inactivated and thereby disturb the homeostasis in the neuronal tissue [229,230]. Moreover, dysfunction of the UPS is observed in a number of neurodegenerative diseases. It has been proposed that polyubiquitin chains accumulate and disrupt cell homeostasis in neurons, for example by forming insoluble deposits [231,232]. Alzheimer's, Parkinson's and Huntington's diseases only represent some the most popular neurodegenerative diseases increasingly linked to the UPS [233-236].
Froyen et al. identified changes in the E3 Ub ligase Mule to be associated with XLID. The Mule gene exhibits either point mutations or copy number gains [1,237]. Because Mule participates in many regulatory pathways in the cell, its alteration can have many and potentially intertwined consequences. The main focus of this work is the investigation of the impact of Mule on BER by ubiquitination and proteasomal degradation of Pol λ and possibly MutYH.

2.4 Aim of the thesis

The aim of this thesis was to explore the influences of mutated Mule, identified in patients suffering from XLID, on the repair capacity of oxidative DNA lesions. The focus lays upon determining:

(i) the status of Mule and proteins important to counteract A:8-oxo-G mispairs,
(ii) the subcellular localization of the corresponding repair proteins,
(iii) the ability to efficiently remove A from A:8-oxo-G mispairs,
(iv) the overall cellular capacity to accurately bypass 8-oxo-G damage, and
(v) the possibility to rescue the observed effects upon modulating Mule levels.

3 Material and Methods

3.1 Common buffers and solutions

GENERAL	**Phosphate buffered saline (PBS) 1x** 137mM NaCl 2.7mM KCl 10mM Na_2HPO_4 1.76mM KH_2PO_4 pH 7.4 (adjusted with HCl)	**PBS-T 0.05%** 137mM NaCl 2.7mM KCl 10mM Na_2HPO_4 1.76mM KH_2PO_4 pH 7.4 (adjusted with HCl) 0.05% (v/v) Tween 20	**Tris/Borate/EDTA (TBE) 1x** 90mM Tris 90mM Boric acid 2mM EDTA pH 8.0
	EDTA pH 8.0 0.5M EDTA*H_2O pH adjusted with NaOH	**EGTA pH 8.0** 0.5M EDTA*H_2O pH adjusted with NaOH	**HEPES pH 7.9** 1M Hepes* H_2O pH adjusted with KOH
	DTT 1M 5g DTT 32.1ml H_2O 326µl 1M Na-Acetat pH 5.2 (adjusted with HCl)	**WCE buffer A** 10mM Tris-HCl pH 7.5 1mM EDTA 1mM DTT 0.1mM PMSF 1.5µM Pepstatin 3µM Bestatin 2µM Leupeptin	**WCE buffer B** 10mM Tris-HCl pH 7.5 1mM EDTA 32% Sucrose 1.28M NaCl 1mM DTT 0.1mM PMSF 1.5µM Pepstatin 3µM Bestatin 2µM Leupeptin
	Fractionation buffer A 10mM Hepes pH 7.9 100mM KCl 1.5mM MgCl2 340mM Sucrose 10% Glycerol 0.1% Triton 100X 1mM DTT 1mM PMSF 1.5µM Pepstatin 3µM Bestatin 2µM Leupeptin	**Fractionation buffer B** 3mM EDTA pH 8.0 0.2mM EGTA pH8.0 1mM DTT 1mM PMSF 1.5µM Pepstatin 3µM Bestatin 2µM Leupeptin	

SDS-PAGE AND IMMUNOBLOT	**SDS loading buffer (Laemmli) 10x** 600mM Tris-HCl pH 6.8 20% SDS 20% Glycerol 0.05% Bromphenol blue 20% β-mercaptoethanol	**Odyssey blocking solution** Odyssey blocking buffer (Li-Cor) 1:2 in PBS-T0.05%	
	TG-gel preparation mix - lower buffer (4xB) 1.5M Tris-HCl pH 8.8 0.4% SDS	**TG-gel preparation mix** - upper buffer (4xC) 0.5M Tris-HCl pH 6.8 0.4% SDS Bromphenol blue	**TG-running buffer 5x** 125mM Tris 0.96M Glycine 0.5% SDS
	TG-transfer buffer 10x 250mM Tris 2M Glycine	**TG-transfer buffer 1x** 100ml trans. buffer 10x 200ml methanol 700ml H_2O	
	TA-gel solution 4x 1.5M Tris-Acetate pH 8.1	**TA-running buffer 20x** 1M Tricine 1M Tris 2% SDS	**TA-transfer buffer 1x** 25mM Tris 192mM Glycine 0.1% SDS 10% Methanol

SEQUENCING GELS	**PA-gel solution 20%** 20% Acrylamide 19:1 0.5% TBE	**Annealing buffer 5x** 100mM Tris-HCl pH 7.5 750mM NaCl	**DNA loading buffer 50x (PA-gel)** 20% Glycerol bromphenol blue xylene cyanol blue
	Denaturating sequencing gel, 7M PA-urea, 10% 420g Urea 250ml Acryl-bis 19:1 (40%) 100ml TBE 10x 350ml H_2O	**Stop buffer 2x (sequencing gel)** 96% Formamide 20mM EDTA pH 8.0 bromphenol blue xylene cyanol blue	**PA-urea running buffer** 1x TBE
	Gel-fixing solution 850ml (=20%) EtOH 96% 250ml (=5%) CH_3COOH 2.9l H_2O		
dNTPs & OLIGOs	**dNTPs preparation** stock of 10mM in TE pH 7.5 working prep: 1mM in TE pH 7.5 titrations diluted in H_2O	**Oligonucleotide preparation** stock of 100μM in TE pH 8.0 working prep: 10μM in TE pH 8.0 labeling concentration of 2μM in TE 8	

3.2 Cell-lines and culturing conditions

3.2.1 Material

- four lymphoblastoid cell-lines, grown in Roswell Park Memorial Institute (RPMI) 1640 medium with L-Glutamine, PAA Laboratories GmbH
- 293T HEK cells, grown in DMEM high glucose (4.5g/l) with stable Glutamine, PAA Laboratories GMbH
- fetal calf serum (FCS) 100%, Gibco
- penicillin-strepomycin 10'000 U/ml, Gibco
- DMSO, Sigma-Aldrich
- Tissue culture testplate 6, TPP
- Tissue culture flask 25, TPP

3.2.2 Lymphoblastoid cell-lines

a. Patient cells

One cell-line from the healthy individual (referred to as "wildtype") and three XLID patient lymphoblastoid cell-lines were used in this project. Patient cell-lines, abbreviated as 444, 106, and p83, were a gift from G. Froyen (Human Genome Laboratory, Leuven, Belgium) and L. Raymond (Cambridge Institute for Medical Research, Cambridge, UK), in whose laboratories they had initially been established [1]. The cells were isolated from the patients' blood and immortalized with Epstein Barr virus as described previously [238]. With microarray-comparative genomic hybridization (array-CGH), quantitative polymerase chain reaction (qPCR) and fluorescence *in situ* hybridization (FISH), the genetic background was characterized. The figure below indicates the three XLID-associated mutations in the Mule gene (Figure 15).

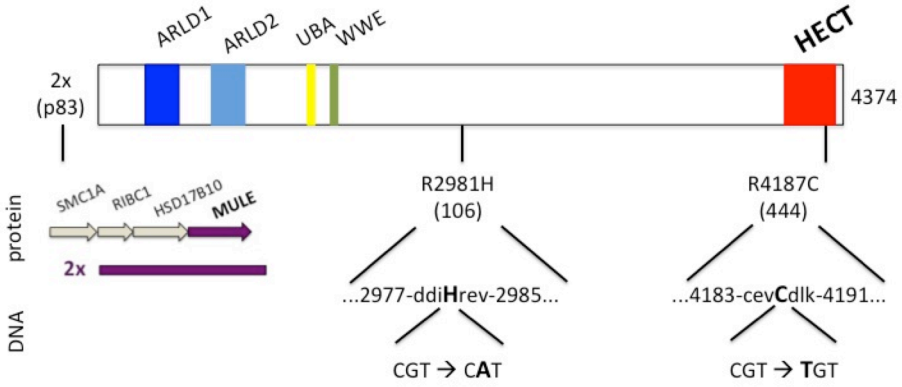

Figure 15. Mutation sites 444, 106 and p83 duplication in Mule.
Identification of mutations on the Mule gene in three XLID patients. The mutated base is indicated in bold, along with the changed codon for the amino acid. (Modified after Svetlana V. Khoronenkova, Grigory L. Dianov. (2011) The emerging role of Mule and ARF in the regulation of base excision repair. *FEBS letters*). Additional data obtained from NCBI gene database and Froyen et al. [1]

Lymphoblastoid cell-line 444 is established from a patient harboring a missense mutation R4187C, positioned within the HECT domain of Mule. The patient is only moderately intellectually disabled, capable to work and care for himself independently, but sometimes has difficulties with articulation and coordination. On the social side, the patient is more introverted and rather timid than average. Several members of his family also carry the mutation.

Cell-line 106, derived from a patient displaying severe symptoms of intellectual disability, has a Mule mutated at the position 2981, where Arg is replaced by His. This patient completely depends on assistance in every day life, lacks speech, has trouble walking as he has flexion deformities of the knees and cannot chew properly. The visceral system is also affected, as he is not toilet trained. The patient has a younger brother that is affected in a similar way. He does not have knee contractures but needs medication for constipation. The uncle (mother's side) of the two boys lives in a mental facility because of comparable symptoms.

P83 cells were obtained from a patient carrying a microduplication at the Xp11.22 locus, which affects the Mule gene. The patient suffers from severe speech delay, decreased tendon reflexes, facial anomalies and social disabilities. His family is affected in a way that several members show mental or locomotor pecularities.

b. Culturing

Cells were grown at 37°C in a 5% CO_2 incubator in RPMI medium supplemented with 15% fetal calf serum (FCS) and 150 U/ml penicillin-streptomycin.
For long-term storage, cells were frozen in FCS with 10% DMSO.

3.2.3 Cell-line HEK 293T

HEK (human embryonic kidney) 293T cells (American Tissue Culture Collection, USA) were grown at 37°C in a 5% CO_2 incubator in DMEM medium supplemented with 10% FCS and 100 U/ml penicillin-streptomycin.

3.3 $CaPO_4$ transduction of lymphoblastoid cell-lines

3.3.1 Material

- HEK 298T cells
- Lymphoblastoid cells (WT, 444, 106, p83)
- DMEM medium with 10% FCS and 100 U/ml penicillin-streptomycin
- RPMI medium with 15% FCS and 100 U/ml penicillin-streptomycin
- Trypan blue, Sigma-Aldrich
- Neubauer counting chamber, Hecht-Assistent
- Plasmid DNA constructs
  - shRNA 1μg/μl: Mule, Scrambled (Open Biosystems)
  - psPAX2 1μg/μl: packing (Open Biosystems)
  - pMD2.G 0.5μg/μl: envelope (Open Biosystems)
  - 2.5M $CaCl_2$
- Hank's Balanced Salt Solution (HBSS) 2x
- Tissue culture dishes 60x16mm, TPP
- Tissue culture testplate 6, TPP
- syringe-filter 0.45μm, TPP
- polybrene (hexadimethrine bromide), Sigma-Aldrich
- puromycin 10μg/ml for selection of transfected lymphoblasts, Gibco

3.3.2 Method

Transduction comprises the introduction of foreign DNA into an eukaryotic cell by using a viral vector. The DNA is randomly integrated into the host genome, where it is transcribed. In our experimental setup, the vector contained information for synthesis of nonspecific short-hairpin RNA (shNs) or shRNA targeting endogenous Mule (shMule) transcript. In addition to shRNA, constructs encoded green-fluorescent protein (GFP), allowing visualization of transduction efficiency and expression level microscopically.
The virus carrying information for synthesis of shNs and shMule RNA was produced in HEK 293T cells, according to following protocol. $2*10^6$ HEK 293T cells were plated in a 6cm dish 24h prior to transfection. The plasmid DNA, prepared as described above, was then pipetted dropwise into bubbling HBSS 2x and incubated for 5min at room-temperature (RT) until a chalky white precipitate formed. The DNA was added to the corresponding 293T HEK dish and mixed by gentle shaking. The cells were incubated for 16h at 37°C in a 5% CO_2 incubator, after which 5ml DMEM medium was exchanged and the cells incubated for another 24h. The virus-containing supernatant was then harvested by filtration through a sterile 0.45μm filter.

Of each lymphoblastoid cell-line, 500'000 cells were counted and plated in a 12-well plate with a final volume of 1ml. The cells were then infected by adding 1ml of respective virus suspension; virus encoding shMule for the knock-down and shNs for the control. To increase the infection-efficiency of lymhoblastoid cells, polybrene was added to the virus-containing supernatant to reach a final concentration of $4\mu g/ml$.
The cells were regularly checked for green fluorescence and the medium exchanged on a two-day basis. After four days, the cells were put under selection with $1\mu g/ml$ puromycin. After ten days the cells were further propagated by transferring to a 6-well plate, and finally flasks six days later.

3.4 Whole-cell extract preparation from lymphoblastoid cell-lines

3.4.1 Material

- PBS 1x
- WCE buffer A and B
- Centrifuge 5417R, Eppendorf
- Rotanta 460 and Rotanta 420R, Hettich
- Tissue grind pestle SC 2ml, Kontes Gerresheimer
- Diagenode Bioruptor Standard sonicator (UCD-200 TM) with Digital 1/Neslab RTE7 Thermo Scientific cooler
- Bio-rad Protein assay, Dye reagent concentrate, Bio-Rad
- Genesys 10 UV Scanning, Thermo Scientific

3.4.2 Harvesting cell pellets

The cells were grown to confluency in the flasks, resuspended and transferred into a 15ml-falcon tube. Cells were pelleted by centrifugation 5min, at RT, 250 rcf; supernatant was removed and cells washed with 5ml cold PBS. From this point, all subsequent steps were performed on ice. Cells were pelleted for a second time, by centrifugation for 10min at 4°C and 250 rcf. The supernatant was removed and the pellet resuspended in 1ml cold PBS. The cells were then transferred into 1.5ml Eppendorf tubes and spun down one last time for 10min at 4°C and 250 rcf. Supernatant was removed and the pellet snap-frozen in liquid nitrogen. Samples were stored at -80°C until use.

3.4.3 Whole-cell extract preparation from lymphoblastoid cell-lines

The protocol for whole-cell extraction was modified after Tanaka et al. [239]. Cell-pellets were thawed on ice, cells resuspended with $250\mu l$ WCE buffer A and let to swell for 20min on ice. Cells were disrupted by 20 strokes with pestle B in Dounce Homogenizer. Next, $125\mu l$ WCE buffer B was added and cells incubated on ice for an additional 5min. They were then sonicated twice for 30s with a 30s interval at 4°C and high power. After centrifugation for 20min at 4°C and 15'000 rcf, supernatant was removed and aliquoted. The samples of WCE were snap-frozen with liquid nitrogen and stored at -80°C until further use.
To determine the protein concentration, the Bradford protein assay was used. The Bradford solution contains Coomassie-Brillant-Blue G-250 with phosphoric acid. Upon adding it to a sample, it forms complexes with the side chains of the proteins therein, mainly the basic and aromatic residues. This reaction changes the absorption, which is photometrically measured at 595nm. To receive the calculation curve, first blank was set and four standards (bovine serum albumin of known concentration) were measured.

3.5 Fractionation of lymphoblastoid cell-lines

3.5.1 Material

- PBS 1x
- Fractionation buffer A and B
- Rotor mixer 10, Greiner
- Centrifuge 5417R, Eppendorf
- Rotanta 460 and Rotanta 420R, Hettich
- Branson Sonifier Cell disruptor B15, Branson Sonic Power Company
- Bio-rad Protein assay, Dye reagent concentrate, Bio-Rad
- Genesys 10 UV Scanning, Thermo Scientific

3.5.2 Harvesting cell pellets

Cell pellets were prepared following the procedure described in subchapter 3.4.2. For subsequent fractionation experiments, frozen as well as fresh cell pellets were used.

3.5.3 Fractionation of lymphoblastoid cell-lines

Protein complexes localized in different cellular compartments can be separated by a fractionation procedure that results in cytoplasmic, nuclear and chromatin fractions. To fractionate lymphoblastoid cells the previously established protocol by Mendez and Stillman [240] was optimized. Cells were resuspended with 200μl fractionation buffer A and let to swell 5min on a rotor at 4°C. Samples were next centrifuged 5min at 4°C and 1700 rcf, yielding supernatant 1 and pellet 1. Supernatant 1 was further clarified by centrifugation for 15min at 4°C and 20'000 rcf; the resulting supernatant represented the cytoplasmic fraction.
Pellet 1 was respuspended with 200μl fractionation buffer B and let 5min on a rotor at 4°C. Centrifugation for 5min at 4°C and 2000 rcf yielded supernatant 2 representing the nucleoplasm, and pellet 2. Pellet 2 was resuspended with 200μl fractionation buffer A and shortly vortexed. It was then sonicated at 30% intensity with 15 pulses and finally centrifuged 5min at 4°C and 20'000 rcf. Supernatant 3 represented the soluble chromatin fraction.
To determine the protein concentration, the Bradford protein assay was applied. To receive the calculation curve blank was set and four standards (bovine serum albumin of known concentration) were measured. The fractions were subsequently subjected to immunoblot analysis. To confirm that each fraction contained expected subcellular components, three proteins were utilized as markers: tubulin for the cytoplasm, fibrilarin in case of nucleoplasam and histone H1 for the soluble chromatin.

3.6 SDS-PAGE

3.6.1 Material

- MiniSpin centrifuge, Eppendorf
- SE250 Mighty Small II for 8x7cm gels, Hoefer
- SDS loading buffer 2x and 10x (Laemmli)
- PageRuler(TM) prestained protein ladder, Fermentas
- HiMark prestained protein standard, Invitrogen
- Immobilon-P transfer membrane, PVDF, Millipore
- TG- and TA-running buffers

- Whattman filter paper, Macherey Nagel
- Mini Trans-Blot Cell, Bio-Rad

Table 4. Protocol for 10% Tris-Glycine gel

	Stacking gel (4.8%)	Separating gel (10%)
H_2O	3.15ml	4ml
lower buffer (4xC)	1.25ml	---
upper buffer (4xB)	---	2ml
40% Acryl-bis 37.5:1	0.6ml	2ml
10% ammonium persulfate	0.05ml	0.08ml
TEMED	0.005ml	0.008
	5ml	8ml

Table 5. Protocol for 7% Tris-Acetate gel

H_2O	9.2ml
4x TA-solution	4ml
40% Acryl-bis 37.5:1	2.8ml
10% ammonium persulfate	0.16ml
TEMED	0.016ml
	16ml

3.6.2 Method

To quantify the protein levels in the WCEs and cell fractions of the four lymphoblastoid cell-lines, sodium dodecyl sulfate polyacrylamide gel electrophoresis (SDS-PAGE) and imunoblot analysis were performed. As the proteins of interest have different sizes, ranging from 30 to 480kD, two different setups were chosen. Proteins of the lower molecular weight were separated on 10% Tris-Glycine gels whereas the high molecular weight proteins were analyzed on 7% Tris-Acetate gels. The protocols for the gel mixes are provided in subchapter 3.6.1.
SDS loading buffer was added to the extracts to reach a final 1x dilution and the samples and everything was subsequently heated for 5min at 95°C. Loading buffer, followed by heating, causes the proteins to denaturate, charges them negatively and breaks disulfide bonds. After heating, samples were shortly spun-down, loaded and run on the gels for 20min at 80V, followed by 125V.

3.7 Immunoblot analysis

3.7.1 Material

- TG- and TA-transfer buffers
- Odyssey blocking solution, Li-cor
- Primary antibodies: in Odyssey blocking buffer 1:2 in PBS 1x, 0.01% NaN_3
  - MutYH (mouse), Abcam (#ab55551), dilution 1:500
  - Pol λ (rabbit), Bethyl Lab. (#A301-640A-1), dilution 1:1000
  - Lasu1/Ureb1 (Mule, rabbit), Bethyl Lab. (#A300-486A), dilution 1:000

  - Tubulin (mouse), Sigma-Aldrich (DM1A), dilution 1:10'000
  - Fibrillarin (mouse), abcam (#ab4566), dilution 1:1000
  - Histone H1 (mouse), Santa Cruz (#sc-8030) dilution 1:500
- Secondary antibodies: in PBS-T 0.05% and 0.01% NaN_3
  - IR-680 Mouse IgG, (from goat), Li-cor, dilution 1:15'000
  - IR-800 Rabbit IgG, (from goat), Li-cor, dilution 1:15'000
- Platform shaker Duomax 1030, Heidolph
- Odyssey CLx infrared scanner, Li-Cor
- GelEval, Frog Dance Software
- Prism, GraphPad Software

3.7.2 Method

To obtain a good-quality blot, it is important to avoid any dirt or bubbles between the gel and the PVDF membrane. Therefore, the blotting sandwich was assembled in H_2O as follows: (i) three Whatman filter papers were laid on a wet sponge, (ii) the gel was placed and the membrane added on the top, after 1min activation in methanol, everything was covered with (iii) another three Whatman filters and a wet sponge. The layers were gently rolled to squeeze out any air.
The transfer occurred in cold either TG- or TA-running buffer, for 1h at RT at 100V, or over-night at 4°C and 30V. The membrane was blocked for 1h in Odyssey blocking buffer 1:2 in PBS-T 0.05%, followed by incubation with the primary antibody of choice for 2h at RT. Before adding the secondary antibody for 1h at RT, the membrane was washed three-times for 5min in PBS-T 0.05% and finally kept in PBS at 4°C.
The pictures were obtained on Odyssey CLx infrared scanner, quantified by GelEval software and analyzed in Prism. Then, a one-sample two-sided t-test was applied.

3.8 DNA oligonucleotides

3.8.1 Material

Oligonucleotides were purchased from Microsynth. The sequences are shown below:
OHü 317: 39mer
5′-TACAACCAAGAGCATACGACGGCCAGTGCCGAATTCACA-3′
BvL 38: P-60mer
5′-GGTGTTGTGTGTTGGTTGTGGTGGTGTTGTGTGGTTGTTGGTGTTGTGTGTGTTGGT GTG-3′
OHü 318: 100mer (**X** = 8-oxo-G)
5′-CACACCAACACACACAACACCAACAACCACACAACACCACCACAACCAACACA CAACACC**X**TGTGAATTCGGCACTGGCCGTCGTATGCTCTTGGTTGTA-3′
OHü 322: 100mer
5′-TACAACCAAGAGCATACGACGGCCAGTGCCGAATTCACA**A**GGTGTTGTGT GTTG GTTGTGGTGGTGTTGTGTGGTTGTTGGTGTTGTGTGTGTTGGTGTG-3′
BvL 37: 35mer
5'-AAAAAAAAAAAAAAAAAAAAAAAAAAAAAAAAAAA-3'

3.8.2 Method

The oligonucleotides were used to prepare DNA substrates for polymerase and glycosylase assays or as trap-DNA. The stock with final concentration of 100μM was prepared by dissolving the oligonucleotides in TE pH 8.0, heating for 10 minutes at 65°C, followed by a short spin-down and storage at -80°C.

3.9 Labeling and annealing of DNA

3.9.1 Material

- Oligonucleotides
  - OHü 317: 39mer, upstream primer
  - OHü 318: 100mer, template
  - OHü 322: 100mer
  - BvL 38: P-60mer, downstream primer
- T4 Polynucleotide Kinase (PNK), Thermo Scientific
- Buffer A PNK 10x, Thermo Scientific
- γP^{32}-ATP, 110 TBq/mmol, Hartmann Analytic
- MicroSpin G-25 column, GE Healthcare
- Annealing buffer 5x
- DNA loading buffer
- 20% PA-gel
- 0.5x TBE running buffer
- X-ray film cassette, Okamoto
- Typox TX-RP blue sensitive film, Raymed Imaging

3.9.2 DNA labeling

To radioactively label OHü 317 oligonucleotide for polymerase, or OHü 322 for glycosylase assay, the reaction was prepared as depicted in Table 6.

Table 6. Protocol for labeling reaction

H_2O	4.5μl
OHü 317/322 (2μM)	2μl
Buffer A PNK 10x	1μl
T4 PNK	0.5μl
γ32-ATP	2μl
	10μl

The labeling reaction was incubated for 1h at 37°C in a water bath, after which 19.5μl of H_2O was added. The labeled DNA was separated from free γP^{32}-ATP by spin-column chromatography on a G-25 column, according to manufacturer's instructions. Briefly, the labeling reaction was added on the top of pre-equilibrated column, and subjected to centrifugation for 2min at 720 rcf. 8μl of annealing buffer 5x was added to purified labeled DNA.

3.9.3 Annealing

The 5' labelled oligonucleotide of interest was annealed to the complementary unlabeled DNA. The annealing of oligonucleotides was achieved by addition of 5pmol of complementary DNA to the labeling reaction, described in 3.9.2., containing 4pmol of labeled primer. The reaction was heated 5min at 95°C, followed by gradual cooling to RT.
For polymerase assays, a substrate containing 1nt-gap opposite an 8-oxo-G damage was generated by annealing radioactively labeled OHü 317 and BvL 38 oligonucleotides to OHü 318 100-mer. The downstream BvL 38 primer contains a phosphorylated 5'-end so that a 1nt-gap substrate resembles as close as possible a natural BER intermediate.
To determine MutYH glycosylase activity, an *in vitro* glycosylase assay was employed. As substrate served double stranded DNA containing the mispaired A opposite an 8-oxo-G lesion. The labeled oligonucleotide OHü 322 carries the faulty A, which can be recognized and excised by MutYH DNA glycosylase.

3.9.4 Annealing check

To test the efficiency of annealing, 20fmol of either (i) labeled or (ii) labeled and annealed DNA template was mixed with DNA loading buffer. Samples were loaded on a 20% PA-gel and separated by electrophoresis for 1.5h at 300V. The position of annealed and non-annealed oligonucleotides on the gel was detected by autoradiography. The non-annealed DNA is lighter and thus migrates faster than the annealed DNA. Based on the difference in signal height, it is possible to conclude whether annealing was successful or not.

3.10 DNA glycosylase assay

3.10.1 Material

- MutYH reaction buffer 10x
  - 250mM Sodium-phosphate buffer pH 6.8
  - 50mM EDTA
  - 15% Glycerol
  - 500μM $ZnCl_2$
  - 75mM $MgCl_2$
- Substrate DNA: 100/100-mer containing A mispaired opposite 8-oxo-G
- recombinant GST-MutYH was purified as described previously [39]
- MutYH dilution buffer
  - 30mM Tris-HCl pH 7.5
  - 1mM EDTA
  - 1mM β-mercaptoethanol
  - 50mM NaCl
  - 30% Glycerol
- Stop buffer 2x
- 10% PA-urea gel
- TBE running buffer 1x
- X-ray film cassette, Okamoto
- Typox TX-RP blue sensitive film, Raymed Imaging
- GelEval, Frog Dance Software
- Prism, GraphPad Software

3.10.2 Method

No efficient *in vitro* DNA glycosylase assay has been established so far to determine the activity of endogenous MutYH in WCE from cells in which MutYH had not been overexpressed. The comparison of endogenous MutYH activity in different lymphoblastoid cell-lines thus represented a challenge, with a series of steps needed to establish the optimal assay conditions. The development of the MutYH glycosylase assay using WCE is described in Figure 18. The optimal reaction conditions are presented in Table 7. To each premix reaction, 4μl of WCEs was added with varying final protein concentrations as indicated in figure legends. For positive control 0.5pmol recombinant GST-MutYH was used, while as negative control served WCE buffer A+B.
The samples were incubated 5min at 37°C. To break the sugar backbone at the position of AP site, 1μl of 2M NaOH was added to each reaction, followed by incubation for 15min at 70°C. The reactions were stopped by adding 11μl stop buffer 2x to each tube. The samples were heated for 5min at 95°C and shortly spun-down. To distinguish between unrepaired and MutYH processed products, samples were loaded on a 10% PA-urea gel and subjected to electrophoresis for 2h at 90W in 1x TBE running buffer. The gel was then exposed on film at -80°C and the positions of DNA oligonucleotides detected on the principle of autoradiography.

Table 7. Protocol for glycosylase reaction premix. All components are listed.

	1r
H_2O	4.55 μl
MutYH dil. Buffer (10x)	1 μl
ATP (40mM)	0.25 μl
Substrate-DNA (100nM)	0.2 μl
WCE (varying conc.)	4 μl
	10 μl

3.10.3 Data analysis

The products of the MutYH glycosylase assay were quantified in GelEval software and analyzed in Prism. Then, a one-sample two-sided t-test was applied.

3.11 DNA polymerase assay

3.11.1 Material

- Polymerase buffer 10x
  - 1M Tris-HCl pH 7.5
  - 10mg/ml BSA
  - 1mM DTT
- Trap-DNA: PolyA 35mer (BvL 37)
- Aphidicolin from Nigrospora sphaerica, Sigma-Aldrich
- Substrate-DNA: 1nt-gap opposite 8-oxo-G
- recombinant Pol λ was purified as described previously [241]
- Pol λ dilution buffer
  - 20mM Tris-HCl pH 7.5

  - 100M NaCl
  - 1mM DTT
  - 20% Glycerol
- dNTPs, Sigma-Aldrich
  - dA/G/TTP stock of 1mM, further diluted with H_2O
  - dC/G/TTP stock of 2mM, further diluted with H_2O
- Stop buffer 2x
- 12.5% PA-urea gel
- TBE running buffer 1x
- Fixing solution
- Gel Dryer Model 583, Bio-Rad
- Storage Phosphor Screen, Molecular Dynamics
- Typhoon 9400 Variable Mode Imager, GE Healthcare
- GelEval, Frog Dance Software
- Prism, GraphPad Software

3.11.2 Method

To assess the differences in the activity and fidelity of repair synthesis between different lymphoblastoid cell-lines, an *in vitro* DNA polymerase assay was performed. A reaction premix was prepared as depicted in Table 8 and contained following components: (i) 1 mM $MgCl_2$ (ii) aphidicolin to inhibit the B-family Pols [242] and (iii) trap-DNA needed to occupy DNAses in the WCEs, thus preventing degradation of the substrate-DNA. To each reaction 5μg of the WCE was added. dNTPs were titrated in the reaction to reach a final concentration of 1, 5 and 10μM, respectively. The 0μM dNTP sample contained H_2O instead dNTPs. The final volume of each reaction was 10μl. A reaction with 5μM dNTPs and WCE buffer A+B represented a negative control, while the positive control contained additional 50fmol Pol λ.

Table 8. Protocol for polymerase reaction premix. All components are listed.

	1 reaction
H_2O	1.2 μl
$MgCl_2$ (100mM)	0.1 μl
Polymerase buffer (10x)	1 μl
Trap-DNA (1.36μg/μl)	1.5 μl
Aphidicolin (10μg/μl)	1 μl
Substrate-DNA (100nM)	0.2 μl
dNTPs (0, 1, 5, 10μM)	1 μl
WCE (1.25μg/μl)	4 μl
	10 μl

All samples were incubated for 30min at 37°C. The reactions were stopped by addition of 10μl stop buffer 2x to each reaction. The formamide in the stop buffer denaturates the proteins and the EDTA captures the metal-ions so that the catalytic activity of the polymerases is additionally inhibited. To denature the DNA, samples were heated for 5min at 95°C.
The products of the polymerase assay were separated on a 12.5% PA-urea gel. Samples were loaded on the gel and subjected to electrophoresis for 3.5h at 90W in 1x TBE running buffer. Upon completion of electrophoresis, the gel was disassembled and fixed for 30min in fixing

solution. It was then vacuum-dried for 2h at 80°C and exposed on a phosphoscreen-casette over-night. The scan was obtained and visualized by Typhoon imager.

3.11.3 Data analysis

The products of the DNA polymerase assay were quantified by GelEval software and analyzed in Prism. Then, a one-sample two-sided t-test was applied.

4 Results

4.1 Protein levels of Mule, MutYH and DNA polymerase λ are individually changed in XLID patient cell-lines

As all three XLID patients carry mutations along the Mule gene, an immunoblot analysis was first performed to investigate the abundance of the proteins. The duplication of the gene in patient p83 leads to an at least two fold increase of Mule. 106 displays a tendency for a slight increase while levels are normal or mildly decreased in 444, when compared to healthy individual (WT) cell-line (Figure 16A and C).

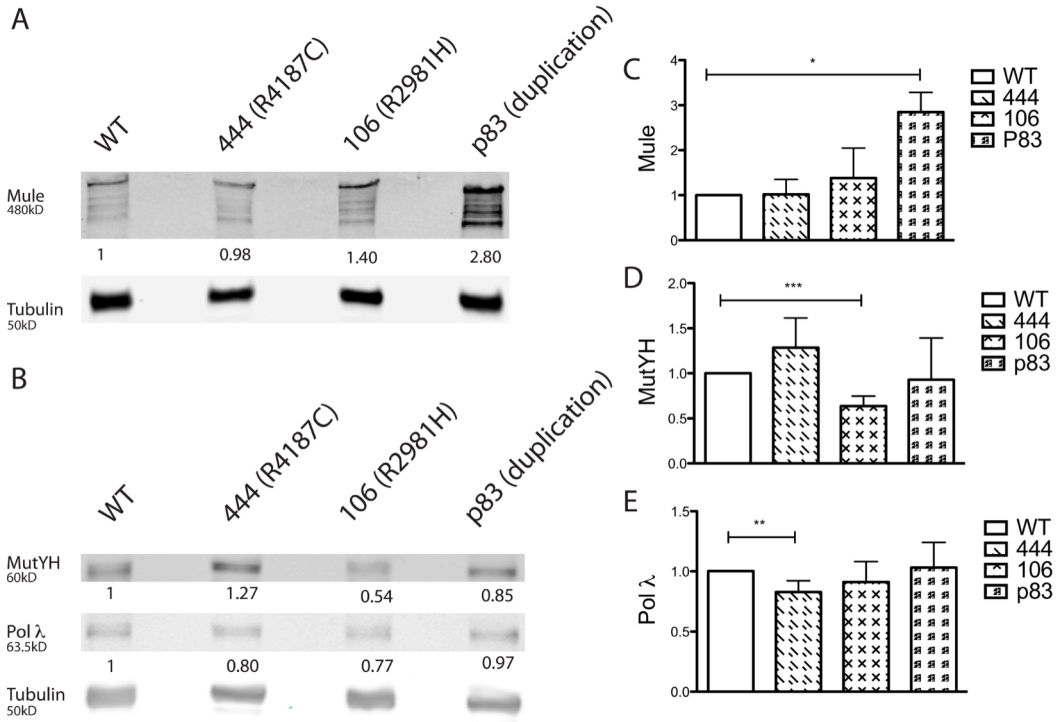

Figure 16. Changes of Mule, MutYH and DNA polymerase λ levels in three XLID patient cell-lines compared to one healthy individual.
Immunoblot analysis of (A) Mule and (B) MutYH and Pol λ protein levels in WCEs obtained from one healthy individual (WT) and three XLID (444, 106 and p83) patient cell-lines relative to tubulin. The numbers below the bands indicate the change in protein amount compared to WT. Quantification of changes in (C) Mule, (D) MutYH and (E) Pol λ protein levels from at least three independently performed experiments as the one in (A) and (B). Error bars indicate S.D., p-values *≤ 0.05, **≤ 0.01, ***≤ 0.001.

The levels of the three DNA repair proteins in WCEs from XLID patient cell-lines were subsequently evaluated by immunoblot analysis. MutYH and Pol λ, the two proteins crucial for efficient and accurate repair of A:8-oxo-G mispairs, were found to be changed. This finding is in agreement with the previous unpublished data obtained in this laboratory (Bosshard M. and van Loon B., unpublished). MutYH levels showed a clear decrease in cell-line 106 when compared to WT, while 444 cell-line had slightly increased amounts of MutYH (Figure 16B and D). Pol λ, was reproducibly reduced by 10% in 444 cell-line (Figure 16B and

E). These findings indicated that the levels of BER proteins MutYH and Pol λ are mis-regulated in XLID patient cells.

4.2 Analysis of MutYH and DNA polymerase λ levels in cytoplasmic, nucleoplasmic and soluble chromatin fractions of XLID patient cell-lines

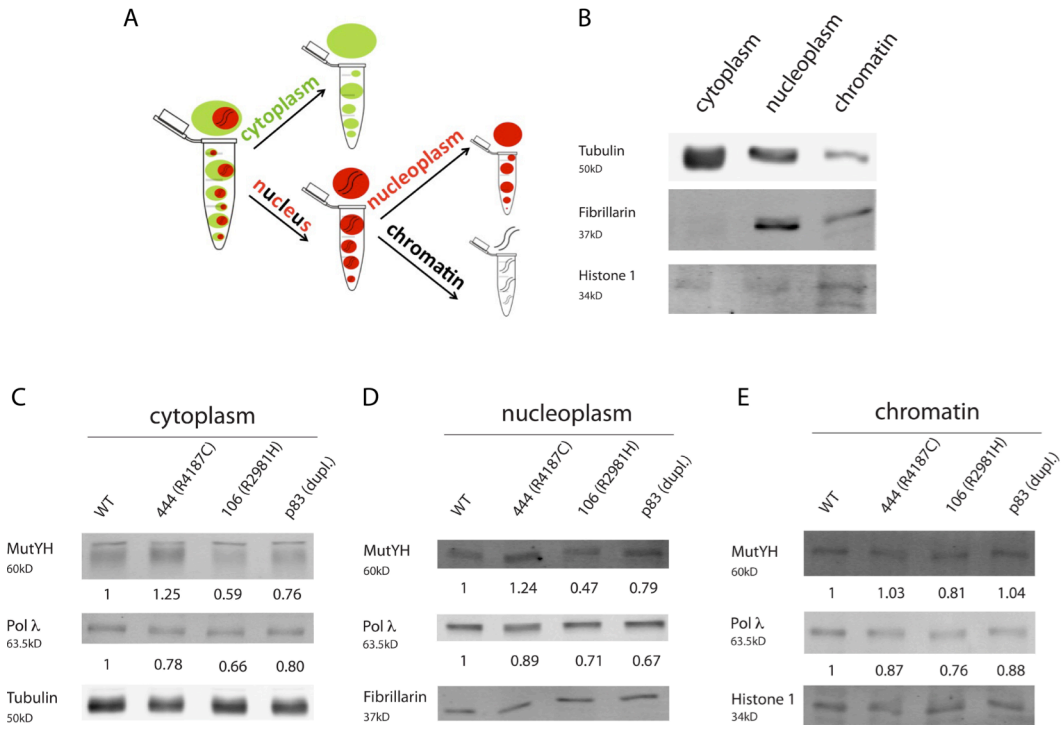

Figure 17. MutYH and DNA polymerase λ levels in cytoplasmic, nucleoplasmic and soluble chromatin fractions of WT, 444, 106 and p83 cell-lines.
(A) Scheme of fractionation principle into cytoplasm, nucleoplasm and soluble chromatin. (B) Immunoblot for compartment markers tubulin, fibrillarin and histone 1 indicating fractionation efficiency. MutYH and Pol λ protein levels in (C) cytoplasm relative to tubulin, (D) nucleoplasm relative to fibrillarin, and (E) soluble chromatin relative to histone 1 in fractionation extracts obtained from one healthy individual (WT) and three XLID (444, 106 and p83) patient cell-lines. The numbers below the bands indicate the change in protein amount compared to WT.

Besides general protein changes observed by WCE analysis, it is possible that the four analyzed cell-lines differ in the subcellular distribution of MutYH and Pol λ, which would directly affect their availability to participate in DNA repair processes. To determine subcellular distribution of these two proteins in lymphoblastoid cells, fractionation into cytoplasm, nucleoplasm and soluble chromatin was performed (Figure 17A). After establishing the conditions applicable to lymphoblastoid cells, the fractions were analyzed by immunoblot for MutYH and Pol λ levels. Three well established marker proteins served to confirm the fractionation efficiency: tubulin for the cytoplasm, fibrillarin in case of nucleoplasam and histone H1 for the soluble chromatin (Figure 17B). Though three markers are predominately present in the expected fractions, slight carryover is observed.
Similar to the WCEs (Figure 16), MutYH levels in the cytoplasmic fraction were increased in 444 but reduced in 106 cell-line. The levels of Pol λ were decreased in 444 cells, as well as 106. This pattern was mirrored in the nucleoplasm, however with additional decrease of both MutYH and Pol λ in p83 cell-line. In the chromatin fraction, the notable changes are a decrease of MutYH in 106 and Pol λ of in all three XLID patient cell-lines.

4.3 Establishment of a MutYH DNA glycosylase assay in whole-cell extracts

To test whether the reduction in MutYH protein levels observed in the XLID patient cells affects overall ability to recognize A:8-oxo-G mispairs and remove the A, an *in vitro* MutYH DNA glycosylase assay was developed. So far no efficient *in vitro* glycosylase assay had been established to determine the activity of endogenous MutYH glycosylase in WCEs.

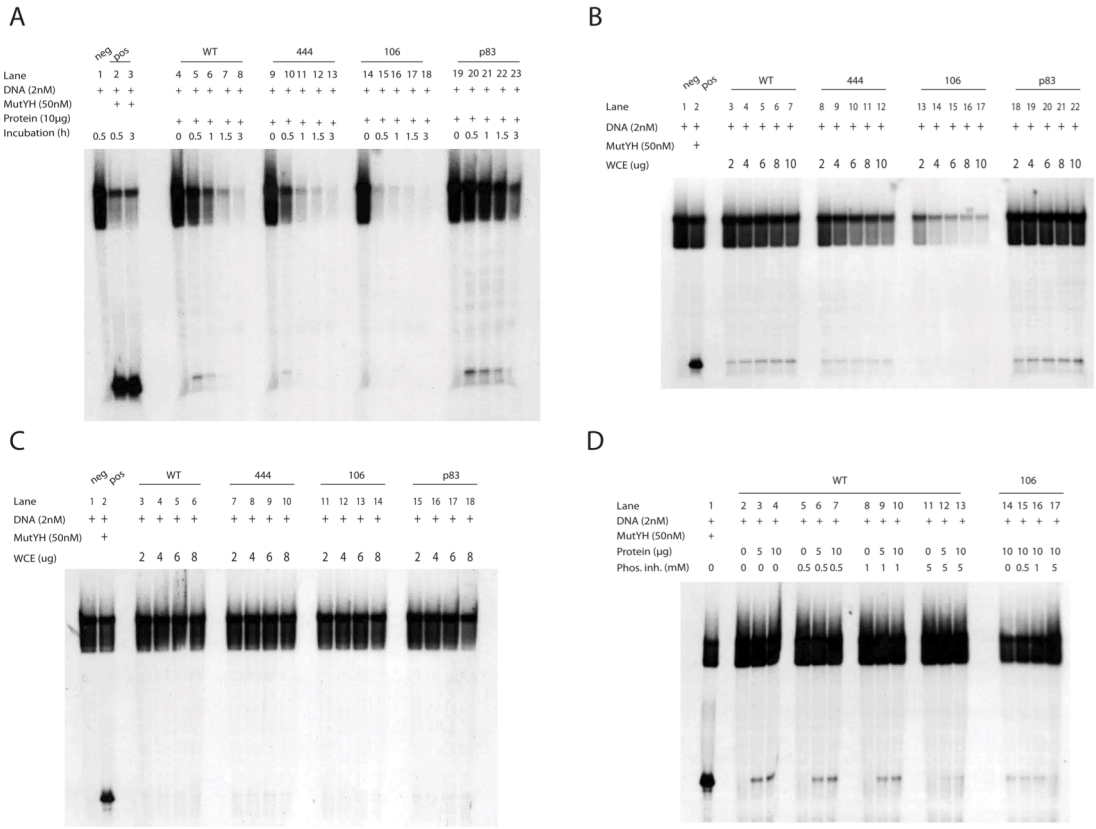

Figure 18. MutYH glycosylase can be measured in whole-cell extracts.
(A) Variation of time from 0 to 180 minutes in the reactions containing WT or XLID (444, 106 or p84) WCEs. (B) Addition of ATP to glycosylase reactions containing different extracts as the one described in (A). (C) Assay using WCEs prepared using sodium phosphate buffer and no sonication. (D) Titration of phosphatase inhibitors in the reactions containing WT or XLID (444, 106 or p84) WCE, with the incubation time of 5 minutes.

First whether the concentration of NaCl present in the reaction affects MutYH activity was tested, since it was shown that at concentrations higher than 200mM MutYH activity was impaired [243,244]. Recombinant MutYH was tested under three different NaCl concentrations (50, 60 or 160mM) (data not shown). Since MutYH was active under all three tested conditions, the protocol for the WCE preparation was chosen so that the final concentration of NaCl in the glycosylase assay did not exceed 160mM NaCl.

Initial time-course experiments using WT and different XLID WCEs revealed that MutYH glycosylase activity can be detected in the extracts (Figure 18A). However, a varying degree of reduction in the substrate signal could be observed with time in all the WCEs, indicating that different extracts contain different amounts of phosphatases (Figure 18A). To divert phosphatases from substrate DNA, ATP was added to the reaction (Figure 18B). Though addition of ATP resulted in slight suppression of phosphatase activity, the effect was by no means sufficient to accurately compare glycosylase activity between the extracts (Figure 18B). Besides ATP to attenuate phosphatases, Tris-HCl in the MutYH reaction buffer was

exchanged with sodium phosphate buffer. Even though the effect of phosphatases still was not evenly distributed between the WCEs, an improvement was observed in reactions containing sodium phosphate buffer, which was therefore used for further experiments (data not shown).

Since it was shown that presence of free DNA inhibits MutYH activity of substrate DNA [245], the WCE were prepared in sodium phosphate buffer, but without the final step involving sonication and shredding of genomic DNA (Figure 18C). Even though the loss of substrate signal was almost completely abolished, indicating that phosphatases have not been present or active in the WCE, the product signal was also almost completely lost (Figure 18C). Thus suggesting that sonication is a necessary step in WCE preparation, needed to remove MutYH bound to the chromatin. Based on these findings following WCEs were prepared according to the initial procedure.

The next important parameter of the assay was the incubation time. Variation of incubation time from 0 to 180 minutes indicated that a longer incubation did not significantly enhance the product signal but gave the phosphatases more time to degrade the substrate DNA (data not shown). The 5min time point was thus chosen as ideal incubation period allowing detection of glycosylase activity and limiting the effect of phosphatases. To understand whether addition of phosphatase inhibitors could further improve the quality of the signal, the 5min condition was used and phosphatase inhibitors were titrated (Figure 18D). The signal reduction was too grave and the improvement of the shorter incubation sufficient so that phosphatase inhibitors were left away. Based on these optimization experiments, final conditions were established as summarized in Table 9.

Table 9. Conditions to assay MutYH glycosylase in whole-cell extracts.
Assay optimization resulted in the final reaction conditions depicted in this table. Besides listed components, during optimization, reactions contained also 35mer PolydA trap-DNA, or the three phosphatase inhibitors (NaF, $Na_4P_2O_7$, $(HOCH_2)_2CHOP(O)(ONa)_2$).

NaCl (final)	ATP	phosphate buffer	incubation time	DNA label
160mM	1mM	25mM, pH 6.8	5min	radioactive

4.4 The XLID patient cell-line 106 has reduced MutYH glycosylase activity compared to the healthy individual

Once the conditions for the glycosylase assay were established, the MutYH activity was compared between the XLID patient cells and cells from a healthy individual. When the glycosylase removes a misincorporated A opposite 8-oxo-G it leaves behind an AP site. In an experimental setup, the sugar backbone is then cleaved by the addition of NaOH, which causes a single-strand break formation and migration of labeled DNA substrate at a lower position under denaturing condition (Figure 19A). As the breakage of the sugar backbone by NaOH is unspecific, it can occur either before or after the phosphate residue at the 3'-end. This is also visible on the gel, as the product faintly separated into two narrow bands (Figure 19B).

In line with the down-regulated MutYH protein levels (Figure 16), the MutYH glycosylase activity is reduced in XLID 106 cell-line (Figure 19B and D). P83 on the other hand shows only minor changes in MutYH levels and no decrease in the activity was detected (Figure 19B and E). 444 is the XLID cell-line with an increase in MutYH protein levels compared to WT

(Figure 16) and similarly elevated MutYH activity is present (Figure 19B and C). Overall, the results of the functional analysis correlate well with the changes observed on the protein level.

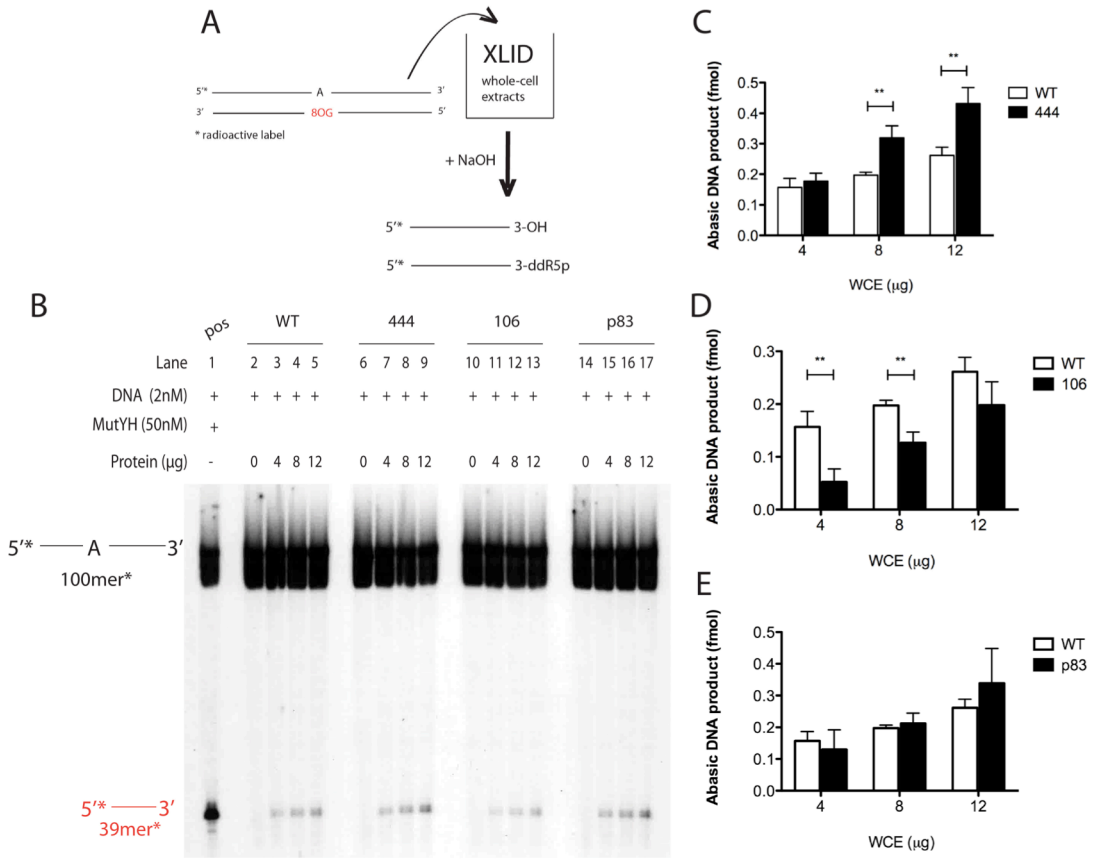

Figure 19. The XLID patient cell-line 106 has reduced MutYH glycosylase activity compared to the healthy individual.
(A) Scheme of DNA glycosylase assay. Whole-cell extracts are incubated and MutYH glycosylase is allowed to work. After final cleavage by addition of NaOH, activity is analyzed and quantified. (B) Removal of misincorporated A by MutYH glycosylase with increasing amount of healthy individual (WT) or XLID patient (444, 106 or p83) WCEs. (C-E) Quantification of MutYH activity present in WT and (C) 444, (D) 106 or (E) p83 WCEs, from three independently performed experiments as the one depicted in (B). Error bars indicate S.D., p-values **≤ 0.01.

4.5 XLID patient cells 444, 106 and p83 misincorporate more frequently dATP opposite 8-oxo-G than cells from the healthy individual

To evaluate the ability of the XLID patient cells to accurately and efficiently bypass 8-oxo-G damage, the WCEs were tested in an *in vitro* DNA polymerase assay (Figure 20A). As a substrate, 1nt-gap DNA substrate containing 8-oxo-G damage opposite the gap was used. The Pols present in the WCE can either incorporate the faulty dATP or the correct dCTP opposite 8-oxo-G, followed by the extension step (Figure 20A).

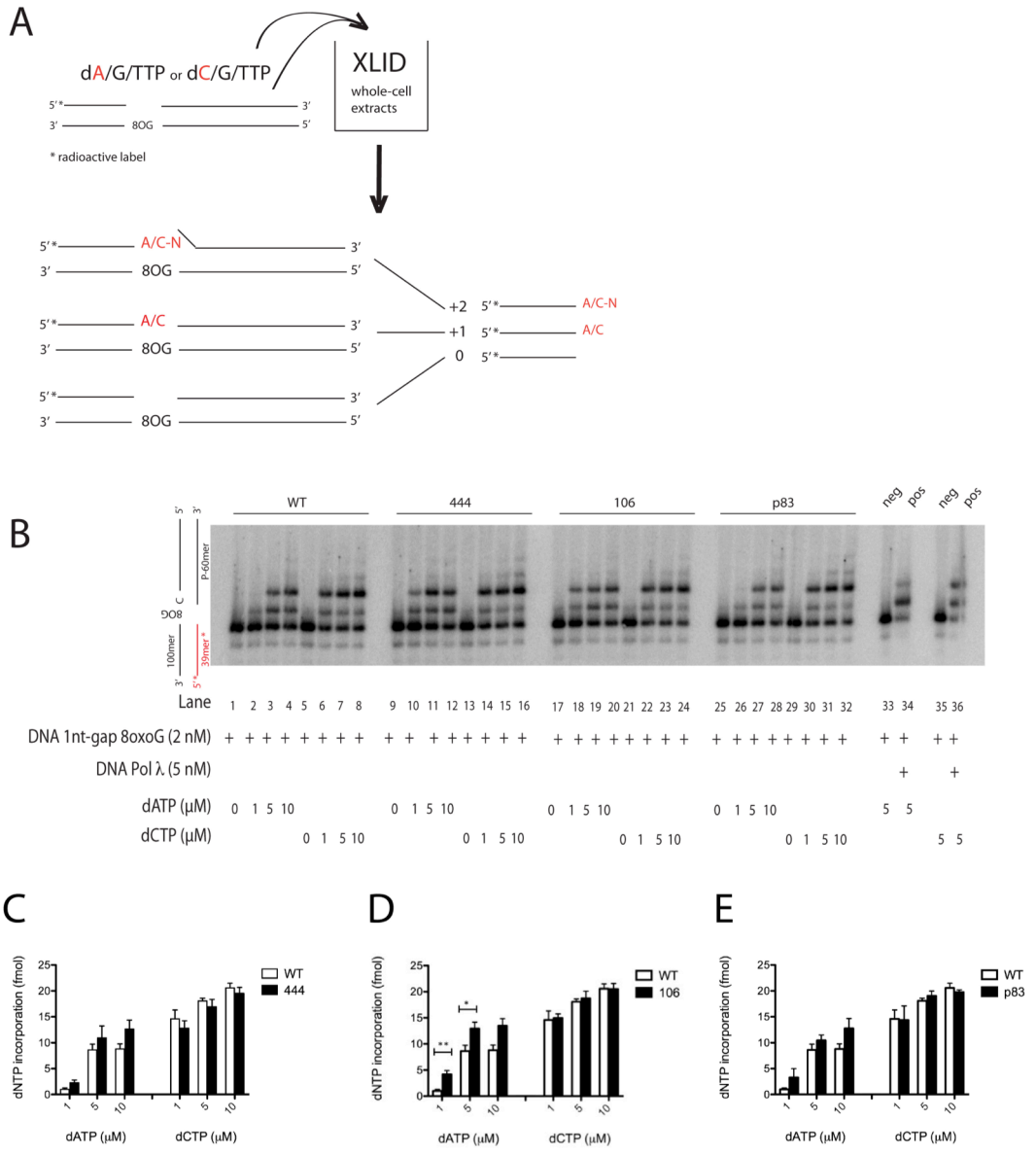

Figure 20. XLID patient cells 444, 106 and p83 misincorporate more frequently the wrong dATP opposite 8-oxo-G than cells from the healthy individual.
(A) Polymerase incorporation scheme. Whole-cell extracts are incubated with dNTPs containing either dATP or dCTP. Products of different lengths are subsequently analyzed and quantified. (B) Incorporation of dATP and dCTP opposite 8-oxo-G at different final concentrations by the healthy individual (WT) or XLID (444, 106 or p83) WCEs. (C-E) Comparison of 8-oxo-G bypass activity between WT and (C) 444, (D) 106 or (E) p83 WCEs, from three independently performed experiments as the one depicted in (B). Error bars indicate S.D., p-values *≤ 0.05, **≤ 0.01.

The XLID patient cell-lines 444, 106 and p83 incorporate more frequently dATP opposite 8-oxo-G than the cells from the healthy individual (Figure 20B-E). The incorporation of accurate dCTP does not significantly differ between WT and XLID cell-lines (Figure 20B-E), and is only slightly reduced in the case of the 444 cell-line (Figure 20B and C). These findings are thus to a certain extent in line with data presented in Figure 16, suggesting that reduced Pol λ protein levels influence cellular ability to accurately and efficiently bypass 8-oxo-G damage.

4.6 Virus transduction of lymphoblastoid cell-lines

The goal of the virus-transduction was to stably knock-down Mule by using short-hairpin RNA (shRNA) methodology. To visualize the approximate extent of transduction-efficiency, the coding plasmid contained the gene for green fluorescent protein (GFP) in addition to information needed for synthesis of shRNA. After ten days of selection with puromycin, more than 50% of the cells were GFP positive, indirectly indicating that the transduction was efficient and that shRNA was expressed in targeted cells (Figure 21).

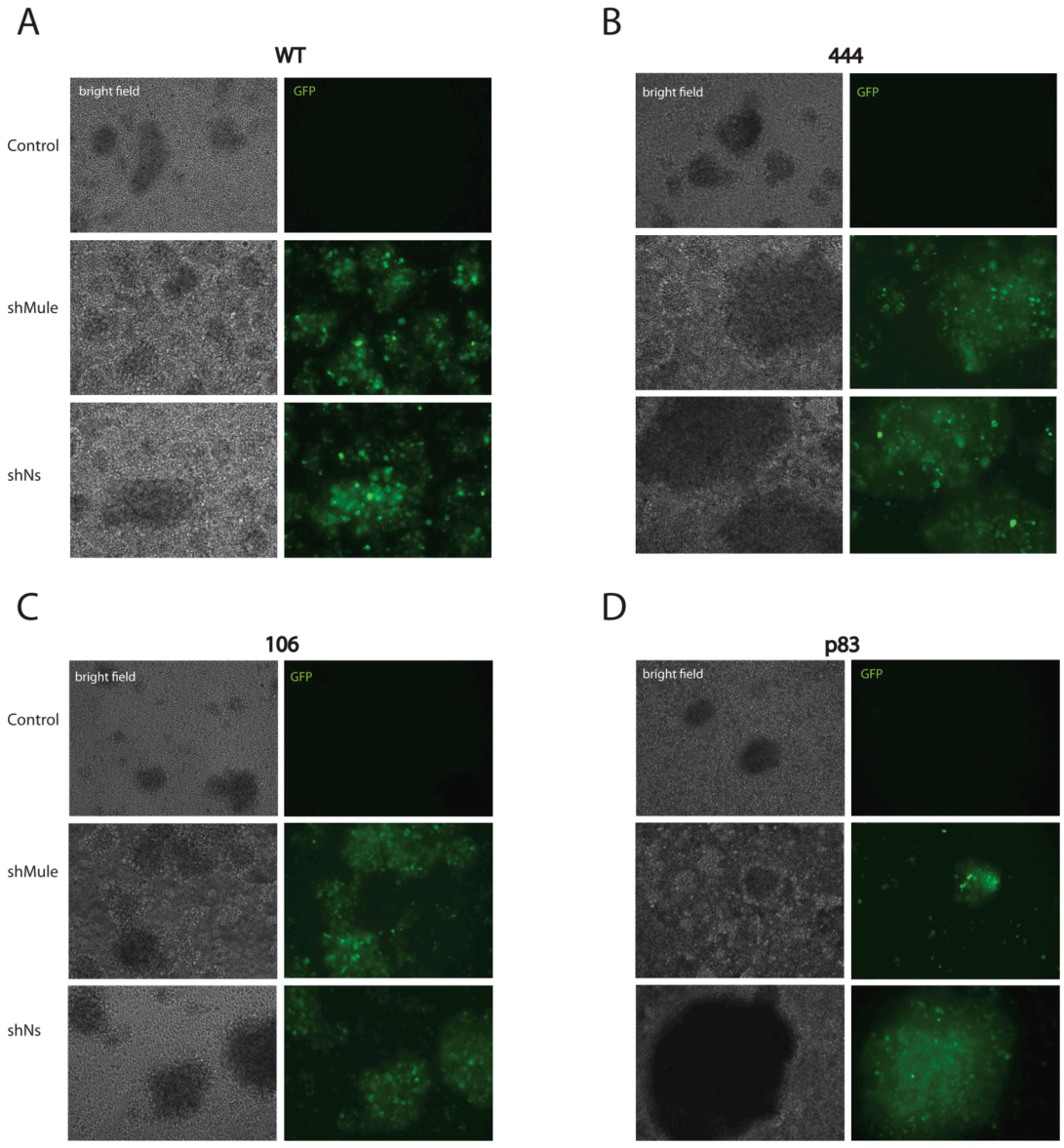

Figure 21. Virus transduction is efficient in all for cell-lines.
(A-D) Healthy individual (WT) and XLID patient (444, 106 and p83) cell-lines have successfully integrated the DNA construct, represented by occurrence of green fluorescent signal.

4.7 DNA glycosylase MutYH and DNA polymerase λ levels after Mule knock-down

The protein levels of the two important factors involved in repair of A:8-oxo-G mispairs, MutYH and Pol λ, are downregulated in XLID patient cells (Figure 16). To test whether reduction of Mule levels can result in restoration of MutYH and Pol λ levels, stable knock-down experiments were performed. Immunoblot analysis showed that the efficiency of Mule knock-down greatly varied between the cell-lines and in some instances was not extremely efficient (Figure 22). This could be explained with the large size of Mule, which makes its knock-down challenging. The strongest effect could be seen in WT cells while it was the least effective in 106 cell-line. Analysis of MutYH and Pol λ protein levels revealed that reduction in Mule levels resulted in an increase of MutYH protein levels in 106 cell-line and over-expression in WT and 444 (Figure 22B and C). Pol λ levels were rescued upon Mule knock-down in 444 XLID cells while in WT cells reduction in Mule lead to Pol λ accumulation (Figure 22B and D). These findings support the idea that Mule directly regulates levels of BER proteins involved in A:8-oxo-G repair as well as that this regulation is misfunctional in XLID patient cells.

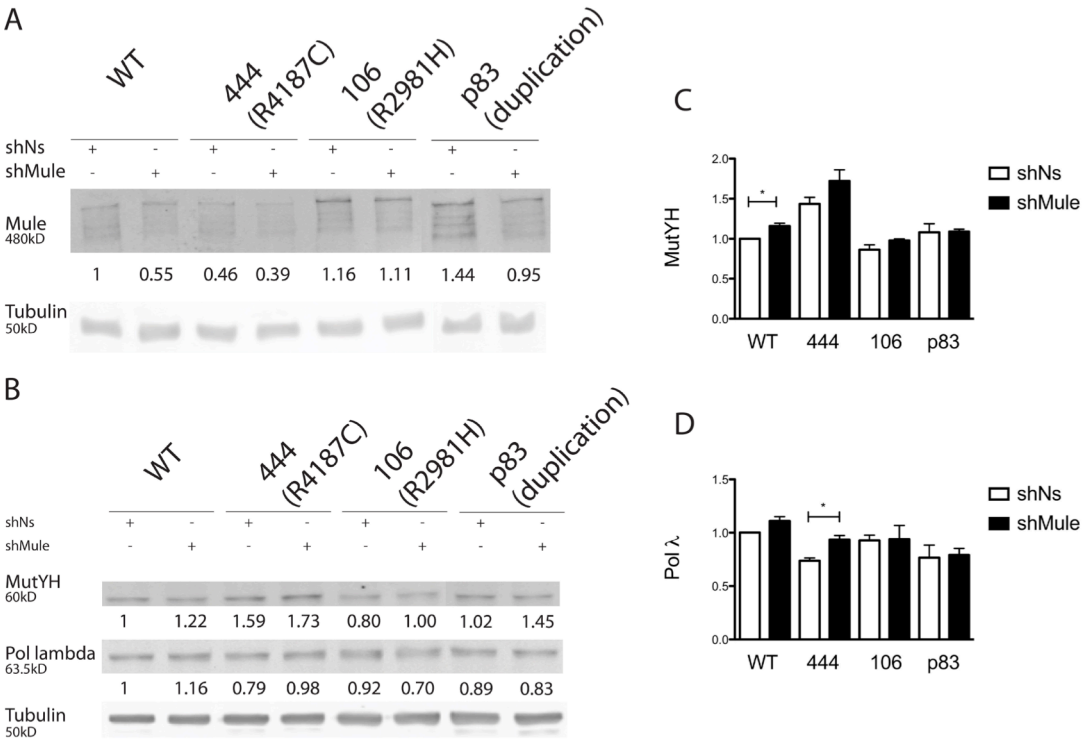

Figure 22. Protein levels of Mule, MutYH and Pol λ after knock-down of Mule.
(A) Immunoblot analysis of Mule protein levels upon knock-down of Mule in the healthy individual (WT) and the XLID patient (444, 106 and p83) cell-lines by shRNA. (B) Changes in MutYH and Pol λ levels detected by immunoblot analysis upon Mule knock-down. Values on graph do not represent values in the figure. (C-D) Quantification of changes in (C) MutYH and (D) Pol λ protein levels between control and knock-down of Mule from three independently performed experiments as the one in (B). Error bars indicate S.D., p-values *≤ 0.05.

4.8 MutYH glycosylase activity after knock-down of Mule

As demonstrated in Figure 19, the activity of MutYH glycosylase is reduced in cell-line 106 together with the protein levels (Figure 16). Therefore, the rescue upon knock-down of Mule was especially interesting for this cell-line. MutYH in 106 cell-line showed only a mild increase on the protein level, compared to the non-silenced condition (Figure 22). This very small change was reflected in slightly elevated glycosylase activity to remove A opposite 8-oxo-G in both WT and 106 cell-lines (Figure 23).

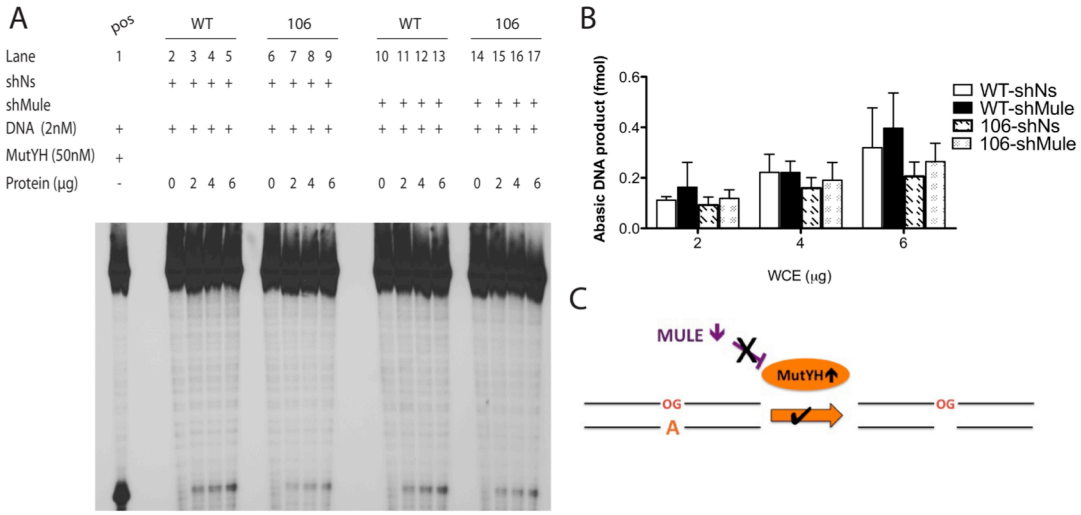

Figure 23. MutYH glycosylase activity is increased in the cell-lines of the healthy individual and of XLID patient 106 upon knock-down of Mule.
(A) Removal of misincorporated A by MutYH glycosylase with increasing amount of healthy individual (WT) or XLID patient 106 WCEs. Both conditions, non-silenced (shNs) and Mule knock-down (shMule) are displayed. (B) Quantification of MutYH activity present in WT and 106 WCEs, from four independently performed experiments as the one depicted in (A). Error bars indicate S.D. (C) Scheme for the rescue of MutYH activity to remove wrong A opposite 8-oxo-G after knock-down of Mule.

4.9 DNA polymerase λ activity after knock-down of Mule

As with the glycosylase assay, the cell-extracts after Mule knock-down were tested in polymerase assays. Since the biggest difference in fidelity was observed between WT and 444 extracts (Figure 20 and 24A), the focus was on the impact of Mule knock-down in these two cell-lines. Comparison of incorrect dATP and correct dCTP incorporation indicated that 444 cells upon Mule knock-down incorporated dCTP equally well as WT cells (Figure 24B). This is not the case for dATP, for which 444 cells were still more error-free. However the dATP incorporation by WT cells with knock-down Mule was much higher than observed previously (Figure 20 and 24A) and thus requires further investigation, before firm conclusions can be drawn.

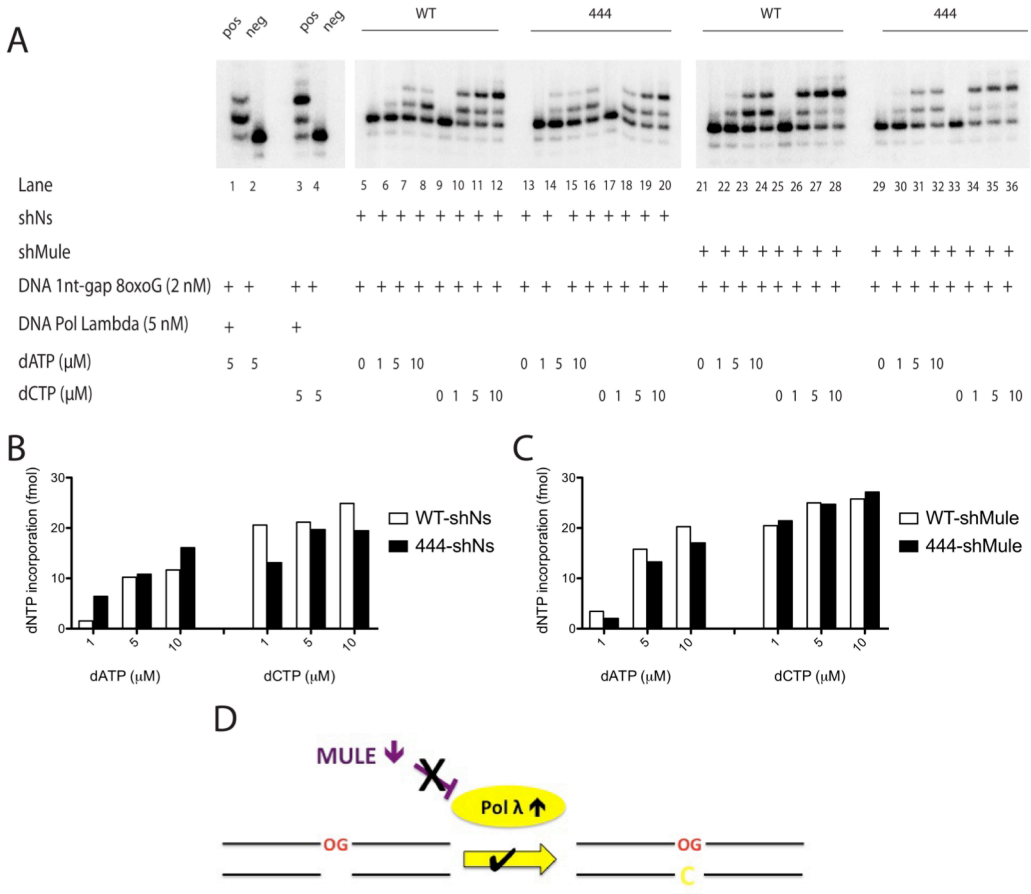

Figure 24. Incorporation of wrong dATP opposite 8-oxo-G in cell-line 444 upon knock-down of Mule.
(A) Incorporation of dATP and dCTP opposite 8-oxo-G at different final concentrations by the healthy individual (WT) or XLID patient 444 WCEs under non-silenced (shNs) and Mule knock-down (shMule) conditions. (B) Comparison of 8-oxo-G bypass activity between shNs and (C) shMule WT and 444 WCEs from the experiment depicted in (B). (D) Scheme for the rescue of Pol λ activity to incorporate correct dCTP opposite 8-oxo-G after knock-down of Mule.

5 Discussion

In this thesis, immortalized lymphoblastoid cells were used to represent the conditions in XLID patients with mutations in the Mule gene. Neuronal cells might behave differently and also the complexity of an organ plays important roles in the preservation of health and onset of disease. However, the chosen setting allowed to test the effects of mutated Mule on oxidative DNA damage repair. Previous research showed that the point mutation of an Arg to a Cys in the HECT domain of Mule in patient cell-line 444 renders the protein hyperactive (Ferrari. E and Hübscher U., unpublished). The neutral amino acid Cys with pH_i 5.05 and the ability to form thioester-bonds replaces the basic Arg with pH_i 11.76 (Figure 15). These alterations might suffice for the structure to change in a way that the activity increases. In 106, the mutation site lies outside the HECT domain and might affect stability, binding to substrates and interaction partners or subcellular localization. To address those questions, *in vitro* analyses with the specific Mule mutations as well as *in vivo* observation of the cells' behavior would be necessary.

The focus of this work lay on the efficiency of oxidative BER in XLID cells. A:8-oxo-G mispairs arise since many Pols preferentially incorporate inaccurate dATP opposite 8-oxo-G [246,247]. The accurate repair of these mispairs depends on MutYH and Pol λ [11,248]. It was observed that amounts of MutYH and Pol λ in the three studied XLID patient cell-lines are lowered. The reduction takes place mainly on the protein level (Figure 16), as mRNA levels are predominantly unchanged between the cell-lines (Markkanen E. and Hübscher U., unpublished). Mule targets Pol λ and putatively MutYH for degradation, which we propose as the direct cause of the altered protein levels in the studied XLID cells. The differences between individual cell-lines likely trace back to the distinct Mule mutations and possible posttranslational modifications stabilizing the proteins [249] and regulating DNA damage response [250]. Epigenetic modifications on the DNA could further even out genetic variations [251-254].

MutYH and Pol λ not only work in the same repair pathway but they are also functionally connected [39]. Subcellular fractions were prepared to identify changes in the cytoplasm, nucleoplasm and soluble chromatin of MutYH and Pol λ between the studied cell-lines (Figure 17). The expectation was that a reduction of MutYH on the chromatin would cause an insufficient recruitment of Pol λ and thus disable efficient BER of 8-oxo-G. The pattern in the cytoplasmic and nucleoplasmic fraction is in line with what was found in WCEs (Figure 17C and D). On the chromatin, 444 shows intact levels of MutYH but a decrease of Pol λ, which most likely arises due to the lower overall Pol λ levels in this cell-line. In 106, there is also less MutYH on the chromatin so that not enough Pol λ can be recruited. On the clinical side, 106 has the most pronounced disabilities. Maybe the shortage of MutYH on the chromosome, as only observed in this cell-line, is at least partially responsible for the degree of XLID. P83 shares similarities with both the others even though the gravest changes could be expected as this cell-line carries a Mule duplication. To draw a quantitative graph over more experiments and make firm conclusions, repetitions have to follow. Moreover, analysis of mitochondrial fractions could provide insight into possible influences of mitochondria in the pathogenesis of XLID, as seen in other cognitive disabilities, peripheral neuropathie and myopathies [255].

In the functional setting of DNA glycosylase and polymerase assays (Figures 19 and 20), the MutYH and Pol λ reduction results in a deficient repair of 8-oxo-G lesions. 106 cell-line fails to remove A opposite 8-oxo-G as well as incorporate correct dCTP at WT efficiency. The dysregulation in 444 cell-line could even have graver consequences, as the high activity of MutYH taking out misincorporated A is followed by a lack of Pol λ, thus boosting the continuous generation of A:8-oxo-G mispairs. This could enhance futile cycles, lead to

oxidized AP sites and eventually increased prevalence of SSBs [256]. P83 again takes a position in between as MutYH activity is comparable to WT but then followed by inaccurate gap-filling.

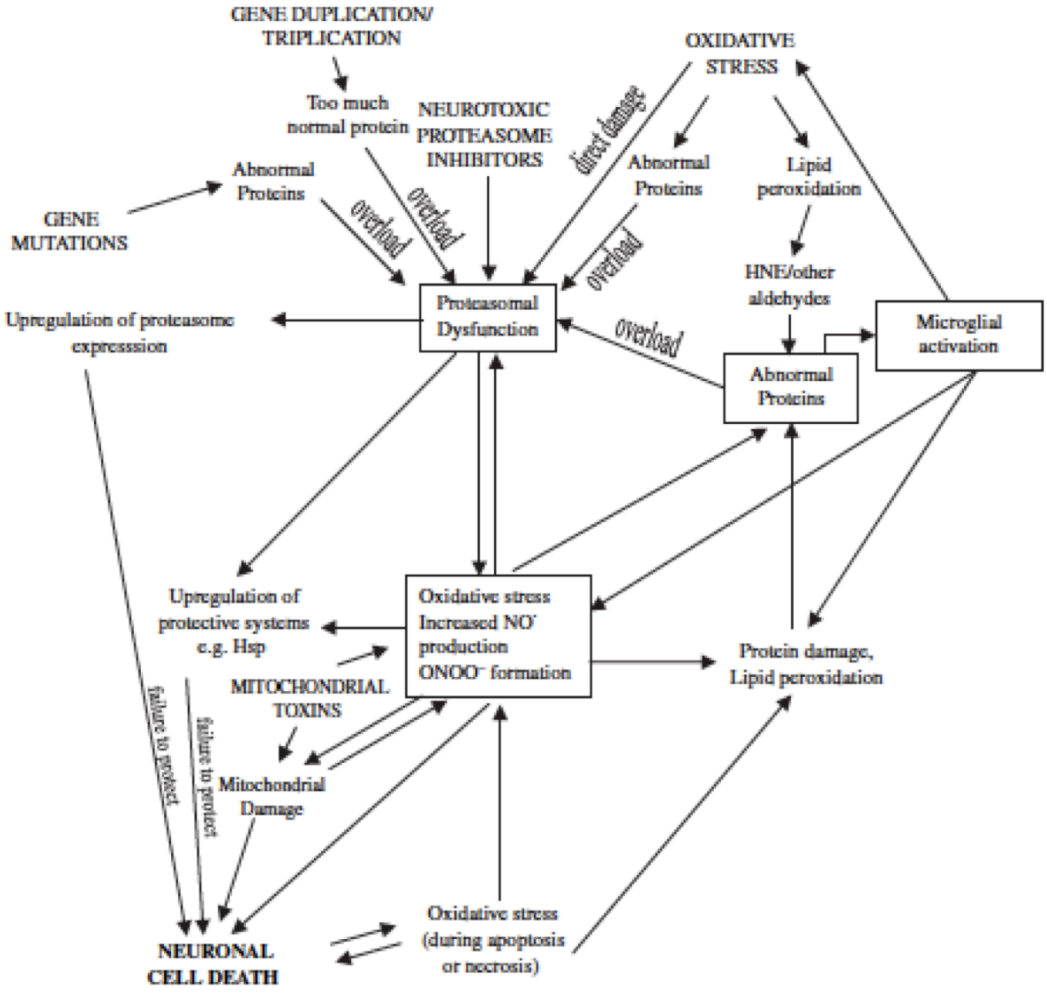

Figure 25. Interplay of mitochondria, oxidative damage and the proteasome in neurodegeneration.
(From Barry Halliwell. (2006) Oxidative stress and neurodegeneration: Where are we now? *Journal of Neurochemistry)*

An interesting observation concerns the activity of Pol λ. It preferentially incorporates dCTP over dATP opposite 8-oxo-G on gapped DNA by a factor of 750 to 1200 [38], ratios that were not obtained in our experimental setup (Figure 20). Previous studies employed recombinant Pol λ, PCNA and RP-A, while here WCEs were used, containing many different factors potentially stimulating as well as inhibiting the reactions. Since other Pols, such as Pol β, are also active on the 8-oxo-G lesion and have a lower fidelity to incorporate dCTP, the higher dATP incorporation detected in XLID WCEs is potentially due to the activity of these proteins. Namely, when Pol λ is present in the cell it binds to the DNA containing 1nt-gap opposite 8-oxo-G and prevents other Pols from acting on this lesion. The reduction in Pol λ levels in the XLID patients possibly results in lower abundance of this Pol at the damage site, which is when Pol β could take over. Finally, the negative influence of Mule on MutYH and Pol λ levels could be shown in a Mule knock-down experiment. Knock-down was not complete but nonetheless there was a tendency of rescue of MutYH and Pol λ protein levels (Figure 22).

The functional impact for MutYH activity in 106 (Figure 23) and Pol λ in 444 (Figure 24) was slightly visible and should be subsequently confirmed in extracts from more efficient knock-downs. Figure 25 presents the network of mechanisms in oxidation-related neurodegeneration, which might partially apply to the pathogenesis of Mule-dependent XLID. The deficient repair of oxidative DNA lesions by MutYH/Pol λ BER leads to persisting A:8-oxo-G mispairs with the risk of G:C→T:A mutations. Altered proteins, mitochondrial dysfunctions and finally apoptosis push the development and progression of neurodegenerative diseases [257]. Stress response and neuroinflammation may further deteriorate the integrity of the delicate neuronal tissue [258,259].
Accumulation or increased activity of Mule in the observed XLID patient cell-lines can have many additional influences. Besides the studied alterations in BER, other targets of the E3 ubiquitin ligase might get out of control (Figure 26). Cell division cycle 6 (Cdc6) [260] and Mcl-1 [155] are important for mitosis and apoptosis. Mule targets them for degradation [157,240,261,262], which prevents the propagation of mutations but may trigger cell death. This could also occur during neurogenesis, which was found altered in various forms of XLID. Structural aspects such as the branched morphology of dendritic spines as well as functional properties of synapses would be limited by a lagging cell cycle [190]. Altered ubiquitination of transcription factors c-Myc [151,263], N-Myc and Myc-interacting zinc finger protein 1 (Miz1) can dysregulate cell cycle control and checkoint activation [264]. The Mule-dependent degradation of N-Myc in neuronal progenitor cells prompts the signal to exit cell cycle and start differentiation [229,230,265]. Mule is indeed increased during brain development and disturbances could either lead the cells to insufficiently differentiate or do so too soon. Besides that, shortage in Myc proteins has been shown to lead to an exaggerated reaction after DNA damage and thereby cause neuronal death [263].

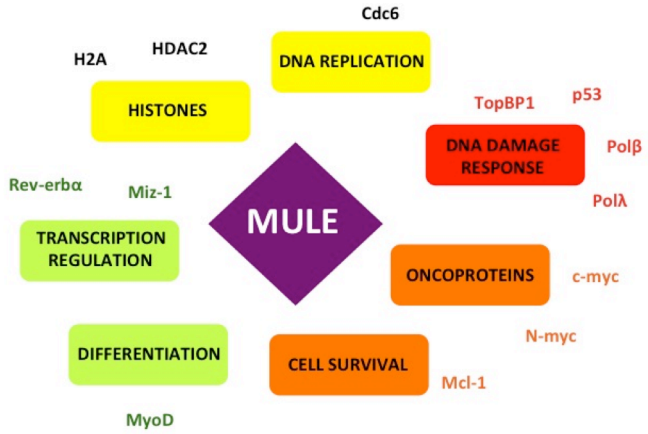

Figure 26. Involvement of Mule in various cellular functions.
See text for more details.

Also histones on the DNA itself are modified by ubiquitination [266] and acetlyation [267], which gave rise to diseases and therapeutical substances such as histone deacetylase inhibitors (HDACis) [268]. Interestingly, overexpression of histone deacetylase 2 (HDAC2) impairs synaptogenesis in the nervous system and inhibits p83 activation after DNA damage [269,270]. Mule has a regulatory function in these processes by modifiying histones directly through ubiquitination and indirectly by degrading HDAC [251,271]. If the activity or affinity of mutated Mule towards these substrates is changed in XLID patients, it can trouble gene transcription in general, DNA damage response through p53, or synaptogenesis.

Other than the involvement with proteins of DNA repair and cell cycle control, Mule ubiquitinates the transcription factor myogenic differentiation factor D (MyoD) and a receptor of the circadian network Rev-erbα [272,273]. MyoD activates muscle specific genes and allows the progenitor cells to differentiate [274-276]. The enactment of the myogenic program requires appropriate activation of the genes involved and also includes the maintenance of progenitor cells (satellite cells) important for muscle regeneration [277,278]. In fact, patients suffering from Mule-associated XLID exhibit flaccid facial expression due to weak muscles and patient 106, even displays flexor deformities preventing him from walking [1]. This could be caused by hampered muscle development due to excessive degradation of MyoD by Mule. Finally, it would be interesting to check the XLID cells for proteins involved in Mule regulation, such as USP7S. Hyperactive or increased levels of Mule could for example be compensated by a decrease in USP7S. Thereby, Mule would rather be degraded after auto-ubiquitination and target its substrates to a lesser degree. Such mechanisms could also assist in the explanation why certain known Mule targets do not show a decrease in the studied XLID cell-lines. On the other side, changes in USP7S also affect the epigenetic regulator ubiquitin-like with PHD and RING finger domains 1 (UHRF1) and thus alter DNA damage response [279]. Moreover, many other substrates of USP7 are involved in proliferation, cell cycle control, DNA repair and apoptosis [164,280-282].

A lesser tolerance of oxidative stress in Mule-dependent XLID suggests the reduction of ROS production or the application of antioxidative agents as therapeutic options. Even though diseases related to oxidative stress present as very heterogeneous - all in etiology, pathology and symptomatology - common concepts might be useful for treatment [283-287]. Dietary adjustments, such as a low-calory diet that is known to increase life expectancy in rats [288,289] and change cognitive functions and neurodegeneration [290-295] could be applied to affect the production of ROS. An other debated mechanism of caloric restriction is the induction of ROS scavengers upon energy shortage [296]. As the restriction necessary to observe the benefits lies high in the range of 20 to 25% [297], the aim is to identify food components with the greatest oxidative potential and reduce their intake selectively. The restriction of proteins in general and Met in particular seem to have the biggest positive impact on life span and disease development [298]. Accumulation of Homocys, (a harmful product from the Met metabolism, has been related to various neurodegenerative diseases and supposedly decreases resistance towards oxidative stress [299]. The degradation of Homocys requires several enzymes as folic acid, vitamin B6 and 12 [300], the supplementation of which can have a beneficial impact on neuronal survival [301,302]. Other ingredients in food can directly combat ROS. They basically include the components important in cellular antioxidative mechanisms: vitamin C, vitamin E, carotenoids, α-lipoic acid, glutathione and others [283,303]. Furthermore, flavanoids, a group of antioxidative agents with the ability to act as metal chelators, feature exciting therapeutic potential [304,305]. They were shown valuable in reducing oxidative stress in neuronal tissue in certain studies and more insight is necessary to pinpoint practical application considering efficient dosage and combinations [306-309]. Further, an interesting new approach is to use cellular detection sensors of ROS and enhance their controlling system, which involves the so-called vitagens. Certain vitagens, such as heme-oxygenase 1 (HO-1) can be induced in brain cells by intake of spices like curcumin [310]. Curcumin additionally contains a variety of polyphenolic molecules that prevent lipid peroxidation and protect from ROS. Also the non-proteinogenic amino acid acetyl-L-carnitine (LAC) found in plants and animals has the ability to induce HO-1, improve mitochondrial functions, stabilize membranes and even enhance repair mechanisms [311-313]. Its therapeutical value lies in the treatment of neurochemical abnormalities, ischemia, aging, neurotropathic pain and even restoring memory function in AD or decreasing oxidative stress in the brain [314-317].

Taken together, the essential merit of understanding disease mechanisms lies in finding therapeutical options, which might not be that far away.

6 Conclusion

Increased oxidative stress is a known factor in the development as well as progression of various neurodegenerative diseases. Neurons with their high oxidative metabolism need a functional repair machinery to combat increased oxidative DNA damage. Since neurons are highly differentiated and do not have an active cell cycle, they are not replaced after their death. While cellular dysregulation in other organs may lead to cancer, degeneration is the most frequent outcome in the nervous system. BER is one pathway to repair non-bulky DNA lesions such as the oxidized base 8-oxo-G. Functional BER with MutYH and Pol λ is crucial to deal with A:8-oxo-G mispairs, which have a highly mutagenic potential for G:C→T:A transversions. Such mutations might cause problems in the nuclear as well as mitochondrial processes and disturb cellular functioning until apoptosis is the outcome. In conclusion, it was shown that XLID patients with mutations in the Mule gene, and subsequently decreased levels in MutYH and Pol λ indeed have a hampered repair of A:8-oxo-G (Figure 27). The mis-regulated repair of A:8-oxo-G mispairs results in preservation of A at the position of C. Among others, this might contribute to the synthesis of aberrant proteins and the subsequent initiation of different cellular responses, resulting in improperly functioning neurons and potential neuronal death during development. It is therefore proposed that certain types of XLID potentially arise due to an impaired response of neurons to oxidative DNA damage.

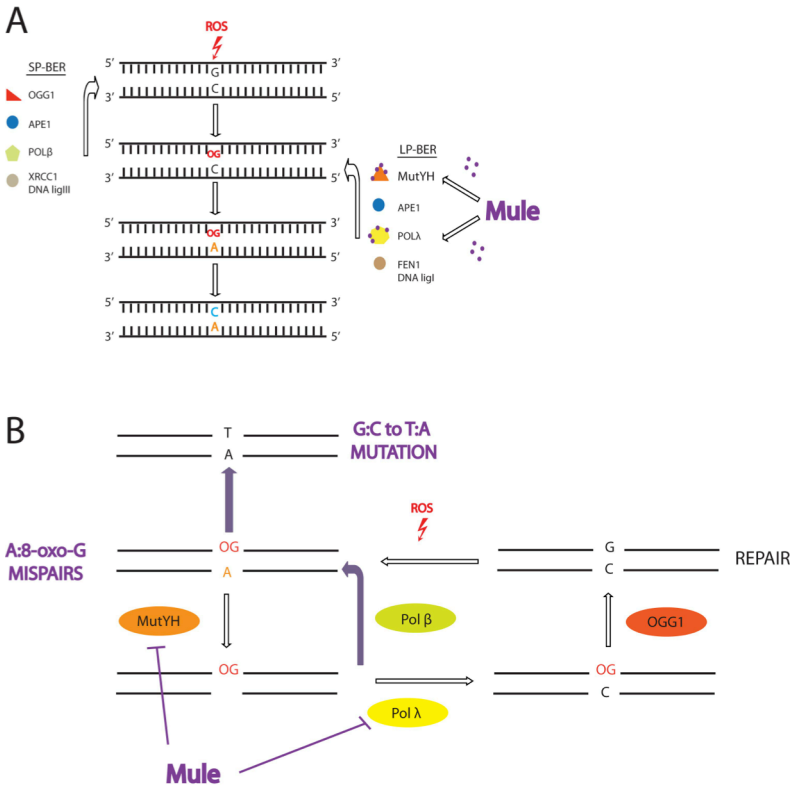

Figure 27. Model: interference of of 8-oxo-G DNA repair by Mule.
(A) SP and LP-BER of 8-oxo-G and the targeting for proteasomal degradation of MutYH and Pol λ. (B) Mule leads to a decrease in glycosylase activity by potentially degrading MutYH. This results in preservation of A:8-oxo-G mispairs and if repair synthesis or even replication takes place at the site of this mispair, G:C→T:A transversion mutations arise. The degradation of Pol λ promotes misincorporation of dATP opposite 8-oxo-G, which is insufficiently removed.

7 Figures and Tables

7.1 Figures

7.2 Tables

8 References

1 Froyen, G. *et al.* Submicroscopic duplications of the hydroxysteroid dehydrogenase HSD17B10 and the E3 ubiquitin ligase HUWE1 are associated with mental retardation. *Am J Hum Genet* **82**, 432-443, doi:10.1016/j.ajhg.2007.11.002 (2008).

2 Cooke, M. S., Evans, M. D., Dizdaroglu, M. & Lunec, J. Oxidative DNA damage: mechanisms, mutation, and disease. *Faseb J* **17**, 1195-1214, doi:10.1096/fj.02-0752rev (2003).

3 Evans, M. D., Dizdaroglu, M. & Cooke, M. S. Oxidative DNA damage and disease: induction, repair and significance. *Mutat Res* **567**, 1-61, doi:10.1016/j.mrrev.2003.11.001 (2004).

4 van Loon, B., Markkanen, E. & Hubscher, U. Oxygen as a friend and enemy: How to combat the mutational potential of 8-oxo-guanine. *DNA Repair (Amst)* **9**, 604-616, doi:10.1016/j.dnarep.2010.03.004 (2010).

5 Boveris, A., Oshino, N. & Chance, B. The cellular production of hydrogen peroxide. *Biochem J* **128**, 617-630 (1972).

6 Klaunig, J. E. & Kamendulis, L. M. The role of oxidative stress in carcinogenesis. *Annu Rev Pharmacol Toxicol* **44**, 239-267, doi:10.1146/annurev.pharmtox.44.101802.121851 (2004).

7 Valko, M., Rhodes, C. J., Moncol, J., Izakovic, M. & Mazur, M. Free radicals, metals and antioxidants in oxidative stress-induced cancer. *Chem Biol Interact* **160**, 1-40, doi:10.1016/j.cbi.2005.12.009 (2006).

8 Finkel, T. Signal transduction by reactive oxygen species. *J Cell Biol* **194**, 7-15, doi:10.1083/jcb.201102095 (2011).

9 Cerutti, P., Ghosh, R., Oya, Y. & Amstad, P. The role of the cellular antioxidant defense in oxidant carcinogenesis. *Environ Health Perspect* **102 Suppl 10**, 123-129 (1994).

10 David, S. S., O'Shea, V. L. & Kundu, S. Base-excision repair of oxidative DNA damage. *Nature* **447**, 941-950, doi:10.1038/nature05978 (2007).

11 Markkanen, E., Castrec, B., Villani, G. & Hubscher, U. A switch between DNA polymerases delta and lambda promotes error-free bypass of 8-oxo-G lesions. *Proc Natl Acad Sci U S A*, doi:10.1073/pnas.1211532109 (2012).

12 Greenman, C. *et al.* Patterns of somatic mutation in human cancer genomes. *Nature* **446**, 153-158, doi:10.1038/nature05610 (2007).

13 Collins, A. R. Oxidative DNA damage, antioxidants, and cancer. *Bioessays* **21**, 238-246, doi:10.1002/(SICI)1521-1878(199903)21:3<238::AID-BIES8>3.0.CO;2-3 (1999).

14 Berquist, B. R. & Wilson, D. M., 3rd. Pathways for repairing and tolerating the spectrum of oxidative DNA lesions. *Cancer Lett* **327**, 61-72, doi:10.1016/j.canlet.2012.02.001 (2012).

15 Hoeijmakers, J. H. DNA damage, aging, and cancer. *N Engl J Med* **361**, 1475-1485, doi:10.1056/NEJMra0804615 (2009).

16 Jackson, S. P. & Bartek, J. The DNA-damage response in human biology and disease. *Nature* **461**, 1071-1078, doi:10.1038/nature08467 (2009).

17 Barnes, D. E. & Lindahl, T. Repair and genetic consequences of endogenous DNA base damage in mammalian cells. *Annu Rev Genet* **38**, 445-476, doi:10.1146/annurev.genet.38.072902.092448 (2004).

18 Dalle-Donne, I. *et al.* Proteins as biomarkers of oxidative/nitrosative stress in diseases: the contribution of redox proteomics. *Mass Spectrom Rev* **24**, 55-99, doi:10.1002/mas.20006 (2005).

19 Krokan, H. E. & Bjoras, M. Base excision repair. *Cold Spring Harb Perspect Biol* **5**, doi:10.1101/cshperspect.a012583 (2013).

20 Robertson, A. B., Klungland, A., Rognes, T. & Leiros, I. DNA repair in mammalian cells: Base excision repair: the long and short of it. *Cell Mol Life Sci* **66**, 981-993, doi:10.1007/s00018-009-8736-z (2009).

21 Fortini, P., Parlanti, E., Sidorkina, O. M., Laval, J. & Dogliotti, E. The type of DNA glycosylase determines the base excision repair pathway in mammalian cells. *J Biol Chem* **274**, 15230-15236 (1999).

22 Jacobs, A. L. & Schar, P. DNA glycosylases: in DNA repair and beyond. *Chromosoma* **121**, 1-20, doi:10.1007/s00412-011-0347-4 (2012).
23 Sung, J. S. & Demple, B. Roles of base excision repair subpathways in correcting oxidized abasic sites in DNA. *Febs J* **273**, 1620-1629, doi:10.1111/j.1742-4658.2006.05192.x (2006).
24 Hazra, T. K. *et al.* Characterization of a novel 8-oxoguanine-DNA glycosylase activity in Escherichia coli and identification of the enzyme as endonuclease VIII. *J Biol Chem* **275**, 27762-27767, doi:10.1074/jbc.M004052200 (2000).
25 Hazra, T. K. *et al.* Identification and characterization of a human DNA glycosylase for repair of modified bases in oxidatively damaged DNA. *Proc Natl Acad Sci U S A* **99**, 3523-3528, doi:10.1073/pnas.062053799 (2002).
26 Dou, H., Mitra, S. & Hazra, T. K. Repair of oxidized bases in DNA bubble structures by human DNA glycosylases NEIL1 and NEIL2. *J Biol Chem* **278**, 49679-49684, doi:10.1074/jbc.M308658200 (2003).
27 Bernstein, N. K. *et al.* Polynucleotide kinase as a potential target for enhancing cytotoxicity by ionizing radiation and topoisomerase I inhibitors. *Anticancer Agents Med Chem* **8**, 358-367 (2008).
28 Hazra, T. K., Izumi, T., Maidt, L., Floyd, R. A. & Mitra, S. The presence of two distinct 8-oxoguanine repair enzymes in human cells: their potential complementary roles in preventing mutation. *Nucleic Acids Res* **26**, 5116-5122 (1998).
29 Nash, H. M. *et al.* Cloning of a yeast 8-oxoguanine DNA glycosylase reveals the existence of a base-excision DNA-repair protein superfamily. *Curr Biol* **6**, 968-980 (1996).
30 Klungland, A. & Bjelland, S. Oxidative damage to purines in DNA: role of mammalian Ogg1. *DNA Repair (Amst)* **6**, 481-488, doi:10.1016/j.dnarep.2006.10.012 (2007).
31 Fortini, P. *et al.* The base excision repair: mechanisms and its relevance for cancer susceptibility. *Biochimie* **85**, 1053-1071 (2003).
32 Fortini, P. *et al.* Different DNA polymerases are involved in the short- and long-patch base excision repair in mammalian cells. *Biochemistry* **37**, 3575-3580, doi:10.1021/bi972999h (1998).
33 Braithwaite, E. K. *et al.* DNA polymerases beta and lambda mediate overlapping and independent roles in base excision repair in mouse embryonic fibroblasts. *PLoS One* **5**, e12229, doi:10.1371/journal.pone.0012229 (2010).
34 Braithwaite, E. K. *et al.* DNA polymerase lambda mediates a back-up base excision repair activity in extracts of mouse embryonic fibroblasts. *J Biol Chem* **280**, 18469-18475, doi:10.1074/jbc.M411864200 (2005).
35 Faucher, F., Doublie, S. & Jia, Z. 8-oxoguanine DNA glycosylases: one lesion, three subfamilies. *Int J Mol Sci* **13**, 6711-6729, doi:10.3390/ijms13066711 (2012).
36 Williams, S. D. & David, S. S. Evidence that MutY is a monofunctional glycosylase capable of forming a covalent Schiff base intermediate with substrate DNA. *Nucleic Acids Res* **26**, 5123-5133 (1998).
37 Hayashi, H. *et al.* Replication-associated repair of adenine:8-oxoguanine mispairs by MYH. *Curr Biol* **12**, 335-339 (2002).
38 Maga, G. *et al.* Replication protein A and proliferating cell nuclear antigen coordinate DNA polymerase selection in 8-oxo-guanine repair. *Proc Natl Acad Sci U S A* **105**, 20689-20694, doi:10.1073/pnas.0811241106 (2008).
39 van Loon, B. & Hubscher, U. An 8-oxo-guanine repair pathway coordinated by MUTYH glycosylase and DNA polymerase lambda. *Proc Natl Acad Sci U S A* **106**, 18201-18206, doi:10.1073/pnas.0907280106 (2009).
40 Ide, H. & Kotera, M. Human DNA glycosylases involved in the repair of oxidatively damaged DNA. *Biol Pharm Bull* **27**, 480-485 (2004).
41 Mohammed, M. Z. *et al.* Development and evaluation of human AP endonuclease inhibitors in melanoma and glioma cell lines. *Br J Cancer* **104**, 653-663, doi:10.1038/sj.bjc.6606058 (2011).
42 Karger, S. *et al.* Distinct pattern of oxidative DNA damage and DNA repair in follicular thyroid tumours. *J Mol Endocrinol* **48**, 193-202, doi:10.1530/JME-11-0119 (2012).

43 Germann, M. W., Johnson, C. N. & Spring, A. M. Recognition of damaged DNA: structure and dynamic markers. *Med Res Rev* **32**, 659-683, doi:10.1002/med.20226 (2012).
44 Dalhus, B., Laerdahl, J. K., Backe, P. H. & Bjoras, M. DNA base repair--recognition and initiation of catalysis. *FEMS Microbiol Rev* **33**, 1044-1078, doi:10.1111/j.1574-6976.2009.00188.x (2009).
45 Hegde, M. L., Hazra, T. K. & Mitra, S. Early steps in the DNA base excision/single-strand interruption repair pathway in mammalian cells. *Cell Res* **18**, 27-47, doi:10.1038/cr.2008.8 (2008).
46 Grin, I. R. & Zharkov, D. O. Eukaryotic endonuclease VIII-like proteins: new components of the base excision DNA repair system. *Biochemistry (Mosc)* **76**, 80-93 (2011).
47 Suzuki, T., Harashima, H. & Kamiya, H. Effects of base excision repair proteins on mutagenesis by 8-oxo-7,8-dihydroguanine (8-hydroxyguanine) paired with cytosine and adenine. *DNA Repair (Amst)* **9**, 542-550, doi:10.1016/j.dnarep.2010.02.004 (2010).
48 Nohmi, T., Kim, S. R. & Yamada, M. Modulation of oxidative mutagenesis and carcinogenesis by polymorphic forms of human DNA repair enzymes. *Mutat Res* **591**, 60-73, doi:10.1016/j.mrfmmm.2005.03.033 (2005).
49 Sampath, H., McCullough, A. K. & Lloyd, R. S. Regulation of DNA glycosylases and their role in limiting disease. *Free Radic Res* **46**, 460-478, doi:10.3109/10715762.2012.655730 (2012).
50 Parker, A. R. & Eshleman, J. R. Human MutY: gene structure, protein functions and interactions, and role in carcinogenesis. *Cell Mol Life Sci* **60**, 2064-2083, doi:10.1007/s00018-003-3053-4 (2003).
51 Takao, M., Zhang, Q. M., Yonei, S. & Yasui, A. Differential subcellular localization of human MutY homolog (hMYH) and the functional activity of adenine:8-oxoguanine DNA glycosylase. *Nucleic Acids Res* **27**, 3638-3644 (1999).
52 Nakabeppu, Y. Regulation of intracellular localization of human MTH1, OGG1, and MYH proteins for repair of oxidative DNA damage. *Prog Nucleic Acid Res Mol Biol* **68**, 75-94 (2001).
53 Markkanen, E., Dorn, J. & Hubscher, U. MUTYH DNA glycosylase: the rationale for removing undamaged bases from the DNA. *Front Genet* **4**, 18, doi:10.3389/fgene.2013.00018 (2013).
54 Lukianova, O. A. & David, S. S. A role for iron-sulfur clusters in DNA repair. *Curr Opin Chem Biol* **9**, 145-151, doi:10.1016/j.cbpa.2005.02.006 (2005).
55 Fromme, J. C., Banerjee, A., Huang, S. J. & Verdine, G. L. Structural basis for removal of adenine mispaired with 8-oxoguanine by MutY adenine DNA glycosylase. *Nature* **427**, 652-656, doi:10.1038/nature02306 (2004).
56 Guan, Y. *et al.* MutY catalytic core, mutant and bound adenine structures define specificity for DNA repair enzyme superfamily. *Nat Struct Biol* **5**, 1058-1064, doi:10.1038/4168 (1998).
57 Parker, A. *et al.* Human homolog of the MutY repair protein (hMYH) physically interacts with proteins involved in long patch DNA base excision repair. *J Biol Chem* **276**, 5547-5555, doi:10.1074/jbc.M008463200 (2001).
58 Kairupan, C. & Scott, R. J. Base excision repair and the role of MUTYH. *Hered Cancer Clin Pract* **5**, 199-209, doi:10.1186/1897-4287-5-4-199 (2007).
59 Parker, A. R. *et al.* Defective human MutY phosphorylation exists in colorectal cancer cell lines with wild-type MutY alleles. *J Biol Chem* **278**, 47937-47945, doi:10.1074/jbc.M306598200 (2003).
60 Boldogh, I. *et al.* hMYH cell cycle-dependent expression, subcellular localization and association with replication foci: evidence suggesting replication-coupled repair of adenine:8-oxoguanine mispairs. *Nucleic Acids Res* **29**, 2802-2809 (2001).
61 Ruggieri, V. *et al.* Loss of MUTYH function in human cells leads to accumulation of oxidative damage and genetic instability. *Oncogene*, doi:10.1038/onc.2012.479 (2012).
62 Parker, A. R. *et al.* Cells with pathogenic biallelic mutations in the human MUTYH gene are defective in DNA damage binding and repair. *Carcinogenesis* **26**, 2010-2018, doi:10.1093/carcin/bgi166 (2005).

63 Nielsen, M., Morreau, H., Vasen, H. F. & Hes, F. J. MUTYH-associated polyposis (MAP). *Crit Rev Oncol Hematol* **79**, 1-16, doi:10.1016/j.critrevonc.2010.05.011 (2011).
64 Kundu, S., Brinkmeyer, M. K., Livingston, A. L. & David, S. S. Adenine removal activity and bacterial complementation with the human MutY homologue (MUTYH) and Y165C, G382D, P391L and Q324R variants associated with colorectal cancer. *DNA Repair (Amst)* **8**, 1400-1410, doi:10.1016/j.dnarep.2009.09.009 (2009).
65 Kinzler, K. W. & Vogelstein, B. Lessons from hereditary colorectal cancer. *Cell* **87**, 159-170 (1996).
66 Goss, K. H. & Groden, J. Biology of the adenomatous polyposis coli tumor suppressor. *J Clin Oncol* **18**, 1967-1979 (2000).
67 Learn, P. A. & Kahlenberg, M. S. Hereditary colorectal cancer syndromes and the role of the surgical oncologist. *Surg Oncol Clin N Am* **18**, 121-144, ix, doi:10.1016/j.soc.2008.08.007 (2009).
68 Paz-Elizur, T. *et al.* DNA repair of oxidative DNA damage in human carcinogenesis: potential application for cancer risk assessment and prevention. *Cancer Lett* **266**, 60-72, doi:10.1016/j.canlet.2008.02.032 (2008).
69 Casorelli, I. *et al.* The Mutyh base excision repair gene influences the inflammatory response in a mouse model of ulcerative colitis. *PLoS One* **5**, e12070, doi:10.1371/journal.pone.0012070 (2010).
70 Morak, M., Massdorf, T., Sykora, H., Kerscher, M. & Holinski-Feder, E. First evidence for digenic inheritance in hereditary colorectal cancer by mutations in the base excision repair genes. *Eur J Cancer* **47**, 1046-1055, doi:10.1016/j.ejca.2010.11.016 (2011).
71 Venesio, T., Balsamo, A., D'Agostino, V. G. & Ranzani, G. N. MUTYH-associated polyposis (MAP), the syndrome implicating base excision repair in inherited predisposition to colorectal tumors. *Front Oncol* **2**, 83, doi:10.3389/fonc.2012.00083 (2012).
72 Kim, C. J. *et al.* Genetic alterations of the MYH gene in gastric cancer. *Oncogene* **23**, 6820-6822, doi:10.1038/sj.onc.1207574 (2004).
73 Barnetson, R. A. *et al.* Germline mutation prevalence in the base excision repair gene, MYH, in patients with endometrial cancer. *Clin Genet* **72**, 551-555, doi:10.1111/j.1399-0004.2007.00900.x (2007).
74 Stanczyk, M. *et al.* The association of polymorphisms in DNA base excision repair genes XRCC1, OGG1 and MUTYH with the risk of childhood acute lymphoblastic leukemia. *Mol Biol Rep* **38**, 445-451, doi:10.1007/s11033-010-0127-x (2011).
75 Gorgens, H. *et al.* Analysis of the base excision repair genes MTH1, OGG1 and MUTYH in patients with squamous oral carcinomas. *Oral Oncol* **43**, 791-795, doi:10.1016/j.oraloncology.2006.10.004 (2007).
76 Oka, S. & Nakabeppu, Y. DNA glycosylase encoded by MUTYH functions as a molecular switch for programmed cell death under oxidative stress to suppress tumorigenesis. *Cancer Sci* **102**, 677-682, doi:10.1111/j.1349-7006.2011.01869.x (2011).
77 Russo, M. T. *et al.* Accumulation of the oxidative base lesion 8-hydroxyguanine in DNA of tumor-prone mice defective in both the Myh and Ogg1 DNA glycosylases. *Cancer Res* **64**, 4411-4414, doi:10.1158/0008-5472.CAN-04-0355 (2004).
78 Xie, Y. *et al.* Deficiencies in mouse Myh and Ogg1 result in tumor predisposition and G to T mutations in codon 12 of the K-ras oncogene in lung tumors. *Cancer Res* **64**, 3096-3102 (2004).
79 Bowling, A. C. & Beal, M. F. Bioenergetic and oxidative stress in neurodegenerative diseases. *Life Sci* **56**, 1151-1171 (1995).
80 Englander, E. W. *et al.* Rat MYH, a glycosylase for repair of oxidatively damaged DNA, has brain-specific isoforms that localize to neuronal mitochondria. *J Neurochem* **83**, 1471-1480 (2002).
81 Lee, H. M. *et al.* Developmental changes in expression and subcellular localization of the DNA repair glycosylase, MYH, in the rat brain. *J Neurochem* **88**, 394-400 (2004).
82 Nguyen, P. V., Marin, L. & Atwood, H. L. Synaptic physiology and mitochondrial function in crayfish tonic and phasic motor neurons. *J Neurophysiol* **78**, 281-294 (1997).
83 Beal, M. F. Does impairment of energy metabolism result in excitotoxic neuronal death in neurodegenerative illnesses? *Ann Neurol* **31**, 119-130, doi:10.1002/ana.410310202 (1992).

84 Lee, H. M. *et al.* Hypoxia induces mitochondrial DNA damage and stimulates expression of a DNA repair enzyme, the Escherichia coli MutY DNA glycosylase homolog (MYH), in vivo, in the rat brain. *J Neurochem* **80**, 928-937 (2002).
85 Fukae, J., Mizuno, Y. & Hattori, N. Mitochondrial dysfunction in Parkinson's disease. *Mitochondrion* **7**, 58-62, doi:10.1016/j.mito.2006.12.002 (2007).
86 Arai, T. *et al.* Up-regulation of hMUTYH, a DNA repair enzyme, in the mitochondria of substantia nigra in Parkinson's disease. *Acta Neuropathol* **112**, 139-145, doi:10.1007/s00401-006-0081-9 (2006).
87 Mariani, E., Polidori, M. C., Cherubini, A. & Mecocci, P. Oxidative stress in brain aging, neurodegenerative and vascular diseases: an overview. *J Chromatogr B Analyt Technol Biomed Life Sci* **827**, 65-75, doi:10.1016/j.jchromb.2005.04.023 (2005).
88 Nakabeppu, Y., Tsuchimoto, D., Yamaguchi, H. & Sakumi, K. Oxidative damage in nucleic acids and Parkinson's disease. *J Neurosci Res* **85**, 919-934, doi:10.1002/jnr.21191 (2007).
89 Wang, A. L., Lukas, T. J., Yuan, M. & Neufeld, A. H. Age-related increase in mitochondrial DNA damage and loss of DNA repair capacity in the neural retina. *Neurobiol Aging* **31**, 2002-2010, doi:10.1016/j.neurobiolaging.2008.10.019 (2010).
90 Brault, L. S., Cooper, C. A., Famula, T. R., Murray, J. D. & Penedo, M. C. Mapping of equine cerebellar abiotrophy to ECA2 and identification of a potential causative mutation affecting expression of MUTYH. *Genomics* **97**, 121-129, doi:10.1016/j.ygeno.2010.11.006 (2011).
91 Hubscher, U., Maga, G. & Spadari, S. Eukaryotic DNA polymerases. *Annu Rev Biochem* **71**, 133-163, doi:10.1146/annurev.biochem.71.090501.150041 (2002).
92 Braithwaite, E. K. *et al.* DNA polymerase lambda protects mouse fibroblasts against oxidative DNA damage and is recruited to sites of DNA damage/repair. *J Biol Chem* **280**, 31641-31647, doi:10.1074/jbc.C500256200 (2005).
93 Lange, S. S., Takata, K. & Wood, R. D. DNA polymerases and cancer. *Nat Rev Cancer* **11**, 96-110, doi:10.1038/nrc2998 (2011).
94 Albertella, M. R., Lau, A. & O'Connor, M. J. The overexpression of specialized DNA polymerases in cancer. *DNA Repair (Amst)* **4**, 583-593, doi:10.1016/j.dnarep.2005.01.005 (2005).
95 Bouwman, P. & Jonkers, J. The effects of deregulated DNA damage signalling on cancer chemotherapy response and resistance. *Nat Rev Cancer* **12**, 587-598, doi:10.1038/nrc3342 (2012).
96 Uchiyama, Y., Takeuchi, R., Kodera, H. & Sakaguchi, K. Distribution and roles of X-family DNA polymerases in eukaryotes. *Biochimie* **91**, 165-170, doi:10.1016/j.biochi.2008.07.005 (2009).
97 Garcia-Diaz, M., Bebenek, K., Kunkel, T. A. & Blanco, L. Identification of an intrinsic 5'-deoxyribose-5-phosphate lyase activity in human DNA polymerase lambda: a possible role in base excision repair. *J Biol Chem* **276**, 34659-34663, doi:10.1074/jbc.M106336200 (2001).
98 Aoufouchi, S. *et al.* Two novel human and mouse DNA polymerases of the polX family. *Nucleic Acids Res* **28**, 3684-3693 (2000).
99 Garcia-Diaz, M. *et al.* DNA polymerase lambda (Pol lambda), a novel eukaryotic DNA polymerase with a potential role in meiosis. *J Mol Biol* **301**, 851-867, doi:10.1006/jmbi.2000.4005 (2000).
100 Garcia-Diaz, M. *et al.* DNA polymerase lambda, a novel DNA repair enzyme in human cells. *J Biol Chem* **277**, 13184-13191, doi:10.1074/jbc.M111601200 (2002).
101 Zhang, X. *et al.* Structure of an XRCC1 BRCT domain: a new protein-protein interaction module. *Embo J* **17**, 6404-6411, doi:10.1093/emboj/17.21.6404 (1998).
102 Fiala, K. A., Duym, W. W., Zhang, J. & Suo, Z. Up-regulation of the fidelity of human DNA polymerase lambda by its non-enzymatic proline-rich domain. *J Biol Chem* **281**, 19038-19044, doi:10.1074/jbc.M601178200 (2006).
103 Ramadan, K., Shevelev, I. V., Maga, G. & Hubscher, U. DNA polymerase lambda from calf thymus preferentially replicates damaged DNA. *J Biol Chem* **277**, 18454-18458, doi:10.1074/jbc.M200421200 (2002).
104 Blanca, G. *et al.* Human DNA polymerases lambda and beta show different efficiencies of translesion DNA synthesis past abasic sites and alternative

mechanisms for frameshift generation. *Biochemistry* **43**, 11605-11615, doi:10.1021/bi049050x (2004).
105 Yamtich, J. & Sweasy, J. B. DNA polymerase family X: function, structure, and cellular roles. *Biochim Biophys Acta* **1804**, 1136-1150, doi:10.1016/j.bbapap.2009.07.008 (2010).
106 Lee, J. W. *et al.* Implication of DNA polymerase lambda in alignment-based gap filling for nonhomologous DNA end joining in human nuclear extracts. *J Biol Chem* **279**, 805-811, doi:10.1074/jbc.M307913200 (2004).
107 Lieber, M. R. The polymerases for V(D)J recombination. *Immunity* **25**, 7-9, doi:10.1016/j.immuni.2006.07.007 (2006).
108 Pavlov, Y. I., Shcherbakova, P. V. & Rogozin, I. B. Roles of DNA polymerases in replication, repair, and recombination in eukaryotes. *Int Rev Cytol* **255**, 41-132, doi:10.1016/S0074-7696(06)55002-8 (2006).
109 Moon, A. F. *et al.* The X family portrait: structural insights into biological functions of X family polymerases. *DNA Repair (Amst)* **6**, 1709-1725, doi:10.1016/j.dnarep.2007.05.009 (2007).
110 Duym, W. W., Fiala, K. A., Bhatt, N. & Suo, Z. Kinetic effect of a downstream strand and its 5'-terminal moieties on single nucleotide gap-filling synthesis catalyzed by human DNA polymerase lambda. *J Biol Chem* **281**, 35649-35655, doi:10.1074/jbc.M607479200 (2006).
111 Markkanen, E. *et al.* Regulation of oxidative DNA damage repair by DNA polymerase lambda and MutYH by cross-talk of phosphorylation and ubiquitination. *Proc Natl Acad Sci U S A* **109**, 437-442, doi:10.1073/pnas.1110449109 (2012).
112 Maga, G. *et al.* 8-oxo-guanine bypass by human DNA polymerases in the presence of auxiliary proteins. *Nature* **447**, 606-608, doi:10.1038/nature05843 (2007).
113 Kunkel, T. A. & Alexander, P. S. The base substitution fidelity of eucaryotic DNA polymerases. Mispairing frequencies, site preferences, insertion preferences, and base substitution by dislocation. *J Biol Chem* **261**, 160-166 (1986).
114 Kobayashi, S., Valentine, M. R., Pham, P., O'Donnell, M. & Goodman, M. F. Fidelity of Escherichia coli DNA polymerase IV. Preferential generation of small deletion mutations by dNTP-stabilized misalignment. *J Biol Chem* **277**, 34198-34207, doi:10.1074/jbc.M204826200 (2002).
115 Hashim, M. F., Schnetz-Boutaud, N. & Marnett, L. J. Replication of template-primers containing propanodeoxyguanosine by DNA polymerase beta. Induction of base pair substitution and frameshift mutations by template slippage and deoxynucleoside triphosphate stabilization. *J Biol Chem* **272**, 20205-20212 (1997).
116 Bebenek, K., Garcia-Diaz, M., Blanco, L. & Kunkel, T. A. The frameshift infidelity of human DNA polymerase lambda. Implications for function. *J Biol Chem* **278**, 34685-34690, doi:10.1074/jbc.M305705200 (2003).
117 Frouin, I., Toueille, M., Ferrari, E., Shevelev, I. & Hubscher, U. Phosphorylation of human DNA polymerase lambda by the cyclin-dependent kinase Cdk2/cyclin A complex is modulated by its association with proliferating cell nuclear antigen. *Nucleic Acids Res* **33**, 5354-5361, doi:10.1093/nar/gki845 (2005).
118 Markkanen, E., Hubscher, U. & van Loon, B. Regulation of oxidative DNA damage repair: the adenine:8-oxo-guanine problem. *Cell Cycle* **11**, 1070-1075, doi:10.4161/cc.11.6.19448 (2012).
119 Wimmer, U., Ferrari, E., Hunziker, P. & Hubscher, U. Control of DNA polymerase lambda stability by phosphorylation and ubiquitination during the cell cycle. *EMBO Rep* **9**, 1027-1033, doi:10.1038/embor.2008.148 (2008).
120 Frouin, E. *et al.* [Hypersensitivity to fluindione (Previscan). Positive skin patch tests]. *Ann Dermatol Venereol* **132**, 1000-1002 (2005).
121 Markkanen, E., van Loon, B., Ferrari, E. & Hubscher, U. Ubiquitylation of DNA polymerase lambda. *FEBS Lett* **585**, 2826-2830, doi:10.1016/j.febslet.2011.03.069 (2011).
122 Hershko, A. & Ciechanover, A. The ubiquitin system. *Annu Rev Biochem* **67**, 425-479, doi:10.1146/annurev.biochem.67.1.425 (1998).
123 Kerscher, O., Felberbaum, R. & Hochstrasser, M. Modification of proteins by ubiquitin and ubiquitin-like proteins. *Annu Rev Cell Dev Biol* **22**, 159-180, doi:10.1146/annurev.cellbio.22.010605.093503 (2006).

124 Komander, D. & Rape, M. The ubiquitin code. *Annu Rev Biochem* **81**, 203-229, doi:10.1146/annurev-biochem-060310-170328 (2012).
125 Weissman, A. M. Themes and variations on ubiquitylation. *Nat Rev Mol Cell Biol* **2**, 169-178, doi:10.1038/35056563 (2001).
126 Dye, B. T. & Schulman, B. A. Structural mechanisms underlying posttranslational modification by ubiquitin-like proteins. *Annu Rev Biophys Biomol Struct* **36**, 131-150, doi:10.1146/annurev.biophys.36.040306.132820 (2007).
127 Husnjak, K. & Dikic, I. Ubiquitin-binding proteins: decoders of ubiquitin-mediated cellular functions. *Annu Rev Biochem* **81**, 291-322, doi:10.1146/annurev-biochem-051810-094654 (2012).
128 Flick, K. *et al.* Proteolysis-independent regulation of the transcription factor Met4 by a single Lys 48-linked ubiquitin chain. *Nat Cell Biol* **6**, 634-641, doi:10.1038/ncb1143 (2004).
129 Thrower, J. S., Hoffman, L., Rechsteiner, M. & Pickart, C. M. Recognition of the polyubiquitin proteolytic signal. *Embo J* **19**, 94-102, doi:10.1093/emboj/19.1.94 (2000).
130 Ye, Y. & Rape, M. Building ubiquitin chains: E2 enzymes at work. *Nat Rev Mol Cell Biol* **10**, 755-764, doi:10.1038/nrm2780 (2009).
131 Chen, Z. J. & Sun, L. J. Nonproteolytic functions of ubiquitin in cell signaling. *Mol Cell* **33**, 275-286, doi:10.1016/j.molcel.2009.01.014 (2009).
132 Ikeda, F. & Dikic, I. Atypical ubiquitin chains: new molecular signals. 'Protein Modifications: Beyond the Usual Suspects' review series. *EMBO Rep* **9**, 536-542, doi:10.1038/embor.2008.93 (2008).
133 Kulathu, Y. & Komander, D. Atypical ubiquitylation - the unexplored world of polyubiquitin beyond Lys48 and Lys63 linkages. *Nat Rev Mol Cell Biol* **13**, 508-523, doi:10.1038/nrm3394 (2012).
134 Spence, J., Sadis, S., Haas, A. L. & Finley, D. A ubiquitin mutant with specific defects in DNA repair and multiubiquitination. *Mol Cell Biol* **15**, 1265-1273 (1995).
135 Dikic, I., Wakatsuki, S. & Walters, K. J. Ubiquitin-binding domains - from structures to functions. *Nat Rev Mol Cell Biol* **10**, 659-671, doi:10.1038/nrm2767 (2009).
136 Finley, D. Recognition and processing of ubiquitin-protein conjugates by the proteasome. *Annu Rev Biochem* **78**, 477-513, doi:10.1146/annurev.biochem.78.081507.101607 (2009).
137 Varshavsky, A. Regulated protein degradation. *Trends Biochem Sci* **30**, 283-286, doi:10.1016/j.tibs.2005.04.005 (2005).
138 Ziv, I. *et al.* A perturbed ubiquitin landscape distinguishes between ubiquitin in trafficking and in proteolysis. *Mol Cell Proteomics* **10**, M111 009753, doi:10.1074/mcp.M111.009753 (2011).
139 Komander, D., Clague, M. J. & Urbe, S. Breaking the chains: structure and function of the deubiquitinases. *Nat Rev Mol Cell Biol* **10**, 550-563, doi:10.1038/nrm2731 (2009).
140 Reyes-Turcu, F. E., Ventii, K. H. & Wilkinson, K. D. Regulation and cellular roles of ubiquitin-specific deubiquitinating enzymes. *Annu Rev Biochem* **78**, 363-397, doi:10.1146/annurev.biochem.78.082307.091526 (2009).
141 Ciechanover, A. The ubiquitin proteolytic system and pathogenesis of human diseases: a novel platform for mechanism-based drug targeting. *Biochem Soc Trans* **31**, 474-481, doi:10.1042/ (2003).
142 Liu, Z., Miao, D., Xia, Q., Hermo, L. & Wing, S. S. Regulated expression of the ubiquitin protein ligase, E3(Histone)/LASU1/Mule/ARF-BP1/HUWE1, during spermatogenesis. *Dev Dyn* **236**, 2889-2898, doi:10.1002/dvdy.21302 (2007).
143 Huibregtse, J. M., Scheffner, M., Beaudenon, S. & Howley, P. M. A family of proteins structurally and functionally related to the E6-AP ubiquitin-protein ligase. *Proc Natl Acad Sci U S A* **92**, 5249 (1995).
144 Pandya, R. K., Partridge, J. R., Love, K. R., Schwartz, T. U. & Ploegh, H. L. A structural element within the HUWE1 HECT domain modulates self-ubiquitination and substrate ubiquitination activities. *J Biol Chem* **285**, 5664-5673, doi:10.1074/jbc.M109.051805 (2010).
145 Kishino, T., Lalande, M. & Wagstaff, J. UBE3A/E6-AP mutations cause Angelman syndrome. *Nat Genet* **15**, 70-73, doi:10.1038/ng0197-70 (1997).

146 Philpot, B. D., Thompson, C. E., Franco, L. & Williams, C. A. Angelman syndrome: advancing the research frontier of neurodevelopmental disorders. *J Neurodev Disord* **3**, 50-56, doi:10.1007/s11689-010-9066-z (2011).
147 Huang, L. *et al.* Structure of an E6AP-UbcH7 complex: insights into ubiquitination by the E2-E3 enzyme cascade. *Science* **286**, 1321-1326 (1999).
148 Rotin, D. & Kumar, S. Physiological functions of the HECT family of ubiquitin ligases. *Nat Rev Mol Cell Biol* **10**, 398-409, doi:10.1038/nrm2690 (2009).
149 Bernassola, F., Karin, M., Ciechanover, A. & Melino, G. The HECT family of E3 ubiquitin ligases: multiple players in cancer development. *Cancer Cell* **14**, 10-21, doi:10.1016/j.ccr.2008.06.001 (2008).
150 Chen, D. *et al.* ARF-BP1/Mule is a critical mediator of the ARF tumor suppressor. *Cell* **121**, 1071-1083, doi:10.1016/j.cell.2005.03.037 (2005).
151 Adhikary, S. *et al.* The ubiquitin ligase HectH9 regulates transcriptional activation by Myc and is essential for tumor cell proliferation. *Cell* **123**, 409-421, doi:10.1016/j.cell.2005.08.016 (2005).
152 Confalonieri, S. *et al.* Alterations of ubiquitin ligases in human cancer and their association with the natural history of the tumor. *Oncogene* **28**, 2959-2968, doi:10.1038/onc.2009.156 (2009).
153 Yang, Y. *et al.* Small molecule inhibitors of HDM2 ubiquitin ligase activity stabilize and activate p53 in cells. *Cancer Cell* **7**, 547-559, doi:10.1016/j.ccr.2005.04.029 (2005).
154 Chen, D., Brooks, C. L. & Gu, W. ARF-BP1 as a potential therapeutic target. *Br J Cancer* **94**, 1555-1558, doi:10.1038/sj.bjc.6603119 (2006).
155 Zhong, Q., Gao, W., Du, F. & Wang, X. Mule/ARF-BP1, a BH3-only E3 ubiquitin ligase, catalyzes the polyubiquitination of Mcl-1 and regulates apoptosis. *Cell* **121**, 1085-1095, doi:10.1016/j.cell.2005.06.009 (2005).
156 Shmueli, A. & Oren, M. Life, death, and ubiquitin: taming the mule. *Cell* **121**, 963-965, doi:10.1016/j.cell.2005.06.018 (2005).
157 Hall, J. R. *et al.* Cdc6 stability is regulated by the Huwe1 ubiquitin ligase after DNA damage. *Mol Biol Cell* **18**, 3340-3350, doi:10.1091/mbc.E07-02-0173 (2007).
158 Parsons, J. L. *et al.* Ubiquitin ligase ARF-BP1/Mule modulates base excision repair. *Embo J* **28**, 3207-3215, doi:10.1038/emboj.2009.243 (2009).
159 Zhang, Y., Xiong, Y. & Yarbrough, W. G. ARF promotes MDM2 degradation and stabilizes p53: ARF-INK4a locus deletion impairs both the Rb and p53 tumor suppression pathways. *Cell* **92**, 725-734 (1998).
160 Yoon, S. Y. *et al.* Over-expression of human UREB1 in colorectal cancer: HECT domain of human UREB1 inhibits the activity of tumor suppressor p53 protein. *Biochem Biophys Res Commun* **326**, 7-17, doi:10.1016/j.bbrc.2004.11.004 (2005).
161 Khoronenkova, S. V. & Dianov, G. L. The emerging role of Mule and ARF in the regulation of base excision repair. *FEBS Lett* **585**, 2831-2835, doi:10.1016/j.febslet.2011.06.015 (2011).
162 Khoronenkova, S. V. & Dianov, G. L. USP7S-dependent inactivation of Mule regulates DNA damage signalling and repair. *Nucleic Acids Res* **41**, 1750-1756, doi:10.1093/nar/gks1359 (2013).
163 Kon, N., Zhong, J., Qiang, L., Accili, D. & Gu, W. Inactivation of arf-bp1 induces p53 activation and diabetic phenotypes in mice. *J Biol Chem* **287**, 5102-5111, doi:10.1074/jbc.M111.322867 (2012).
164 Nicholson, B. & Suresh Kumar, K. G. The multifaceted roles of USP7: new therapeutic opportunities. *Cell Biochem Biophys* **60**, 61-68, doi:10.1007/s12013-011-9185-5 (2011).
165 Khoronenkova, S. V. *et al.* ATM-dependent downregulation of USP7/HAUSP by PPM1G activates p53 response to DNA damage. *Mol Cell* **45**, 801-813, doi:10.1016/j.molcel.2012.01.021 (2012).
166 Sowa, M. E., Bennett, E. J., Gygi, S. P. & Harper, J. W. Defining the human deubiquitinating enzyme interaction landscape. *Cell* **138**, 389-403, doi:10.1016/j.cell.2009.04.042 (2009).
167 Saxena, S. & Caroni, P. Selective neuronal vulnerability in neurodegenerative diseases: from stressor thresholds to degeneration. *Neuron* **71**, 35-48, doi:10.1016/j.neuron.2011.06.031 (2011).

168 Herrup, K. & Yang, Y. Cell cycle regulation in the postmitotic neuron: oxymoron or new biology? *Nat Rev Neurosci* **8**, 368-378, doi:10.1038/nrn2124 (2007).
169 Kruman, II. Why do neurons enter the cell cycle? *Cell Cycle* **3**, 769-773 (2004).
170 Yang, Y., Geldmacher, D. S. & Herrup, K. DNA replication precedes neuronal cell death in Alzheimer's disease. *J Neurosci* **21**, 2661-2668 (2001).
171 Hanawalt, P. C. Emerging links between premature ageing and defective DNA repair. *Mech Ageing Dev* **129**, 503-505, doi:10.1016/j.mad.2008.03.007 (2008).
172 See, V. & Loeffler, J. P. Oxidative stress induces neuronal death by recruiting a protease and phosphatase-gated mechanism. *J Biol Chem* **276**, 35049-35059, doi:10.1074/jbc.M104988200 (2001).
173 Graeber, M. B. & Moran, L. B. Mechanisms of cell death in neurodegenerative diseases: fashion, fiction, and facts. *Brain Pathol* **12**, 385-390 (2002).
174 Katyal, S. & McKinnon, P. J. DNA repair deficiency and neurodegeneration. *Cell Cycle* **6**, 2360-2365 (2007).
175 Orii, K. E., Lee, Y., Kondo, N. & McKinnon, P. J. Selective utilization of nonhomologous end-joining and homologous recombination DNA repair pathways during nervous system development. *Proc Natl Acad Sci U S A* **103**, 10017-10022, doi:10.1073/pnas.0602436103 (2006).
176 Kety, S. S. The circulation, metabolism, and functional activity of the human brain. *Neurochem Res* **16**, 1073-1078 (1991).
177 Halliwell, B. Oxidative stress and neurodegeneration: where are we now? *J Neurochem* **97**, 1634-1658, doi:10.1111/j.1471-4159.2006.03907.x (2006).
178 Boveris, A. & Chance, B. The mitochondrial generation of hydrogen peroxide. General properties and effect of hyperbaric oxygen. *Biochem J* **134**, 707-716 (1973).
179 Barzilai, A. The contribution of the DNA damage response to neuronal viability. *Antioxid Redox Signal* **9**, 211-218, doi:10.1089/ars.2007.9.ft-6 (2007).
180 Beal, M. F. Aging, energy, and oxidative stress in neurodegenerative diseases. *Ann Neurol* **38**, 357-366, doi:10.1002/ana.410380304 (1995).
181 Federico, A. *et al.* Mitochondria, oxidative stress and neurodegeneration. *J Neurol Sci* **322**, 254-262, doi:10.1016/j.jns.2012.05.030 (2012).
182 Moos, T. & Morgan, E. H. The metabolism of neuronal iron and its pathogenic role in neurological disease: review. *Ann N Y Acad Sci* **1012**, 14-26 (2004).
183 Shin, S. Y. *et al.* Hydrogen peroxide negatively modulates Wnt signaling through downregulation of beta-catenin. *Cancer Lett* **212**, 225-231, doi:10.1016/j.canlet.2004.03.003 (2004).
184 Serrano, F. & Klann, E. Reactive oxygen species and synaptic plasticity in the aging hippocampus. *Ageing Res Rev* **3**, 431-443, doi:10.1016/j.arr.2004.05.002 (2004).
185 Zhu, D. *et al.* Hydrogen peroxide alters membrane and cytoskeleton properties and increases intercellular connections in astrocytes. *J Cell Sci* **118**, 3695-3703, doi:10.1242/jcs.02507 (2005).
186 Lin, H. J., Wang, X., Shaffer, K. M., Sasaki, C. Y. & Ma, W. Characterization of H2O2-induced acute apoptosis in cultured neural stem/progenitor cells. *FEBS Lett* **570**, 102-106, doi:10.1016/j.febslet.2004.06.019 (2004).
187 Butterfield, D. A. & Lauderback, C. M. Lipid peroxidation and protein oxidation in Alzheimer's disease brain: potential causes and consequences involving amyloid beta-peptide-associated free radical oxidative stress. *Free Radic Biol Med* **32**, 1050-1060 (2002).
188 Mohsenzadegan, M. & Mirshafiey, A. The immunopathogenic role of reactive oxygen species in Alzheimer disease. *Iran J Allergy Asthma Immunol* **11**, 203-216, doi:011.03/ijaai.203216 (2012).
189 Montine, K. S. *et al.* Isoprostanes and related products of lipid peroxidation in neurodegenerative diseases. *Chem Phys Lipids* **128**, 117-124, doi:10.1016/j.chemphyslip.2003.10.010 (2004).
190 Humeau, Y., Gambino, F., Chelly, J. & Vitale, N. X-linked mental retardation: focus on synaptic function and plasticity. *J Neurochem* **109**, 1-14, doi:10.1111/j.1471-4159.2009.05881.x (2009).

191 Wang, X. *et al.* Genomic and biochemical approaches in the discovery of mechanisms for selective neuronal vulnerability to oxidative stress. *BMC Neurosci* **10**, 12, doi:10.1186/1471-2202-10-12 (2009).
192 Foster, T. C. Calcium homeostasis and modulation of synaptic plasticity in the aged brain. *Aging Cell* **6**, 319-325, doi:10.1111/j.1474-9726.2007.00283.x (2007).
193 Andersen, J. K. Oxidative stress in neurodegeneration: cause or consequence? *Nat Med* **10 Suppl**, S18-25, doi:10.1038/nrn1434 (2004).
194 Ljungman, M. & Lane, D. P. Transcription - guarding the genome by sensing DNA damage. *Nat Rev Cancer* **4**, 727-737, doi:10.1038/nrc1435 (2004).
195 Borgesius, N. Z. *et al.* Accelerated age-related cognitive decline and neurodegeneration, caused by deficient DNA repair. *J Neurosci* **31**, 12543-12553, doi:10.1523/JNEUROSCI.1589-11.2011 (2011).
196 Hegde, M. L. *et al.* Oxidative genome damage and its repair: implications in aging and neurodegenerative diseases. *Mech Ageing Dev* **133**, 157-168, doi:10.1016/j.mad.2012.01.005 (2012).
197 Wilson, D. M., 3rd & McNeill, D. R. Base excision repair and the central nervous system. *Neuroscience* **145**, 1187-1200, doi:10.1016/j.neuroscience.2006.07.011 (2007).
198 Melis, J. P., van Steeg, H. & Luijten, M. Oxidative DNA Damage and Nucleotide Excision Repair. *Antioxid Redox Signal*, doi:10.1089/ars.2012.5036 (2012).
199 Nouspikel, T. & Hanawalt, P. C. Terminally differentiated human neurons repair transcribed genes but display attenuated global DNA repair and modulation of repair gene expression. *Mol Cell Biol* **20**, 1562-1570 (2000).
200 Swain, U. & Rao, K. S. Age-dependent decline of DNA base excision repair activity in rat cortical neurons. *Mech Ageing Dev* **133**, 186-194, doi:10.1016/j.mad.2012.01.001 (2012).
201 Bosshard, M., Markkanen, E. & van Loon, B. Base excision repair in physiology and pathology of the central nervous system. *Int J Mol Sci* **13**, 16172-16222, doi:10.3390/ijms131216172 (2012).
202 Li, P. *et al.* Mechanistic insight into DNA damage and repair in ischemic stroke: exploiting the base excision repair pathway as a model of neuroprotection. *Antioxid Redox Signal* **14**, 1905-1918, doi:10.1089/ars.2010.3451 (2011).
203 Sheng, Z. *et al.* 8-Oxoguanine causes neurodegeneration during MUTYH-mediated DNA base excision repair. *J Clin Invest*, doi:10.1172/JCI65053 (2012).
204 Siegel, C. & McCullough, L. D. NAD+ depletion or PAR polymer formation: which plays the role of executioner in ischaemic cell death? *Acta Physiol (Oxf)* **203**, 225-234, doi:10.1111/j.1748-1716.2010.02229.x (2011).
205 Chaitanya, G. V., Steven, A. J. & Babu, P. P. PARP-1 cleavage fragments: signatures of cell-death proteases in neurodegeneration. *Cell Commun Signal* **8**, 31, doi:10.1186/1478-811X-8-31 (2010).
206 Elmore, S. Apoptosis: a review of programmed cell death. *Toxicol Pathol* **35**, 495-516, doi:10.1080/01926230701320337 (2007).
207 Jellinger, K. A. Cell death mechanisms in neurodegeneration. *J Cell Mol Med* **5**, 1-17 (2001).
208 Ying, W. & Xiong, Z. G. Oxidative stress and NAD+ in ischemic brain injury: current advances and future perspectives. *Curr Med Chem* **17**, 2152-2158 (2010).
209 Mattson, M. P. Apoptosis in neurodegenerative disorders. *Nat Rev Mol Cell Biol* **1**, 120-129, doi:10.1038/35040009 (2000).
210 Chiurazzi, P., Tabolacci, E. & Neri, G. X-linked mental retardation (XLMR): from clinical conditions to cloned genes. *Crit Rev Clin Lab Sci* **41**, 117-158, doi:10.1080/10408360490443013 (2004).
211 Froyen, G. *et al.* Detection of genomic copy number changes in patients with idiopathic mental retardation by high-resolution X-array-CGH: important role for increased gene dosage of XLMR genes. *Hum Mutat* **28**, 1034-1042, doi:10.1002/humu.20564 (2007).
212 Chiurazzi, P., Schwartz, C. E., Gecz, J. & Neri, G. XLMR genes: update 2007. *Eur J Hum Genet* **16**, 422-434, doi:10.1038/sj.ejhg.5201994 (2008).
213 Shea, S. E. Intellectual disability (mental retardation). *Pediatr Rev* **33**, 110-121; quiz 120-111, doi:10.1542/pir.33-3-110 (2012).

214 Ropers, H. H. X-linked mental retardation: many genes for a complex disorder. *Curr Opin Genet Dev* **16**, 260-269, doi:10.1016/j.gde.2006.04.017 (2006).
215 Bauters, M. *et al.* Detection and validation of copy number variation in X-linked mental retardation. *Cytogenet Genome Res* **123**, 44-53, doi:10.1159/000184691 (2008).
216 Skuse, D. H. X-linked genes and mental functioning. *Hum Mol Genet* **14 Spec No 1**, R27-32, doi:10.1093/hmg/ddi112 (2005).
217 Turner, G. Finding genes on the X chromosome by which homo may have become sapiens. *Am J Hum Genet* **58**, 1109-1110 (1996).
218 Graves, J. A., Gecz, J. & Hameister, H. Evolution of the human X--a smart and sexy chromosome that controls speciation and development. *Cytogenet Genome Res* **99**, 141-145, doi:71585 (2002).
219 Zechner, U. *et al.* A high density of X-linked genes for general cognitive ability: a run-away process shaping human evolution? *Trends Genet* **17**, 697-701 (2001).
220 Gijsbers, A. C. *et al.* X-chromosome duplications in males with mental retardation: pathogenic or benign variants? *Clin Genet* **79**, 71-78, doi:10.1111/j.1399-0004.2010.01438.x (2011).
221 Stevenson, R. E. & Schwartz, C. E. Clinical and molecular contributions to the understanding of X-linked mental retardation. *Cytogenet Genome Res* **99**, 265-275, doi:71603 (2002).
222 Ropers, H. H. & Hamel, B. C. X-linked mental retardation. *Nat Rev Genet* **6**, 46-57, doi:10.1038/nrg1501 (2005).
223 Govek, E. E. *et al.* The X-linked mental retardation protein oligophrenin-1 is required for dendritic spine morphogenesis. *Nat Neurosci* **7**, 364-372, doi:10.1038/nn1210 (2004).
224 Ramakers, G. J. Rho proteins, mental retardation and the cellular basis of cognition. *Trends Neurosci* **25**, 191-199 (2002).
225 Scheiffele, P., Fan, J., Choih, J., Fetter, R. & Serafini, T. Neuroligin expressed in nonneuronal cells triggers presynaptic development in contacting axons. *Cell* **101**, 657-669 (2000).
226 Dean, C. *et al.* Neurexin mediates the assembly of presynaptic terminals. *Nat Neurosci* **6**, 708-716, doi:10.1038/nn1074 (2003).
227 Berry-Kravis, E., Knox, A. & Hervey, C. Targeted treatments for fragile X syndrome. *J Neurodev Disord* **3**, 193-210, doi:10.1007/s11689-011-9074-7 (2011).
228 Franco, M., Seyfried, N. T., Brand, A. H., Peng, J. & Mayor, U. A novel strategy to isolate ubiquitin conjugates reveals wide role for ubiquitination during neural development. *Mol Cell Proteomics* **10**, M110 002188, doi:10.1074/mcp.M110.002188 (2011).
229 Zhao, X. *et al.* The HECT-domain ubiquitin ligase Huwe1 controls neural differentiation and proliferation by destabilizing the N-Myc oncoprotein. *Nat Cell Biol* **10**, 643-653, doi:10.1038/ncb1727 (2008).
230 D'Arca, D. *et al.* Huwe1 ubiquitin ligase is essential to synchronize neuronal and glial differentiation in the developing cerebellum. *Proc Natl Acad Sci U S A* **107**, 5875-5880, doi:10.1073/pnas.0912874107 (2010).
231 Bence, N. F., Sampat, R. M. & Kopito, R. R. Impairment of the ubiquitin-proteasome system by protein aggregation. *Science* **292**, 1552-1555, doi:10.1126/science.292.5521.1552 (2001).
232 Mayer, R. J., Lowe, J., Lennox, G., Doherty, F. & Landon, M. Intermediate filaments and ubiquitin: a new thread in the understanding of chronic neurodegenerative diseases. *Prog Clin Biol Res* **317**, 809-818 (1989).
233 Cripps, D. *et al.* Alzheimer disease-specific conformation of hyperphosphorylated paired helical filament-Tau is polyubiquitinated through Lys-48, Lys-11, and Lys-6 ubiquitin conjugation. *J Biol Chem* **281**, 10825-10838, doi:10.1074/jbc.M512786200 (2006).
234 van Leeuwen, F. W., Hol, E. M. & Fischer, D. F. Frameshift proteins in Alzheimer's disease and in other conformational disorders: time for the ubiquitin-proteasome system. *J Alzheimers Dis* **9**, 319-325 (2006).
235 Ross, C. A. & Pickart, C. M. The ubiquitin-proteasome pathway in Parkinson's disease and other neurodegenerative diseases. *Trends Cell Biol* **14**, 703-711, doi:10.1016/j.tcb.2004.10.006 (2004).

236 Bennett, E. J. *et al.* Global changes to the ubiquitin system in Huntington's disease. *Nature* **448**, 704-708, doi:10.1038/nature06022 (2007).
237 Froyen, G. *et al.* Copy-number gains of HUWE1 due to replication- and recombination-based rearrangements. *Am J Hum Genet* **91**, 252-264, doi:10.1016/j.ajhg.2012.06.010 (2012).
238 Hui-Yuen, J., McAllister, S., Koganti, S., Hill, E. & Bhaduri-McIntosh, S. Establishment of Epstein-Barr virus growth-transformed lymphoblastoid cell lines. *J Vis Exp*, doi:10.3791/3321 (2011).
239 Tanaka, M., Lai, J. S. & Herr, W. Promoter-selective activation domains in Oct-1 and Oct-2 direct differential activation of an snRNA and mRNA promoter. *Cell* **68**, 755-767 (1992).
240 Mendez, J. & Stillman, B. Chromatin association of human origin recognition complex, cdc6, and minichromosome maintenance proteins during the cell cycle: assembly of prereplication complexes in late mitosis. *Mol Cell Biol* **20**, 8602-8612 (2000).
241 Shimazaki, N. *et al.* Over-expression of human DNA polymerase lambda in E. coli and characterization of the recombinant enzyme. *Genes Cells* **7**, 639-651 (2002).
242 Pedrali-Noy, G. & Spadari, S. Effect of aphidicolin on viral and human DNA polymerases. *Biochem Biophys Res Commun* **88**, 1194-1202 (1979).
243 Lu, A. L. & Fawcett, W. P. Characterization of the recombinant MutY homolog, an adenine DNA glycosylase, from yeast Schizosaccharomyces pombe. *J Biol Chem* **273**, 25098-25105 (1998).
244 Shinmura, K. *et al.* Adenine excisional repair function of MYH protein on the adenine:8-hydroxyguanine base pair in double-stranded DNA. *Nucleic Acids Res* **28**, 4912-4918 (2000).
245 Slupska, M. M., Luther, W. M., Chiang, J. H., Yang, H. & Miller, J. H. Functional expression of hMYH, a human homolog of the Escherichia coli MutY protein. *J Bacteriol* **181**, 6210-6213 (1999).
246 Shibutani, S., Takeshita, M. & Grollman, A. P. Translesional synthesis on DNA templates containing a single abasic site. A mechanistic study of the "A rule". *J Biol Chem* **272**, 13916-13922 (1997).
247 Kalam, M. A. & Basu, A. K. Mutagenesis of 8-oxoguanine adjacent to an abasic site in simian kidney cells: tandem mutations and enhancement of G-->T transversions. *Chem Res Toxicol* **18**, 1187-1192, doi:10.1021/tx050119r (2005).
248 Villani, G. *et al.* In vitro gap-directed translesion DNA synthesis of an abasic site involving human DNA polymerases epsilon, lambda, and beta. *J Biol Chem* **286**, 32094-32104, doi:10.1074/jbc.M111.246611 (2011).
249 Hegde, M. L., Izumi, T. & Mitra, S. Oxidized base damage and single-strand break repair in mammalian genomes: role of disordered regions and posttranslational modifications in early enzymes. *Prog Mol Biol Transl Sci* **110**, 123-153, doi:10.1016/B978-0-12-387665-2.00006-7 (2012).
250 Jackson, S. P. & Durocher, D. Regulation of DNA damage responses by ubiquitin and SUMO. *Mol Cell* **49**, 795-807, doi:10.1016/j.molcel.2013.01.017 (2013).
251 Zhang, J. *et al.* Mule determines the apoptotic response to HDAC inhibitors by targeted ubiquitination and destruction of HDAC2. *Genes Dev* **25**, 2610-2618, doi:10.1101/gad.170605.111 (2011).
252 Robertson, K. D. DNA methylation and human disease. *Nat Rev Genet* **6**, 597-610, doi:10.1038/nrg1655 (2005).
253 Weake, V. M. & Workman, J. L. Inducible gene expression: diverse regulatory mechanisms. *Nat Rev Genet* **11**, 426-437, doi:10.1038/nrg2781 (2010).
254 Daniel, F. I., Cherubini, K., Yurgel, L. S., de Figueiredo, M. A. & Salum, F. G. The role of epigenetic transcription repression and DNA methyltransferases in cancer. *Cancer* **117**, 677-687, doi:10.1002/cncr.25482 (2011).
255 Mancuso, C. *et al.* Mitochondrial dysfunction, free radical generation and cellular stress response in neurodegenerative disorders. *Front Biosci* **12**, 1107-1123 (2007).
256 Demple, B. & DeMott, M. S. Dynamics and diversions in base excision DNA repair of oxidized abasic lesions. *Oncogene* **21**, 8926-8934, doi:10.1038/sj.onc.1206178 (2002).

257 Sayre, L. M., Perry, G. & Smith, M. A. Oxidative stress and neurotoxicity. *Chem Res Toxicol* **21**, 172-188, doi:10.1021/tx700210j (2008).
258 de Nadal, E., Ammerer, G. & Posas, F. Controlling gene expression in response to stress. *Nat Rev Genet* **12**, 833-845, doi:10.1038/nrg3055 (2011).
259 Obulesu, M. & Jhansilakshmi, M. Neuroinflammation in Alzheimer's Disease: An understanding of physiology and pathology. *Int J Neurosci*, doi:10.3109/00207454.2013.831852 (2013).
260 Lau, E., Zhu, C., Abraham, R. T. & Jiang, W. The functional role of Cdc6 in S-G2/M in mammalian cells. *EMBO Rep* **7**, 425-430, doi:10.1038/sj.embor.7400624 (2006).
261 Duursma, A. & Agami, R. p53-Dependent regulation of Cdc6 protein stability controls cellular proliferation. *Mol Cell Biol* **25**, 6937-6947, doi:10.1128/MCB.25.16.6937-6947.2005 (2005).
262 Duursma, A. M. & Agami, R. CDK-dependent stabilization of Cdc6: linking growth and stress signals to activation of DNA replication. *Cell Cycle* **4**, 1725-1728 (2005).
263 Adhikary, S. & Eilers, M. Transcriptional regulation and transformation by Myc proteins. *Nat Rev Mol Cell Biol* **6**, 635-645, doi:10.1038/nrm1703 (2005).
264 Herold, S. *et al.* Miz1 and HectH9 regulate the stability of the checkpoint protein, TopBP1. *Embo J* **27**, 2851-2861, doi:10.1038/emboj.2008.200 (2008).
265 Bernard, O., Drago, J. & Sheng, H. L-myc and N-myc influence lineage determination in the central nervous system. *Neuron* **9**, 1217-1224 (1992).
266 West, M. H. & Bonner, W. M. Histone 2B can be modified by the attachment of ubiquitin. *Nucleic Acids Res* **8**, 4671-4680 (1980).
267 Fukuda, H., Sano, N., Muto, S. & Horikoshi, M. Simple histone acetylation plays a complex role in the regulation of gene expression. *Brief Funct Genomic Proteomic* **5**, 190-208, doi:10.1093/bfgp/ell032 (2006).
268 Tan, J., Cang, S., Ma, Y., Petrillo, R. L. & Liu, D. Novel histone deacetylase inhibitors in clinical trials as anti-cancer agents. *J Hematol Oncol* **3**, 5, doi:10.1186/1756-8722-3-5 (2010).
269 Guan, J. S. *et al.* HDAC2 negatively regulates memory formation and synaptic plasticity. *Nature* **459**, 55-60, doi:10.1038/nature07925 (2009).
270 LeBoeuf, M. *et al.* Hdac1 and Hdac2 act redundantly to control p63 and p53 functions in epidermal progenitor cells. *Dev Cell* **19**, 807-818, doi:10.1016/j.devcel.2010.10.015 (2010).
271 Liu, Z., Oughtred, R. & Wing, S. S. Characterization of E3Histone, a novel testis ubiquitin protein ligase which ubiquitinates histones. *Mol Cell Biol* **25**, 2819-2831, doi:10.1128/MCB.25.7.2819-2831.2005 (2005).
272 Noy, T., Suad, O., Taglicht, D. & Ciechanover, A. HUWE1 ubiquitinates MyoD and targets it for proteasomal degradation. *Biochem Biophys Res Commun* **418**, 408-413, doi:10.1016/j.bbrc.2012.01.045 (2012).
273 Yin, L., Joshi, S., Wu, N., Tong, X. & Lazar, M. A. E3 ligases Arf-bp1 and Pam mediate lithium-stimulated degradation of the circadian heme receptor Rev-erb alpha. *Proc Natl Acad Sci U S A* **107**, 11614-11619, doi:10.1073/pnas.1000438107 (2010).
274 Berkes, C. A. & Tapscott, S. J. MyoD and the transcriptional control of myogenesis. *Semin Cell Dev Biol* **16**, 585-595, doi:10.1016/j.semcdb.2005.07.006 (2005).
275 Bentzinger, C. F., Wang, Y. X. & Rudnicki, M. A. Building muscle: molecular regulation of myogenesis. *Cold Spring Harb Perspect Biol* **4**, doi:10.1101/cshperspect.a008342 (2012).
276 Yokoyama, S. & Asahara, H. The myogenic transcriptional network. *Cell Mol Life Sci* **68**, 1843-1849, doi:10.1007/s00018-011-0629-2 (2011).
277 Sousa-Victor, P., Munoz-Canoves, P. & Perdiguero, E. Regulation of skeletal muscle stem cells through epigenetic mechanisms. *Toxicol Mech Methods* **21**, 334-342, doi:10.3109/15376516.2011.557873 (2011).
278 Kang, J. S. & Krauss, R. S. Muscle stem cells in developmental and regenerative myogenesis. *Curr Opin Clin Nutr Metab Care* **13**, 243-248, doi:10.1097/MCO.0b013e328336ea98 (2010).
279 Chen, H. *et al.* DNA damage regulates UHRF1 stability via the SCF(beta-TrCP) E3 ligase. *Mol Cell Biol* **33**, 1139-1148, doi:10.1128/MCB.01191-12 (2013).

280 Fang, Z. & Luna, E. J. Supervillin-mediated Suppression of p53 Protein Enhances Cell Survival. *J Biol Chem* **288**, 7918-7929, doi:10.1074/jbc.M112.416842 (2013).
281 Giovinazzi, S., Morozov, V. M., Summers, M. K., Reinhold, W. C. & Ishov, A. M. USP7 and Daxx regulate mitosis progression and taxane sensitivity by affecting stability of Aurora-A kinase. *Cell Death Differ* **20**, 721-731, doi:10.1038/cdd.2012.169 (2013).
282 Ma, H. *et al.* M phase phosphorylation of the epigenetic regulator UHRF1 regulates its physical association with the deubiquitylase USP7 and stability. *Proc Natl Acad Sci U S A* **109**, 4828-4833, doi:10.1073/pnas.1116349109 (2012).
283 Firuzi, O., Miri, R., Tavakkoli, M. & Saso, L. Antioxidant therapy: current status and future prospects. *Curr Med Chem* **18**, 3871-3888 (2011).
284 Melo, A. *et al.* Oxidative stress in neurodegenerative diseases: mechanisms and therapeutic perspectives. *Oxid Med Cell Longev* **2011**, 467180, doi:10.1155/2011/467180 (2011).
285 Uttara, B., Singh, A. V., Zamboni, P. & Mahajan, R. T. Oxidative stress and neurodegenerative diseases: a review of upstream and downstream antioxidant therapeutic options. *Curr Neuropharmacol* **7**, 65-74, doi:10.2174/157015909787602823 (2009).
286 Dukhande, V. V., Kawikova, I., Bothwell, A. L. & Lai, J. C. Neuroprotection against neuroblastoma cell death induced by depletion of mitochondrial glutathione. *Apoptosis*, doi:10.1007/s10495-013-0836-4 (2013).
287 Wu, J. Q., Kosten, T. R. & Zhang, X. Y. Free radicals, antioxidant defense systems, and schizophrenia. *Prog Neuropsychopharmacol Biol Psychiatry*, doi:10.1016/j.pnpbp.2013.02.015 (2013).
288 Ross, M. H. Length of life and caloric intake. *Am J Clin Nutr* **25**, 834-838 (1972).
289 Trepanowski, J. F., Canale, R. E., Marshall, K. E., Kabir, M. M. & Bloomer, R. J. Impact of caloric and dietary restriction regimens on markers of health and longevity in humans and animals: a summary of available findings. *Nutr J* **10**, 107, doi:10.1186/1475-2891-10-107 (2011).
290 Pitsikas, N., Carli, M., Fidecka, S. & Algeri, S. Effect of life-long hypocaloric diet on age-related changes in motor and cognitive behavior in a rat population. *Neurobiol Aging* **11**, 417-423 (1990).
291 Witte, A. V., Fobker, M., Gellner, R., Knecht, S. & Floel, A. Caloric restriction improves memory in elderly humans. *Proc Natl Acad Sci U S A* **106**, 1255-1260, doi:10.1073/pnas.0808587106 (2009).
292 Calingasan, N. Y. & Gibson, G. E. Dietary restriction attenuates the neuronal loss, induction of heme oxygenase-1 and blood-brain barrier breakdown induced by impaired oxidative metabolism. *Brain Res* **885**, 62-69 (2000).
293 Hofer, T. *et al.* Long-term effects of caloric restriction or exercise on DNA and RNA oxidation levels in white blood cells and urine in humans. *Rejuvenation Res* **11**, 793-799, doi:10.1089/rej.2008.0712 (2008).
294 Skrha, J. Effect of caloric restriction on oxidative markers. *Adv Clin Chem* **47**, 223-247 (2009).
295 Ribeiro, L. C. *et al.* Caloric restriction improves basal redox parameters in hippocampus and cerebral cortex of Wistar rats. *Brain Res* **1472**, 11-19, doi:10.1016/j.brainres.2012.07.021 (2012).
296 Laganiere, S. & Yu, B. P. Effect of chronic food restriction in aging rats. II. Liver cytosolic antioxidants and related enzymes. *Mech Ageing Dev* **48**, 221-230 (1989).
297 Hubert, M. F., Laroque, P., Gillet, J. P. & Keenan, K. P. The effects of diet, ad Libitum feeding, and moderate and severe dietary restriction on body weight, survival, clinical pathology parameters, and cause of death in control Sprague-Dawley rats. *Toxicol Sci* **58**, 195-207 (2000).
298 Lopez-Torres, M. & Barja, G. Lowered methionine ingestion as responsible for the decrease in rodent mitochondrial oxidative stress in protein and dietary restriction possible implications for humans. *Biochim Biophys Acta* **1780**, 1337-1347, doi:10.1016/j.bbagen.2008.01.007 (2008).

299 Calabrese, V. *et al.* Redox homeostasis and cellular stress response in aging and neurodegeneration. *Methods Mol Biol* **610**, 285-308, doi:10.1007/978-1-60327-029-8_17 (2010).
300 Obeid, R. & Herrmann, W. Mechanisms of homocysteine neurotoxicity in neurodegenerative diseases with special reference to dementia. *FEBS Lett* **580**, 2994-3005, doi:10.1016/j.febslet.2006.04.088 (2006).
301 Stott, D. J. *et al.* Randomized controlled trial of homocysteine-lowering vitamin treatment in elderly patients with vascular disease. *Am J Clin Nutr* **82**, 1320-1326 (2005).
302 Morris, M. S. The role of B vitamins in preventing and treating cognitive impairment and decline. *Adv Nutr* **3**, 801-812, doi:10.3945/an.112.002535 (2012).
303 Cantuti-Castelvetri, I., Shukitt-Hale, B. & Joseph, J. A. Neurobehavioral aspects of antioxidants in aging. *Int J Dev Neurosci* **18**, 367-381 (2000).
304 Tapas, A. R., Sakarkar, D. M. & Kakde, R. B. Flavonoids as Nutraceuticals: A Review. *Trop J Pharm Res* **7**, 1089-1099 (2008).
305 Brown, J. E. & Rice-Evans, C. A. Luteolin-rich artichoke extract protects low density lipoprotein from oxidation in vitro. *Free Radic Res* **29**, 247-255 (1998).
306 Devasagayam, T. P. *et al.* Free radicals and antioxidants in human health: current status and future prospects. *J Assoc Physicians India* **52**, 794-804 (2004).
307 Herbert, V. Prooxidant effects of antioxidant vitamins. Introduction. *J Nutr* **126**, 1197S-1200S (1996).
308 Zaidi, S. M. K. R., Al-Qirim, T. M., Hoda, N. & Banu, N. Modulation of restraint stress induced oxidative changes in rats by antioxidant vitamins. *J Nutr Biochem* **14**, 633-636, doi:Doi 10.1016/S0955-2863(03)00117-7 (2003).
309 Devore, E. E. *et al.* Dietary antioxidants and long-term risk of dementia. *Arch Neurol* **67**, 819-825, doi:10.1001/archneurol.2010.144 (2010).
310 Scapagnini, G. *et al.* Caffeic acid phenethyl ester and curcumin: a novel class of heme oxygenase-1 inducers. *Mol Pharmacol* **61**, 554-561 (2002).
311 Rao, K. V., Mawal, Y. R. & Qureshi, I. A. Progressive decrease of cerebral cytochrome C oxidase activity in sparse-fur mice: role of acetyl-L-carnitine in restoring the ammonia-induced cerebral energy depletion. *Neurosci Lett* **224**, 83-86 (1997).
312 Ahmed, H. H. Modulatory effects of vitamin E, acetyl-L-carnitine and alpha-lipoic acid on new potential biomarkers for Alzheimer's disease in rat model. *Exp Toxicol Pathol* **64**, 549-556, doi:10.1016/j.etp.2010.11.012 (2012).
313 Abdul, H. M., Calabrese, V., Calvani, M. & Butterfield, D. A. Acetyl-L-carnitine-induced up-regulation of heat shock proteins protects cortical neurons against amyloid-beta peptide 1-42-mediated oxidative stress and neurotoxicity: implications for Alzheimer's disease. *J Neurosci Res* **84**, 398-408, doi:10.1002/jnr.20877 (2006).
314 Malaguarnera, M. Acetyl-L-carnitine in hepatic encephalopathy. *Metab Brain Dis*, doi:10.1007/s11011-013-9376-4 (2013).
315 Patel, S. P., Sullivan, P. G., Lyttle, T. S., Magnuson, D. S. & Rabchevsky, A. G. Acetyl-L-carnitine treatment following spinal cord injury improves mitochondrial function correlated with remarkable tissue sparing and functional recovery. *Neuroscience* **210**, 296-307, doi:10.1016/j.neuroscience.2012.03.006 (2012).
316 Zhou, P. *et al.* Acetyl-L-carnitine attenuates homocysteine-induced Alzheimer-like histopathological and behavioral abnormalities. *Rejuvenation Res* **14**, 669-679, doi:10.1089/rej.2011.1195 (2011).
317 Rump, T. J. *et al.* Acetyl-L-carnitine protects neuronal function from alcohol-induced oxidative damage in the brain. *Free Radic Biol Med* **49**, 1494-1504, doi:10.1016/j.freeradbiomed.2010.08.011 (2010).

Acknowledgements

My greatest thanks go to Barbara van Loon and Ulrich Hübscher. They generously invited me into their laboratories, provided valuable inputs, helped in the evaluation of the collected data and writing of the thesis. My next appreciation goes to Matthias Bosshard, whose project I joined. He guided me during my first experiences in the laboratory and was never shy to offer his help. Further, I thank the Swiss National Foundation, which sponsored this thesis work (31003A_133100/1) and Hanspeter Nägeli, who gave his feedback as co-referee.
Also the whole van Loon and Hübscher group contributed many small and big things to this project: Antonia Furrer, Nicole Grosse, Marcel Rösinger, Ralph Imhof, Enni Markkanen, Elena Ferrari, Julia Dorn as well as visitors from Boston Dragon Fu, from Pavia Giovanni Maga and Emmanuele Crespan and from Oxford Grigory Dianov and Svetlana Khoronenkova.
The actors behind the scenes, Peter Binz, Rachele Vescio and Paula Raposo made sure that utensils were always ready and worked properly. My fellow students, Sarah Wyck and Samia Bachmann, completed the team of inspiring and encouraging people. All the lab of the Institute of Veterinary Biochemistry and Molecular Biology created a very friendly surrounding, which made working here a pleasure every day.
Last but not least, I thank my mother and brother, Irene and Matthias Gattiker. They stood by my side during all the ups and downs and supported me every day. It was a very intensive time, in which I not only learned a lot scientifically but also personally.

Curriculum vitae

Personal:

Name	Cristina Manuela Gattiker
Date of birth	May 29th, 1989
Place of birth	Zürich, Switzerland
Nationality	Swiss
Hometown	Richterswil ZH, Switzerland

Education:

30.01.2014	Veterinary degree (med. vet.) from the Vetsuisse Faculty, University of Zürich, Switzerland
2012-2013	Veterinary dissertation thesis under the supervision of Dr. sc. nat. Barbara van Loon at the Institute of Veterinary Biochemistry and Molecular Biology of the Vetsuisse Faculty, University of Zürich, Switzerland
2008 - 2013	Studies in Veterinary Medicine at the Vetsuisse Faculty, University of Zürich, Switzerland
01.09.2008	Matura at Kantonsschule Limmattal, Urdorf ZH, Switzerland
2002 - 2008	High school (Gymnasium) at Kantonsschule Limmattal, Urdorf ZH, Switzerland
2006 -2007	High school exchange year at Christian School of York, York PA, USA
1996 - 2002	Primary school, Unterengstringen ZH, Switzerland

Work:

2012 - present	Caretaking assistant at Tierklinik Aarau West, Oberentfelden AG, Switzerland
2012 - 2013	Surgery assistant in the department of Small Animal Surgery at Tierspital Zürich, Switzerland
2011 - 2013	Caretaker at Tierspital Zürich, Switzerland Office assistant in the department of Livestock Surgery at Tierspital Zürich, Switzerland Caretaking assistant at the Clinic of Zoo Animals, Exotic Pets and Wildlife at Tierspital Zürich, Switzerland
2007 - 2013	Private English teacher
2010 - 2012	Student representative at Vetsuisse-Lehrkommission, Zürich
2010 - 2011	Immunology tutor at Tierspital Zürich, Switzerland
2009 - 2012	Anesthetic assistant at Tierspital Zürich, Switzerland
2008 - 2012	Committee member of the Fachverein für Veterinärmedizin, Zürich
2008 - 2011	Service assistant at Cafe Bar Infinito, Zürich, Switzerland